Laser Spectroscopy combined with mass spectrometry

Jos Oomens

FELIX Laboratory, Radboud University

Nijmegen, The Netherlands

joso@science.ru.nl


FELIX
Free Electron Laser for Infrared eXperiments

Free Electron Laser: widely tunable, high intensity

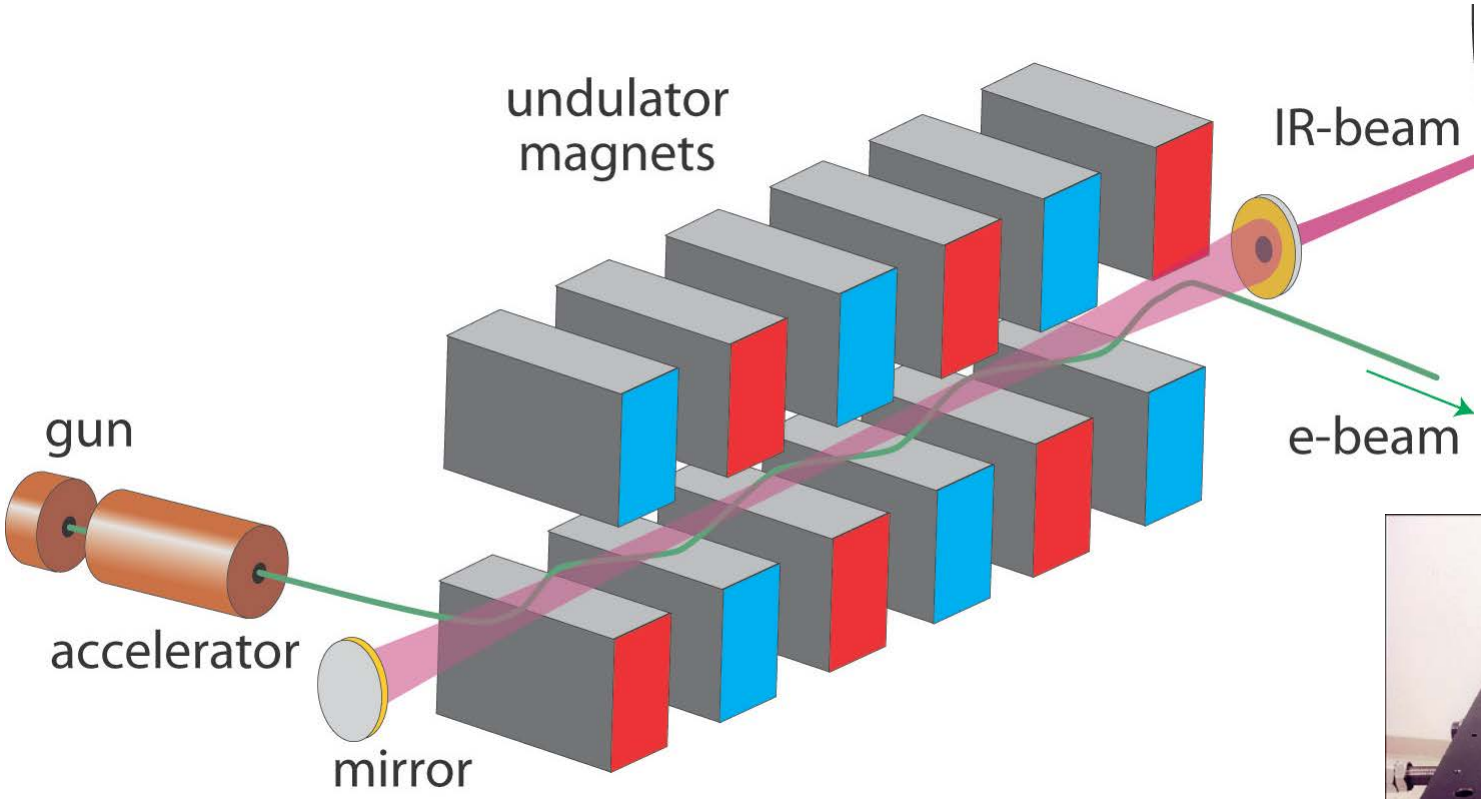

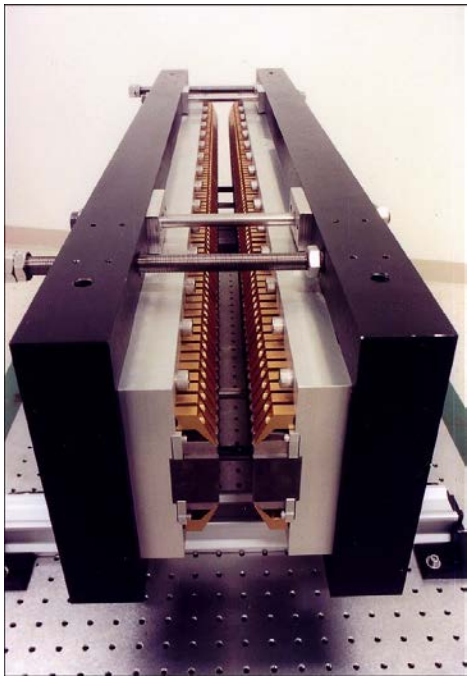

undulator

FELIX - Free Electron Laser

Electron energy < 45MeV

Wavelength tunable 5 – 200 μm

Pulse energy <100 mJ per 5 μs pulse

FWHM bandwidth >0.4% of λ

International user facility

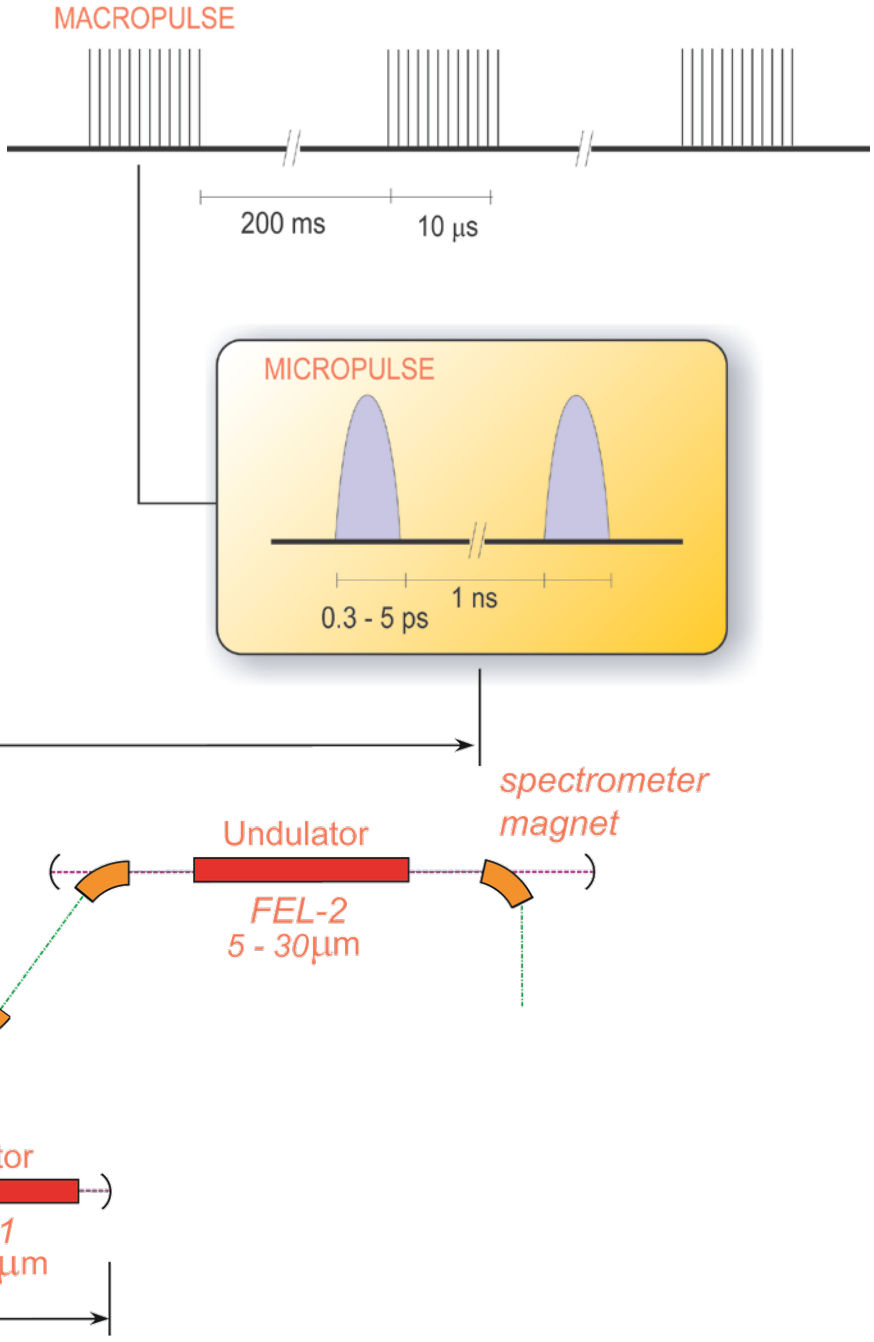

Other common IR laser sources

CO_2 laser

line tunable 9-11 μm

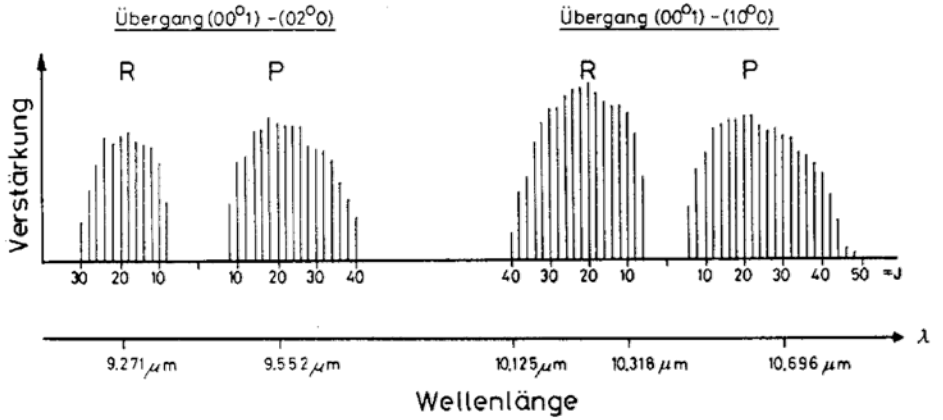

1064 nm ~1.5 μm ~3.0 μm

OPO: $h\nu_{pump} = h\nu_{signal} + h\nu_{idler}$

tuning range depends on NL crystal transparency

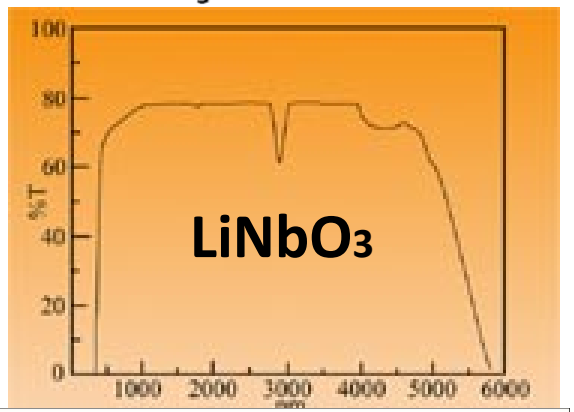

~3.0 μm 1064 nm dye laser

DFG: $h\nu = h\nu_{pump} - h\nu_{tune}$

tuning range depends on NL crystal transparency

Quantum cascade / diode laser

narrow tuning range

Far IR Time-Domain Spectrometer

THz range (<100 cm-1)

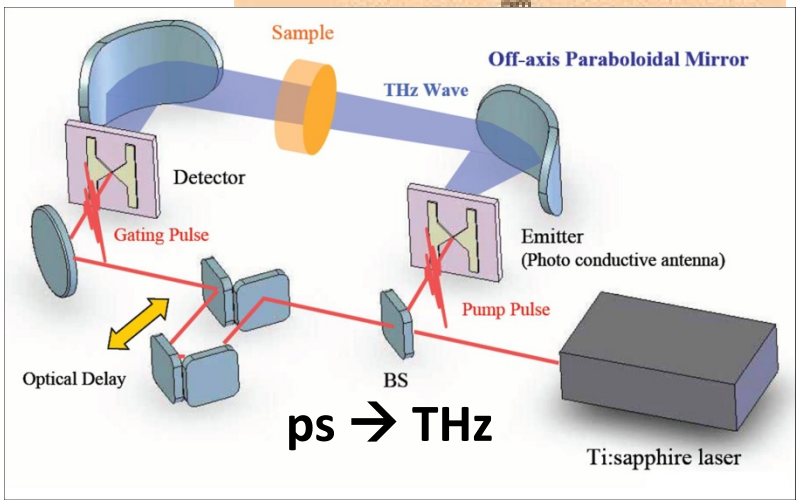

Infrared spectroscopy

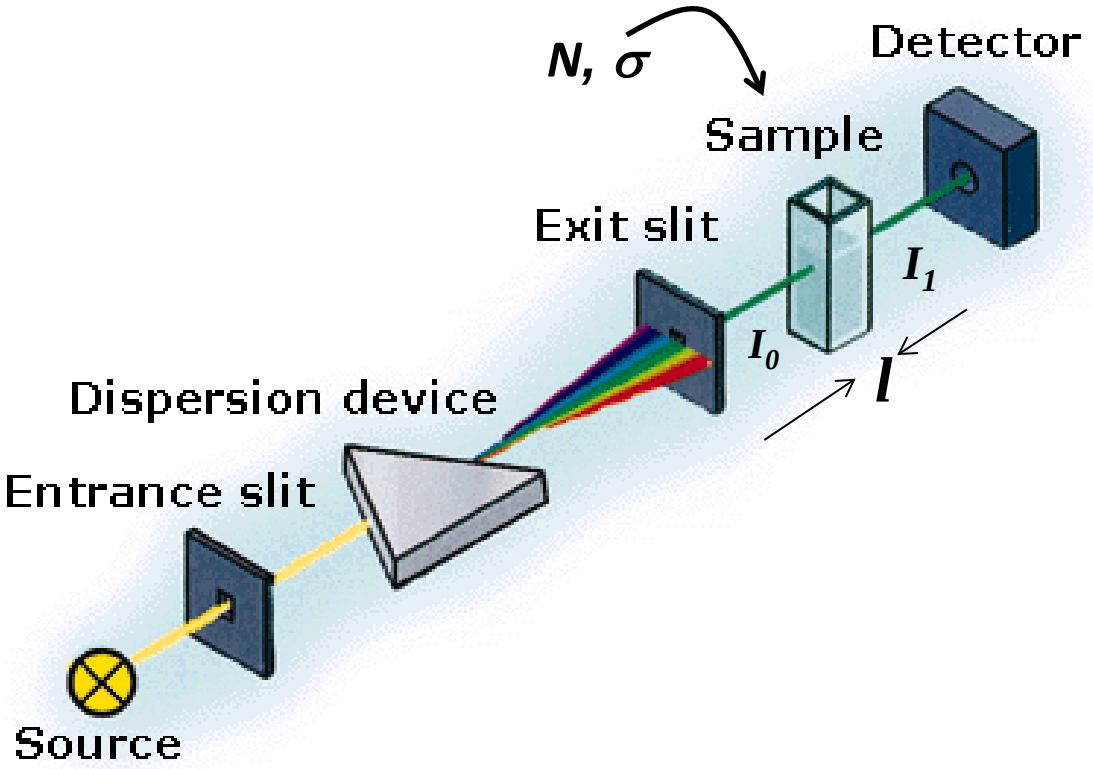

Typical values:

$$\sigma(\lambda)\, l\, n \sim 0.1 - 1$$

$\sigma \sim 10^{-19}$ cm^2

$l \sim 10$ cm

$\rightarrow n \sim 10^{18}$ cm^{-3}

What if we have only 10^6 molecules cm^{-3}?

$$T(\lambda) = I_1 / I_0 = e^{-\sigma(\lambda)\, l\, n}$$

Lambert-Beer law

vibrational spectroscopy in polyatomic molecules

Normal modes may resemble local modes

One (or few) oscillator contributes <u>dominantly</u> to normal mode

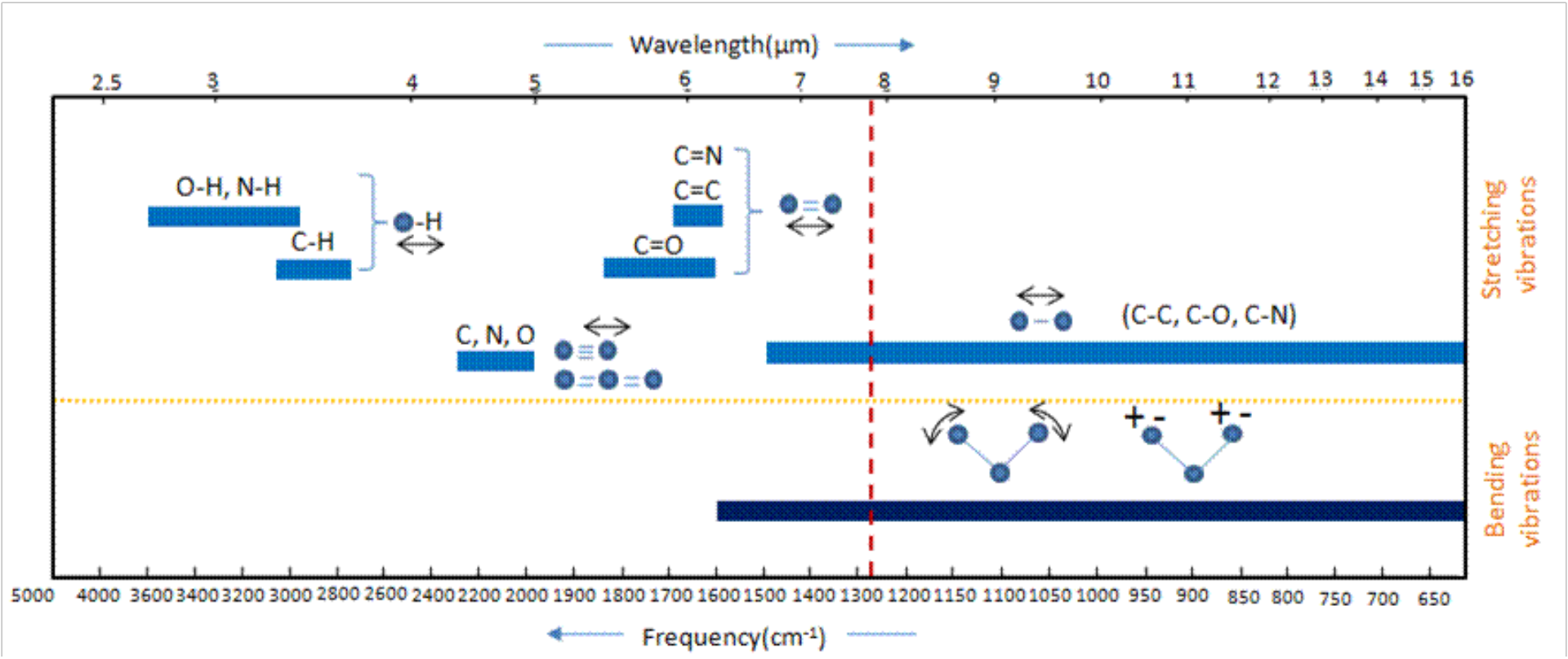

The QM 1-dim harmonic oscillator – a diatomic molecule

Linear restoring force: $F(x) = -kx$

Harmonic potential: $V(x) = \frac{1}{2}kx^2$

Taylor expansion of potential: $V(x) = V_0 + \left[\frac{dV}{dx}\right]_{x=0} x + \frac{1}{2}\left[\frac{dV}{dx}\right]_{x=0} x^2 + \cdots$

constant

0 at equilibrium

Hamiltonian: $H = -\frac{\hbar^2}{2\mu}\frac{\partial^2}{\partial x^2} + \frac{1}{2}kx^2 \quad \Rightarrow \quad H\psi = E\psi$

Solutions: $E_v = (v + \frac{1}{2})\hbar\omega$ and $\psi_v(x) \sim H_v \cdot e^{-\frac{1}{2}\alpha x^2}$

Vibrational wavefunctions: $\psi_v(x) \sim H_v \cdot e^{-\frac{1}{2}\alpha x^2}$

Hermite polynomials

$$H_n(x) = (-1)^n e^{x^2} \frac{d^n}{dx^n} e^{-x^2}$$

$$H_0(x) = 1$$
$$H_1(x) = 2x$$
$$H_2(x) = 4x^2 - 2$$
$$H_3(x) = 8x^3 - 12x$$
$$H_4(x) = 16x^4 - 48x^2 + 12$$
$$H_5(x) = 32x^5 - 160x^3 + 120x$$
$$H_6(x) = 64x^6 - 480x^4 + 720x^2 - 120$$
$$H_7(x) = 128x^7 - 1344x^5 + 3360x^3 - 1680x$$
$$H_8(x) = 256x^8 - 3584x^6 + 13440x^4 - 13440x^2 + 1680$$
$$H_9(x) = 512x^9 - 9216x^7 + 48384x^5 - 80640x^3 + 30240x$$
$$H_{10}(x) = 1024x^{10} - 23040x^8 + 161280x^6 - 403200x^4 + 302400x^2 - 30240$$

Vibrationele golffuncties met Hermite polynomen

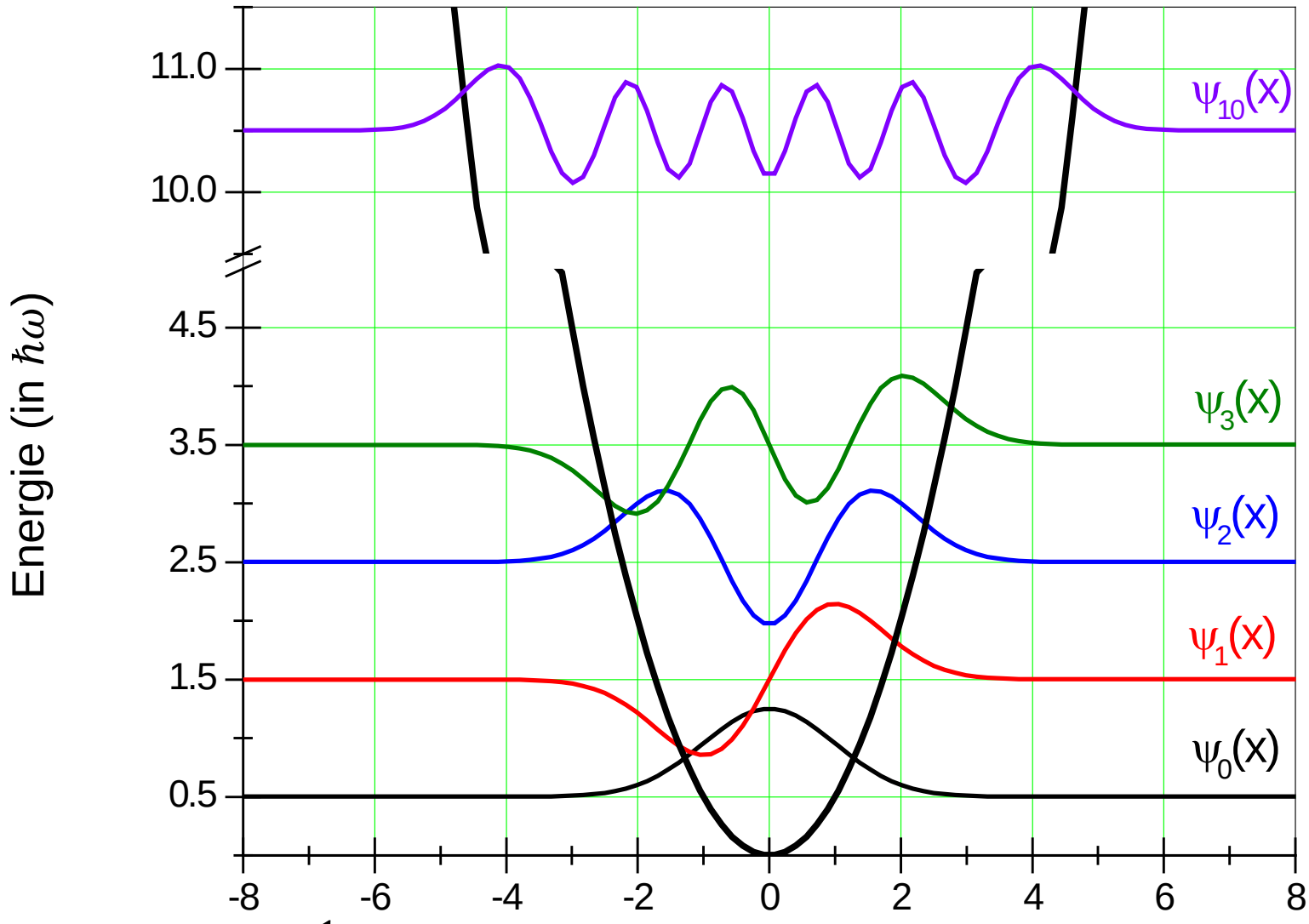

$E_v = \hbar\omega(v + {}^1/_2)$

voor $\alpha = [4\pi^2 k\mu/h^2]^{1/2} = 1$

Vibrationele waarschijnlijkheidsverdeling

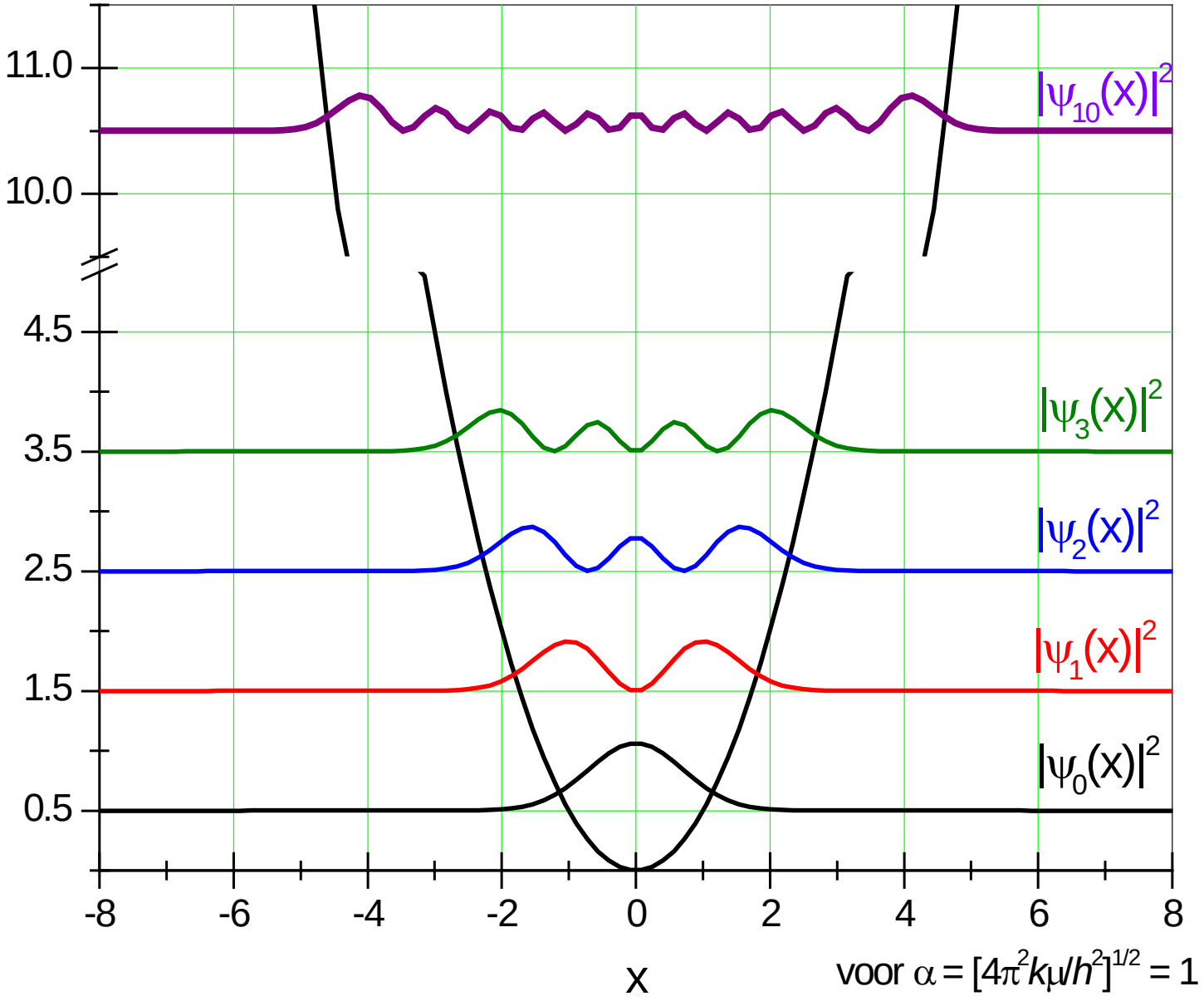

Intensities / selection rules: tranition dipole moment

Taylor expansion for dipole moment: $\mu(x) = \mu_0 + \left[\frac{d\mu}{dx}\right]_{x=0} x + \cdots$

$$TDM = \int_{-\infty}^{\infty} \psi_v \mu(x) \psi_{v'} dx =$$

$$\mu_0 \int_{-\infty}^{\infty} \psi_v \psi_{v'} dx + \left[\frac{d\mu}{dx}\right]_{x=0} \int_{-\infty}^{\infty} \psi_v x \psi_{v'} dx$$

0 due to orthogonality

dipole derivative

$\Delta v = 1$

Vibrational wavefunctions are orthogonal

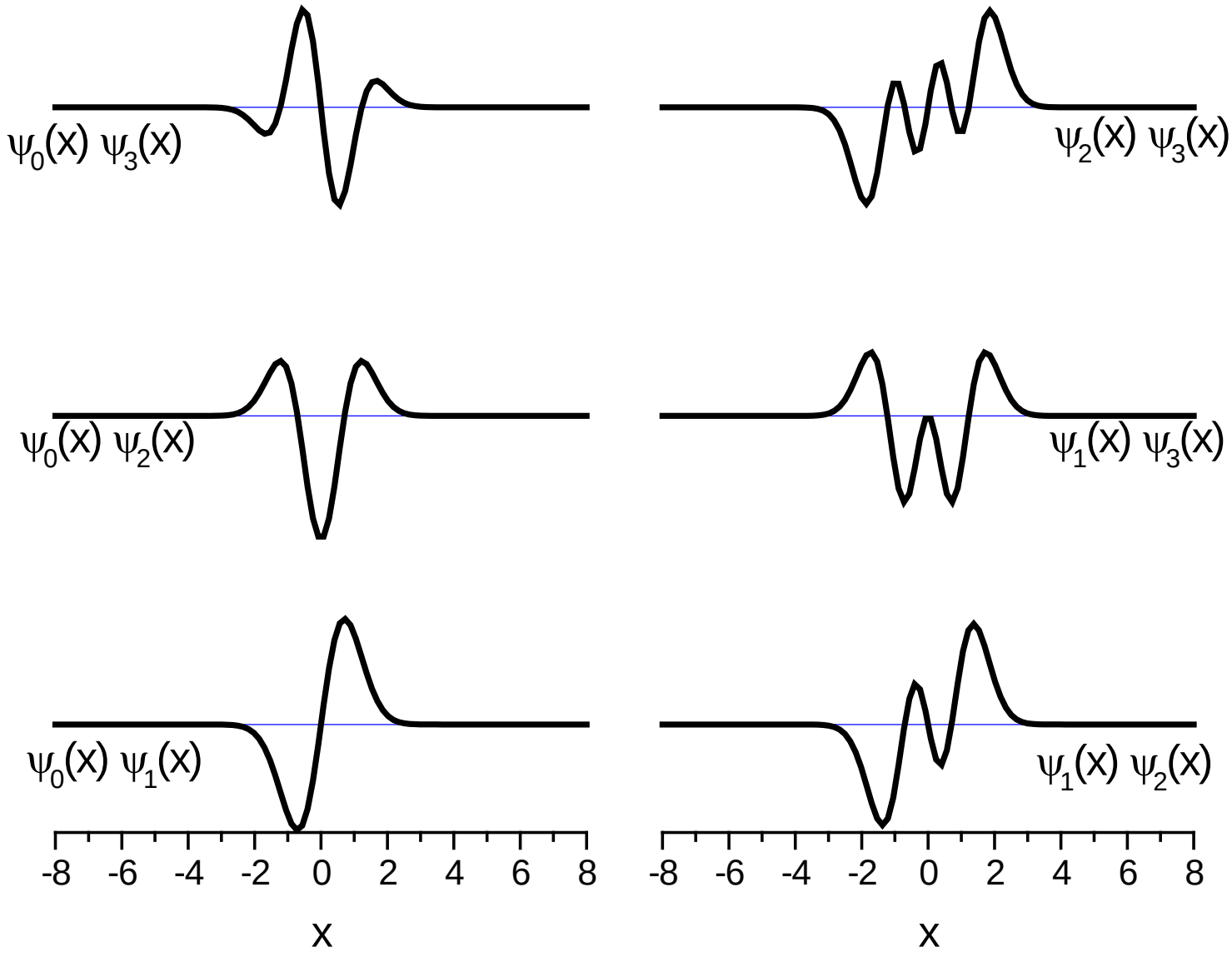

Overlap vibrational wavefunctions → selection rules

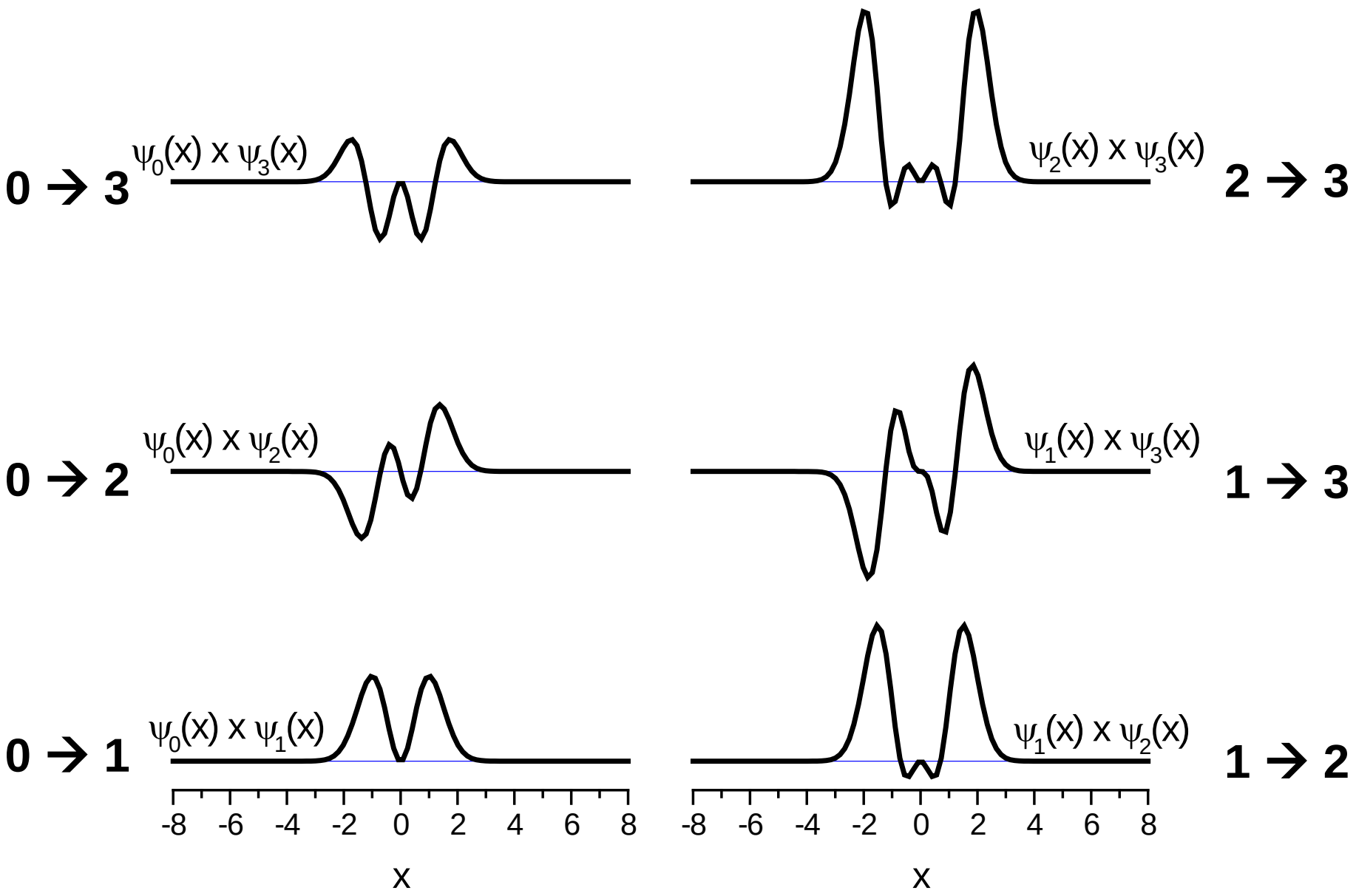

CH stretch normal mode

voor C_2H_4 (D_{2h})

TABLE 16.5 The Character Table for the D_{2h} Point Group

	E	$C_2(z)$	$C_2(y)$	$C_2(x)$	i	$\sigma(xy)$	$\sigma(xz)$	$\sigma(yz)$		
A_g	1	1	1	1	1	1	1	1		x^2, y^2, z^2
B_{1g}	1	1	−1	−1	1	1	−1	−1	R_z	xy
B_{2g}	1	−1	1	−1	1	−1	1	−1	R_y	xz
B_{3g}	1	−1	−1	1	1	−1	−1	1	R_x	yz
A_u	1	1	1	1	−1	−1	−1	−1		
B_{1u}	1	1	−1	−1	−1	−1	1	1	z	
B_{2u}	1	−1	1	−1	−1	1	−1	1	y	
B_{3u}	1	−1	−1	1	−1	1	1	−1	x	

B1u

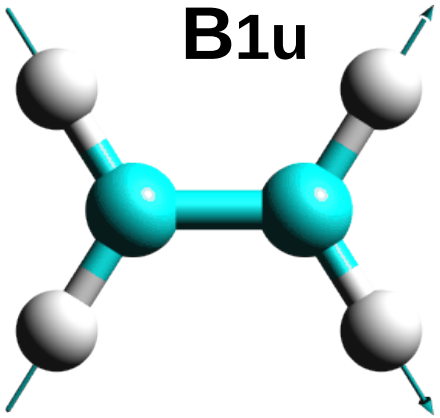

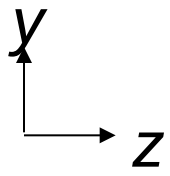

Ag

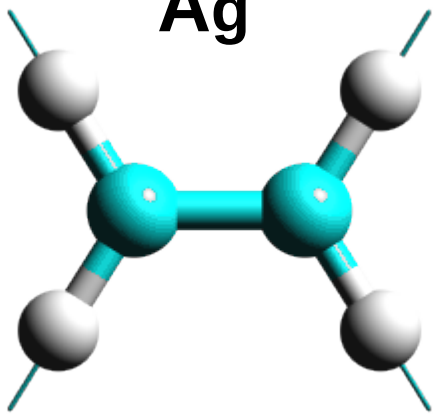

B3g

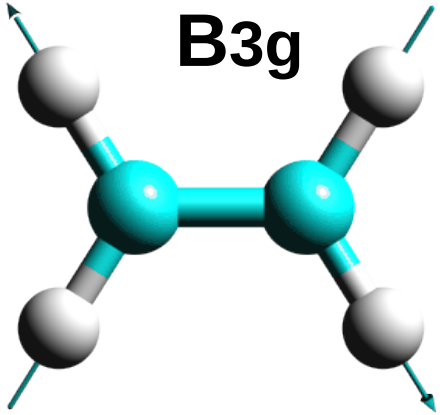

B2u

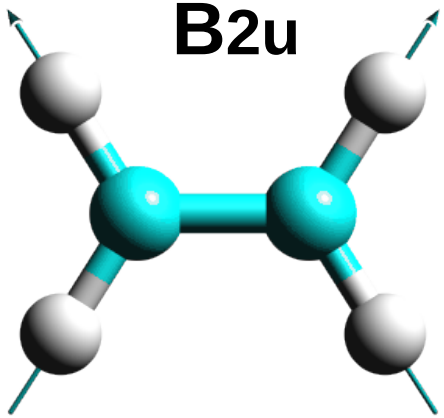

Vibrational structure of molecules

3N – 6 vibrational normal modes / frequencies

Complete orthogonal set

Vibrations assumed to be harmonic oscillations

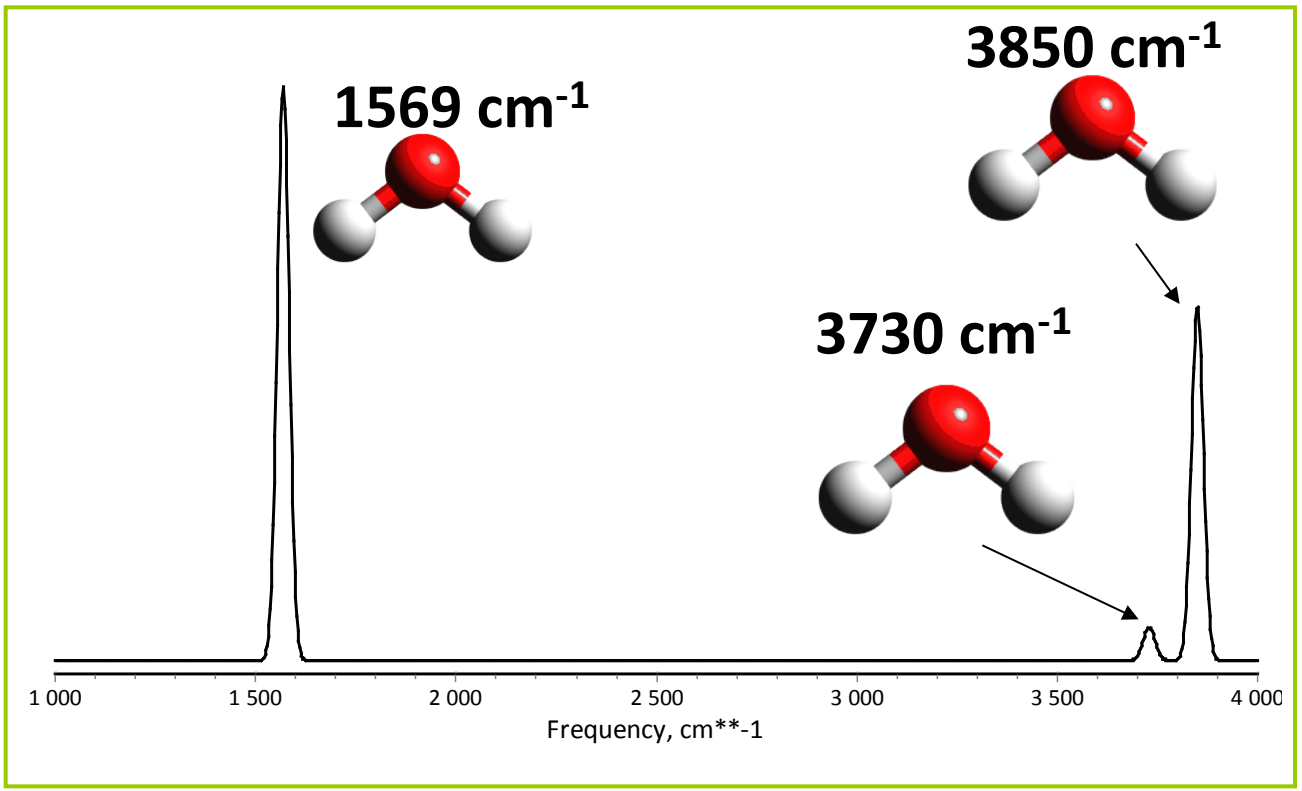

F(z) = –kz

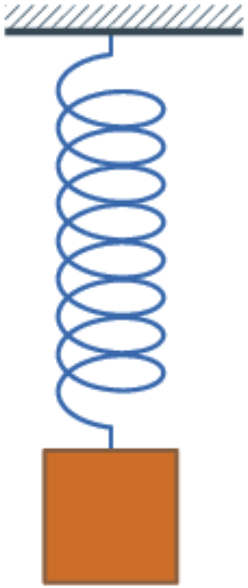

Normal modes – localized vs. delocalized

NH bend 1561 cm-1

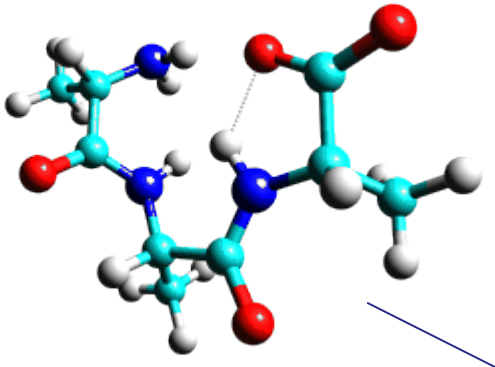

CO stretch 1729 cm-1

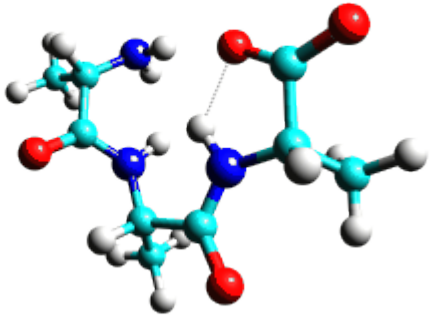

CH stretch 3094 cm-1

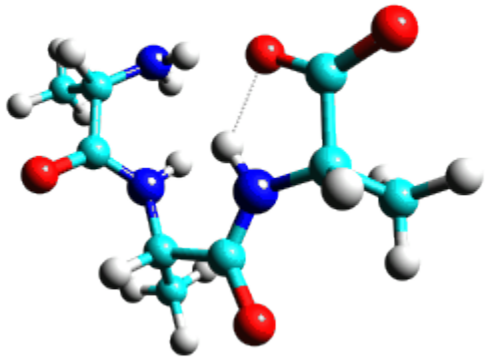

delocalized 661 cm-1

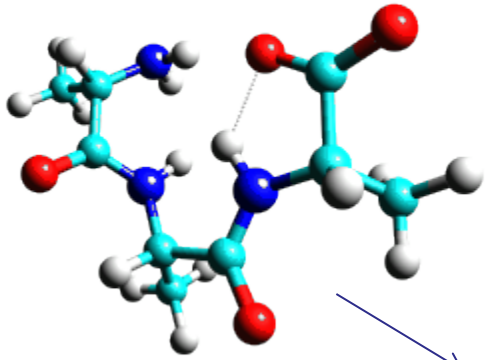

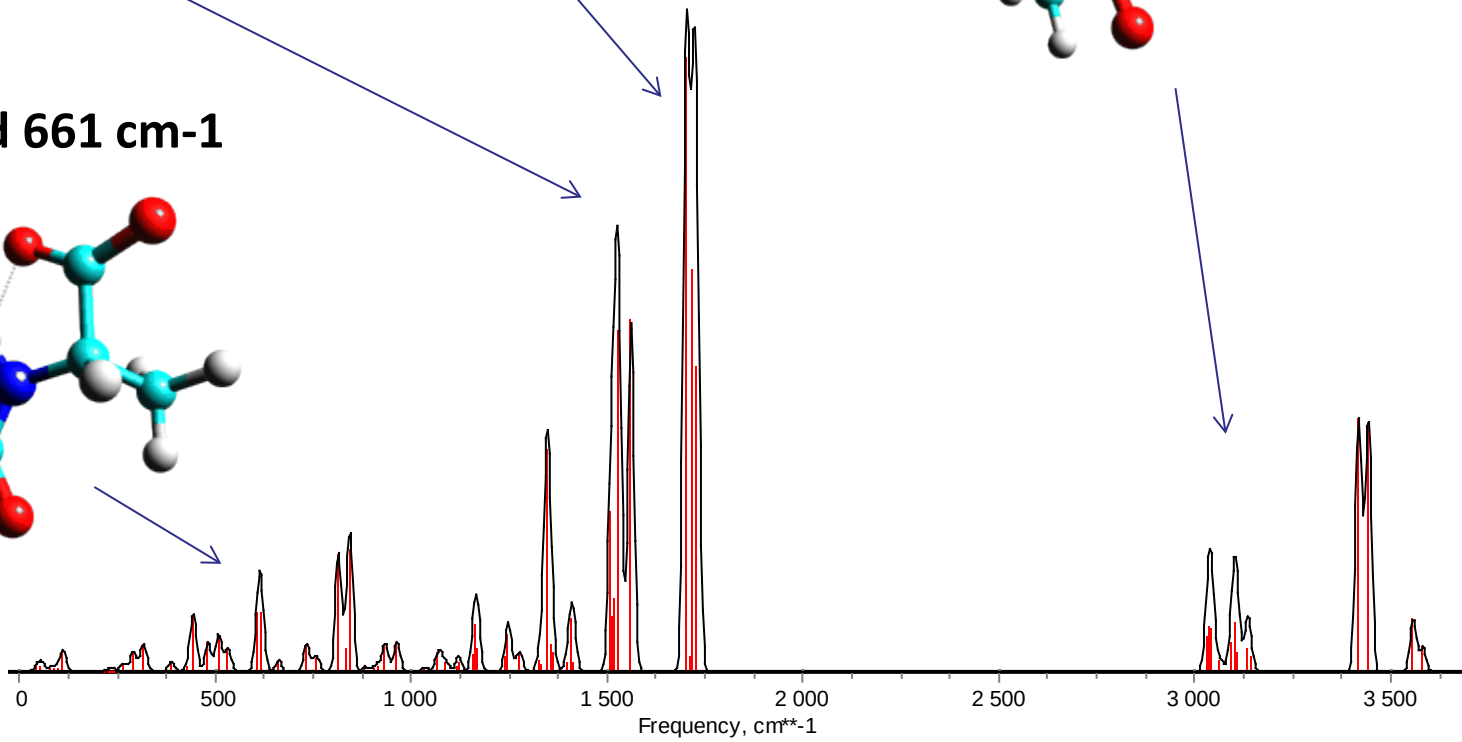

Anharmonicity – Morse potential

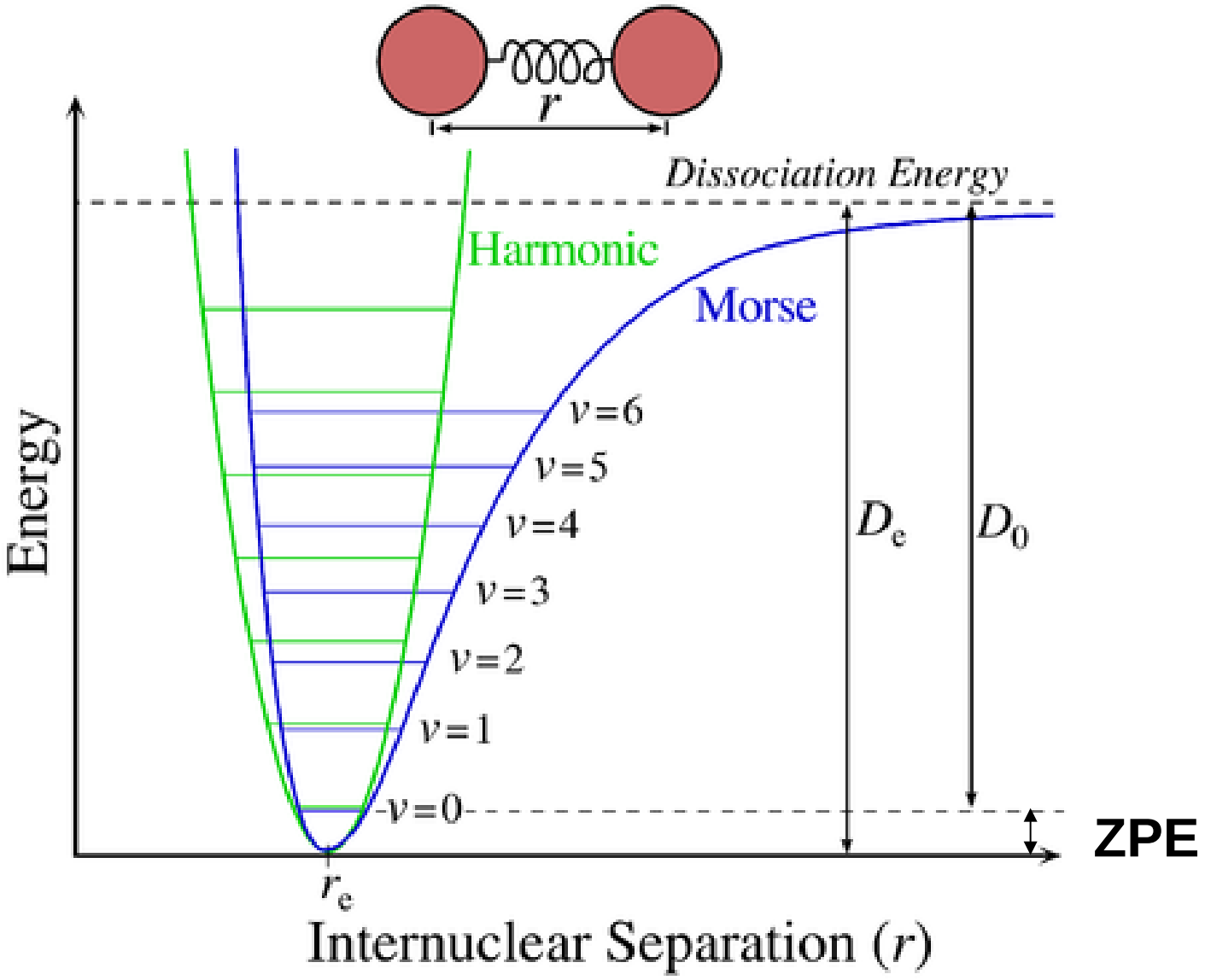

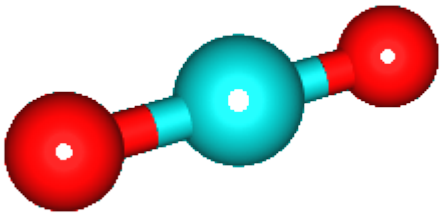

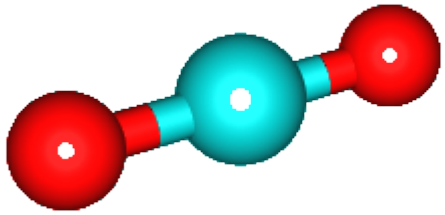

What determines spectral linewidth?

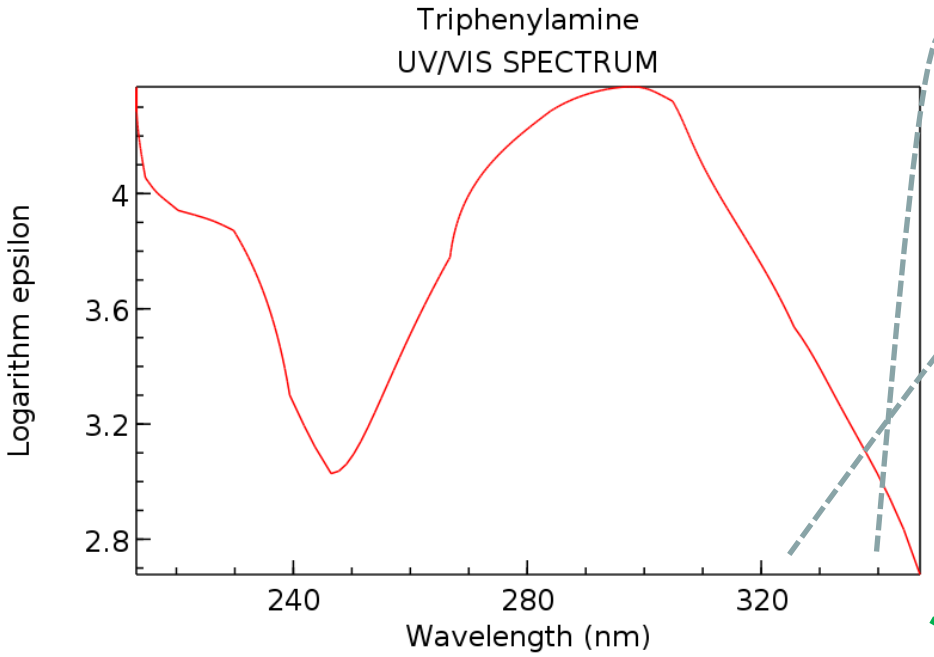

NIST Chemistry WebBook (http://webbook.nist.gov/chemistry)

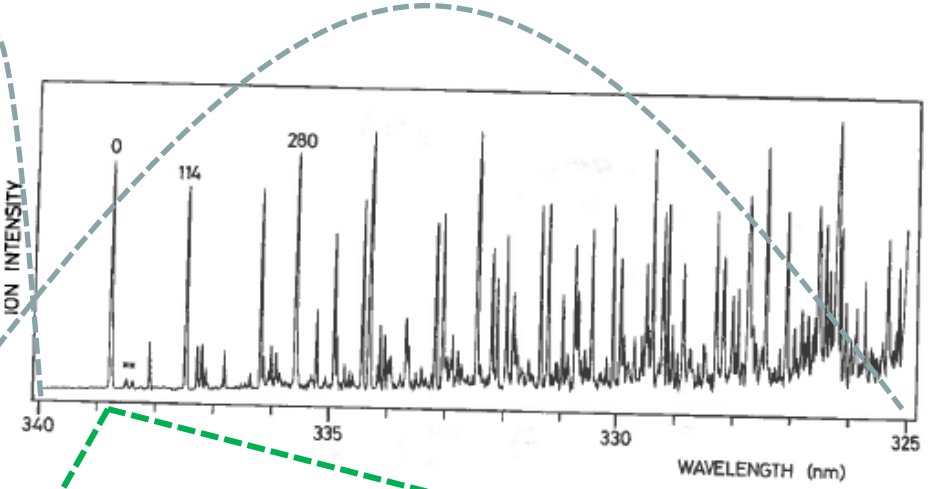

Figure 2.2: *Vibrationally resolved (1+1)-REMPI spectrum of jet-cooled TPA using 100 mJ/cm² for excitation and ionization. The stronger peaks in the spectrum are all off scale. Clear structure is observed up to at least 1000 cm⁻¹ above the S_1 origin.*

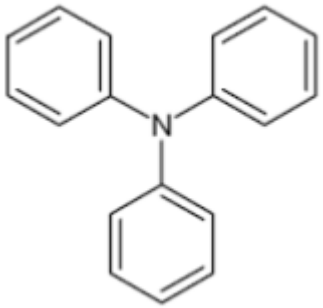

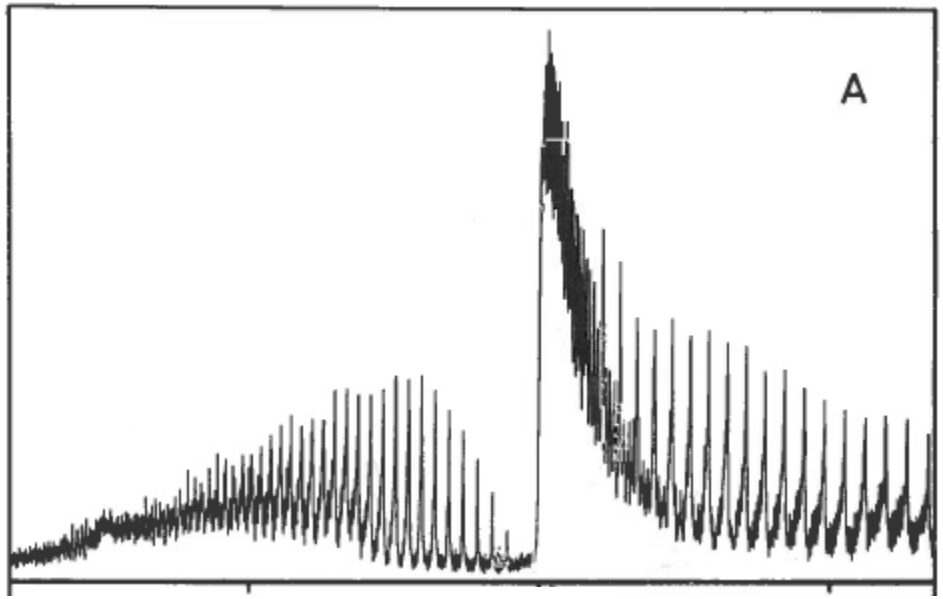

Berden, Meijer, et al.

What determines spectral linewidth?

Homogeneous broadening
- lifetime (excited state)
- pressure broadening
- transit time

Inhomogeneous broadening
- solvent (or environment) interactions
- Doppler broadening (velocity distribution)
- conformeric heterogeneity

Unresolved fine structure (rotational, T-dependent)
Instrumental resolution

supersonic molecular beam expansion

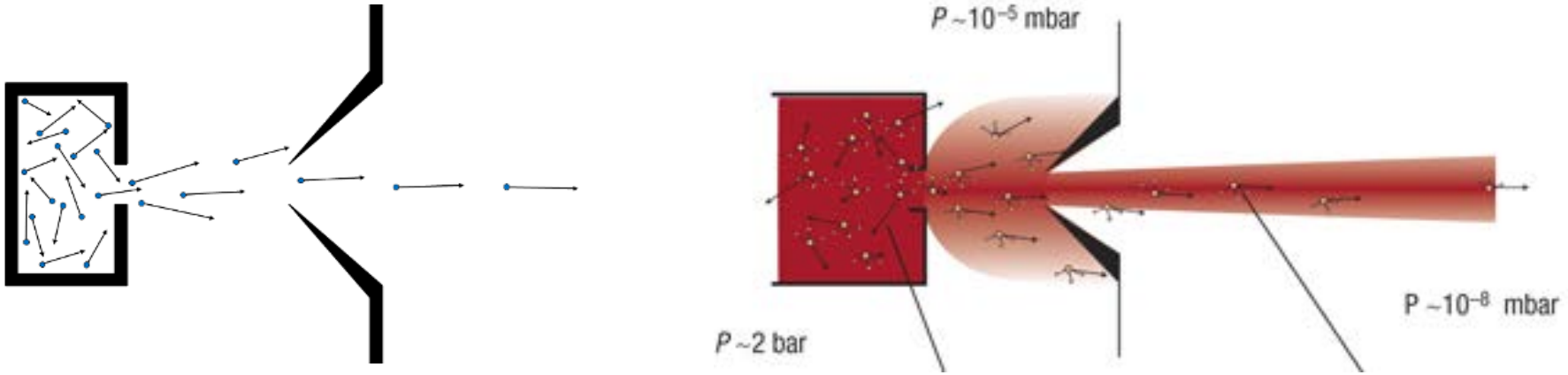

Temperature lowered (conservation of energy):

1. Fewer quantum states populated (Boltzmann distribution)
   - rotational: pop ~ $(2J+1)\exp[E_J/kT]$
   - vibrational: pop ~ $g \bullet \exp[E_v/kT]$
2. Fewer conformational structures populated (freeze out)
3. All molecules move in same direction
4. All molecules move with same velocity (no collisions)
   - reduce Doppler broadening
   - low velocity spread = low temperature
   - no interactions, molecules are isolated
5. Stabilize weakly bound complexes (e.g. M-Ar)

Laser Probes of Conformational Isomerization in Flexible Molecules and Complexes

Timothy S. Zwier†

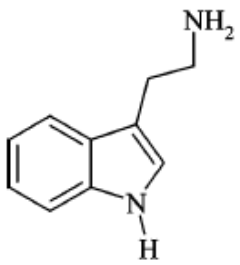

Tryptamine

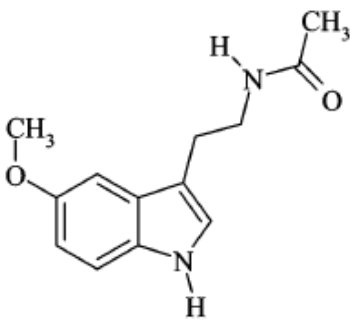

Melatonin

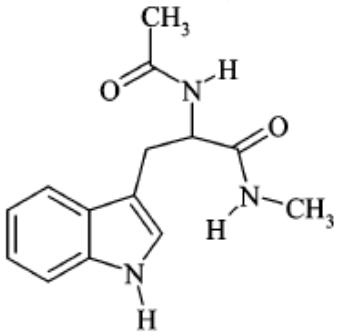

N-acetyl tryptophan methyl amide (NATMA)

11 128 164

Complexity gap

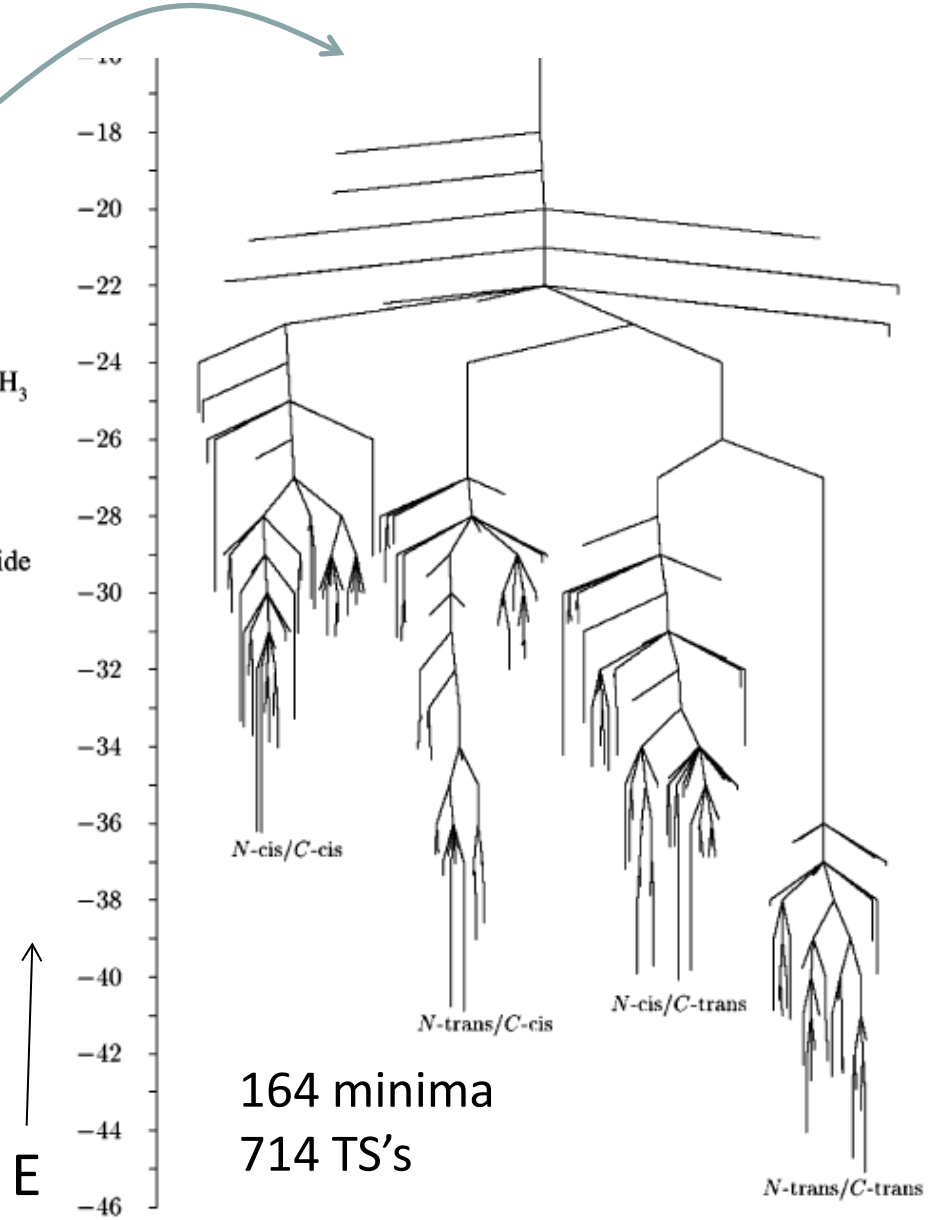

164 minima
714 TS's

Conformational energy landscape

As function of two torsional coordinates

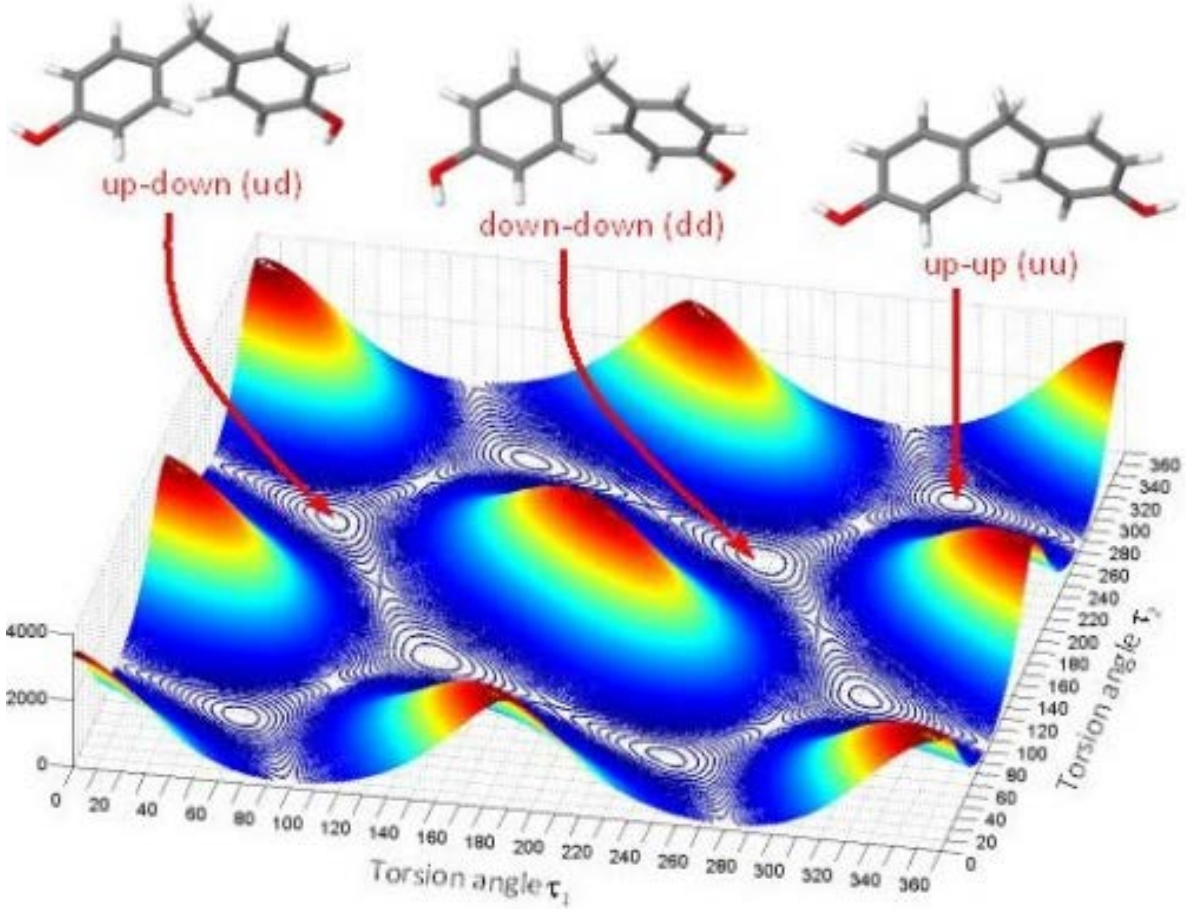

As function of multiple coordinates: hypersurface

Maxwell Boltzmann velocity distribution

$$f(v) = \sqrt{\left(\frac{m}{2\pi kT}\right)^3} 4\pi v^2 e^{-\frac{mv^2}{2kT}}$$

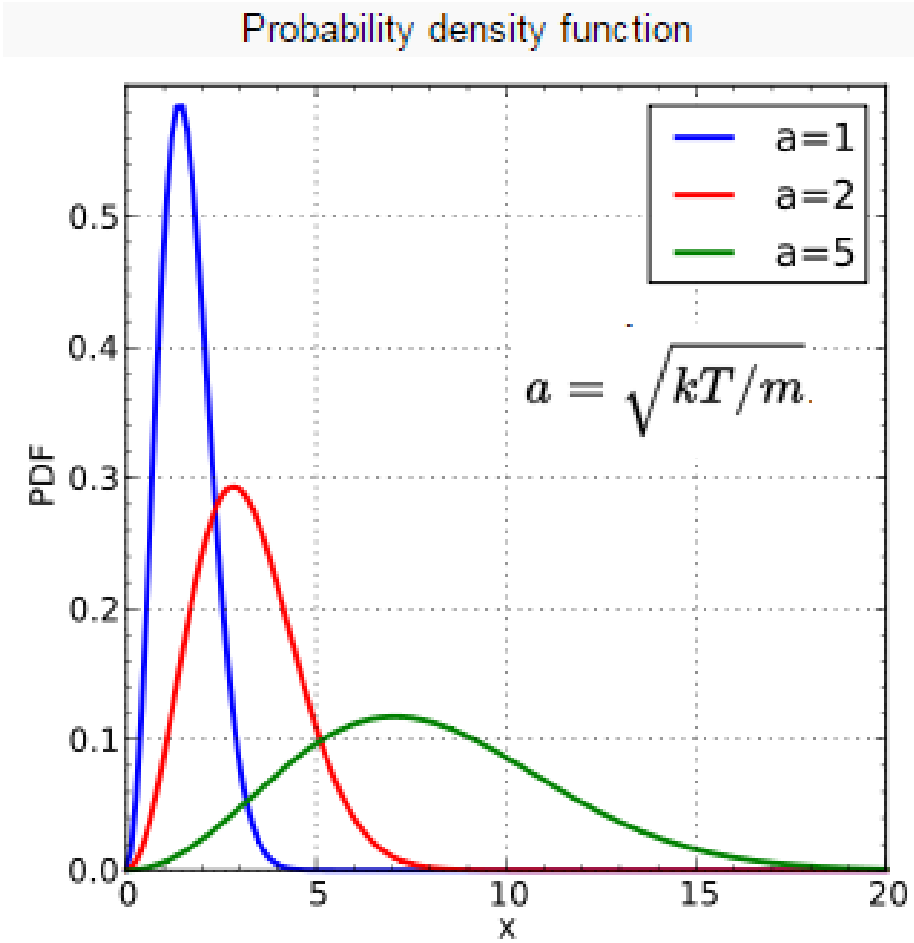

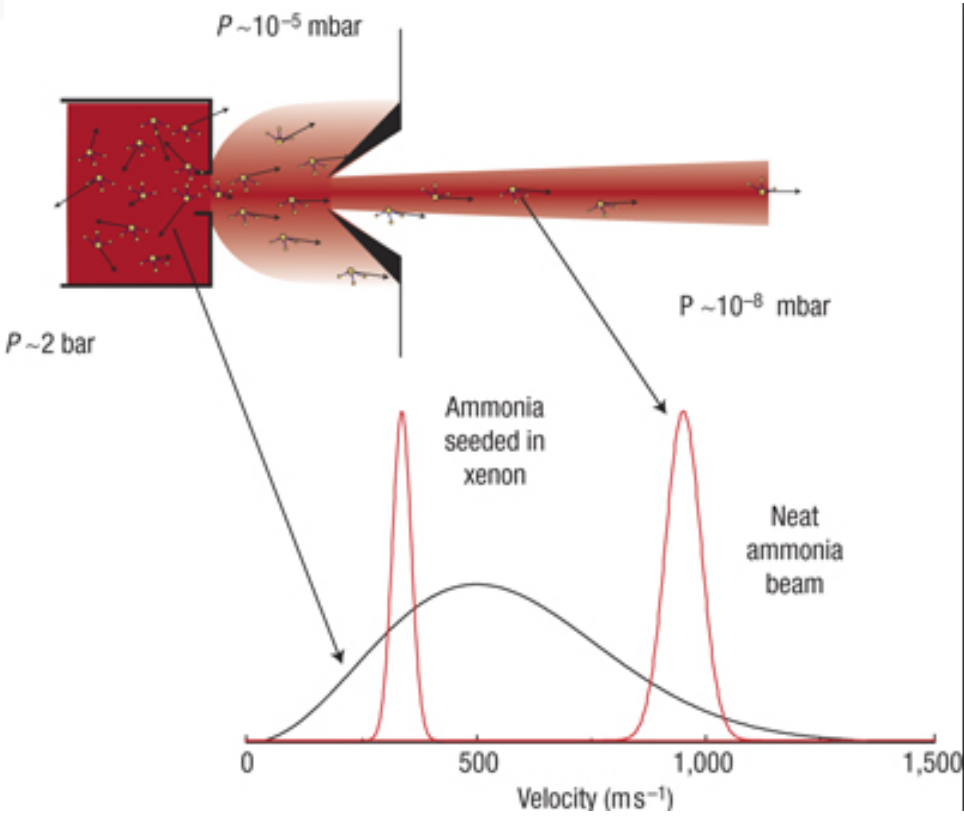

Typical molecular beam parameters

Terminal velocity ~ 500 – 1000 m/s (depend on seed gas $v_\infty \sim \sqrt{1/m}$)
Beam diameter ~ several mm
Density ~ 10^{14} cm^{-3}
Seed ratio ~ 1 – 10 percent

$$I(\nu) = I_0 e^{-\sigma(\nu) n l}$$

$$\sigma(\nu) n l \approx 10^{-16} cm^2 \, 10^{12} cm^{-3} \, 10^{-1} cm$$

$$\approx 10^{-5}$$

can hardly detect attenuation of light beam

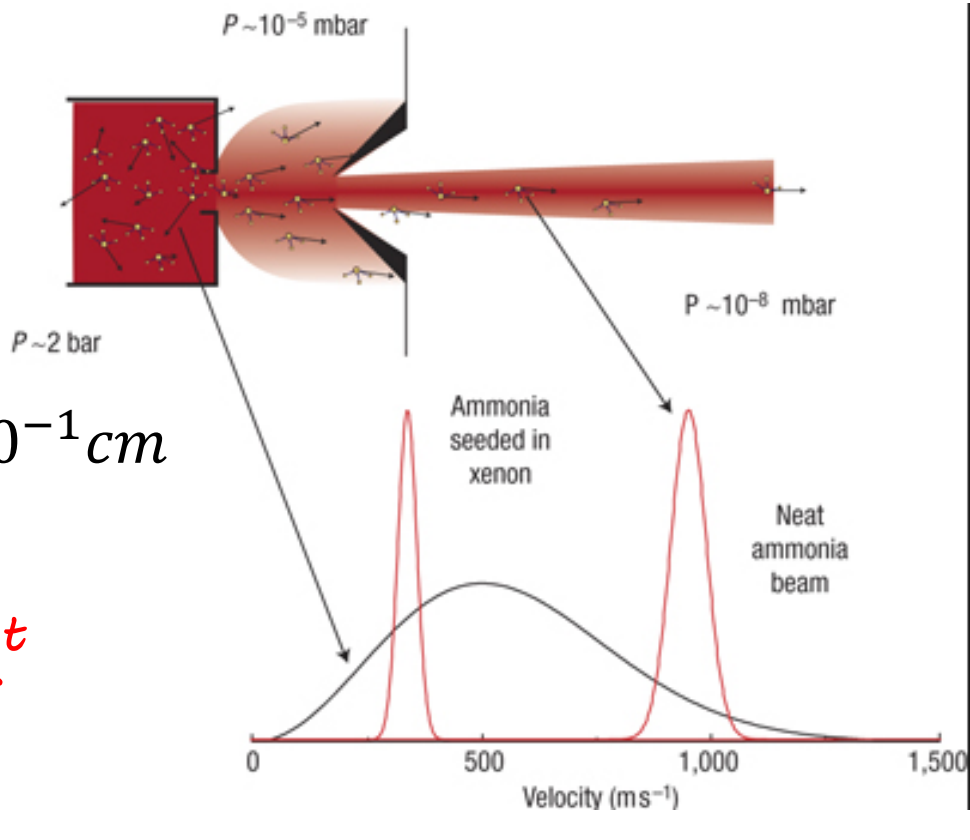

Spectroscopy in molecular beam

Cavity enhanced methods

Cavity ring down spectroscopy

determine decay time instead of attenuation of intensity. Insensitive to intensity fluctuations

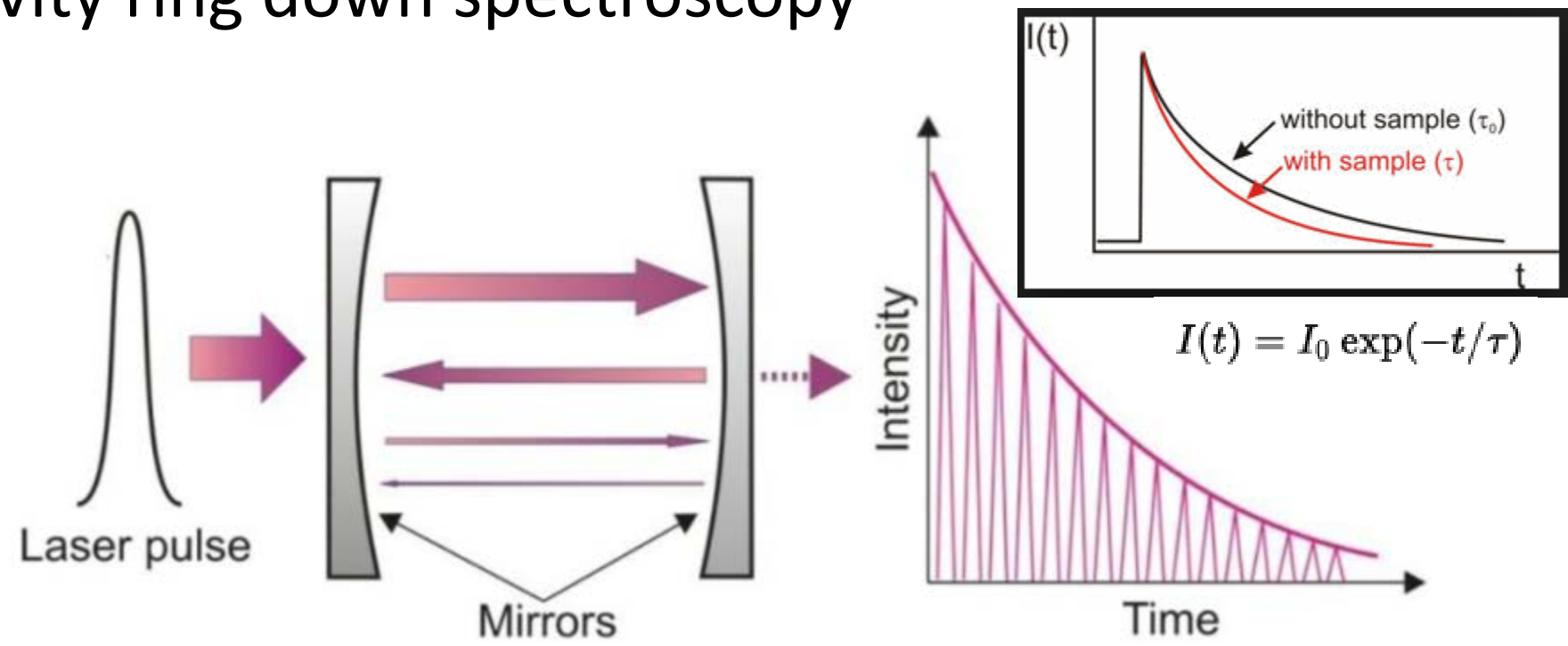

$$\tau = \frac{n}{c} \cdot \frac{l}{1 - R + X + \alpha l}$$

molecular absorption (λ dependent)

other losses

mirror reflectivity = 0·99999…

Note: $R = R(\lambda)$

Action spectroscopy in molecular beam

UV/vis (electronic spectroscopy)

fluorescence quantum yield!

Laser induced fluorescence (LIF)

detect **fluorescence** with photomultiplier

- Tune laser λ: excitation spectrum
- Fixed λ, disperse fluorescence: ground state spectrum

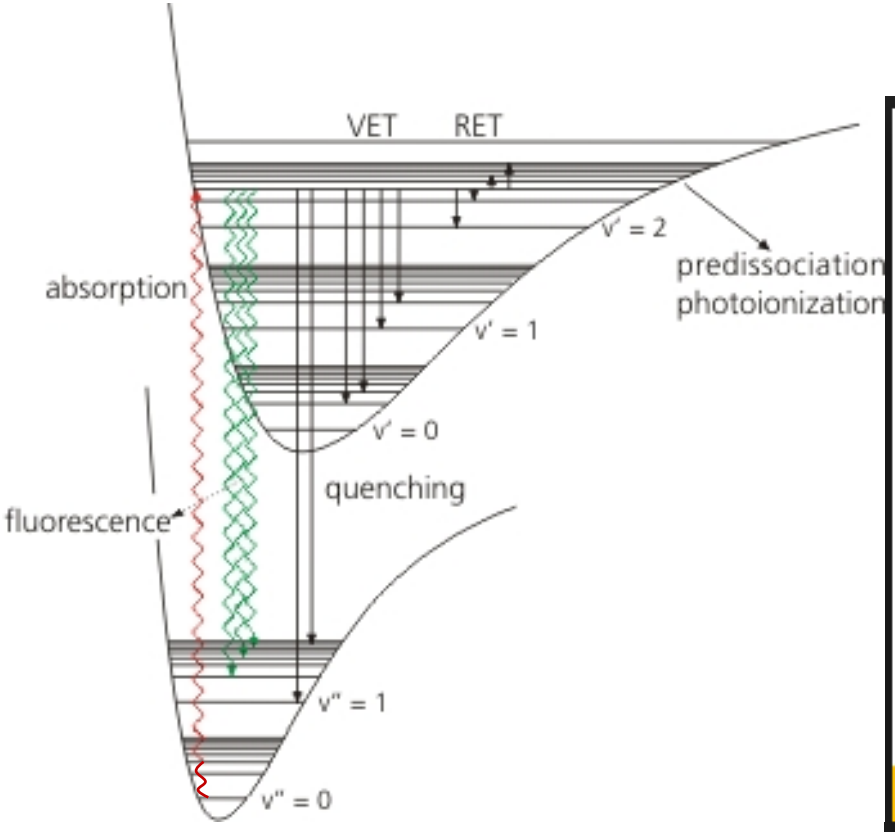

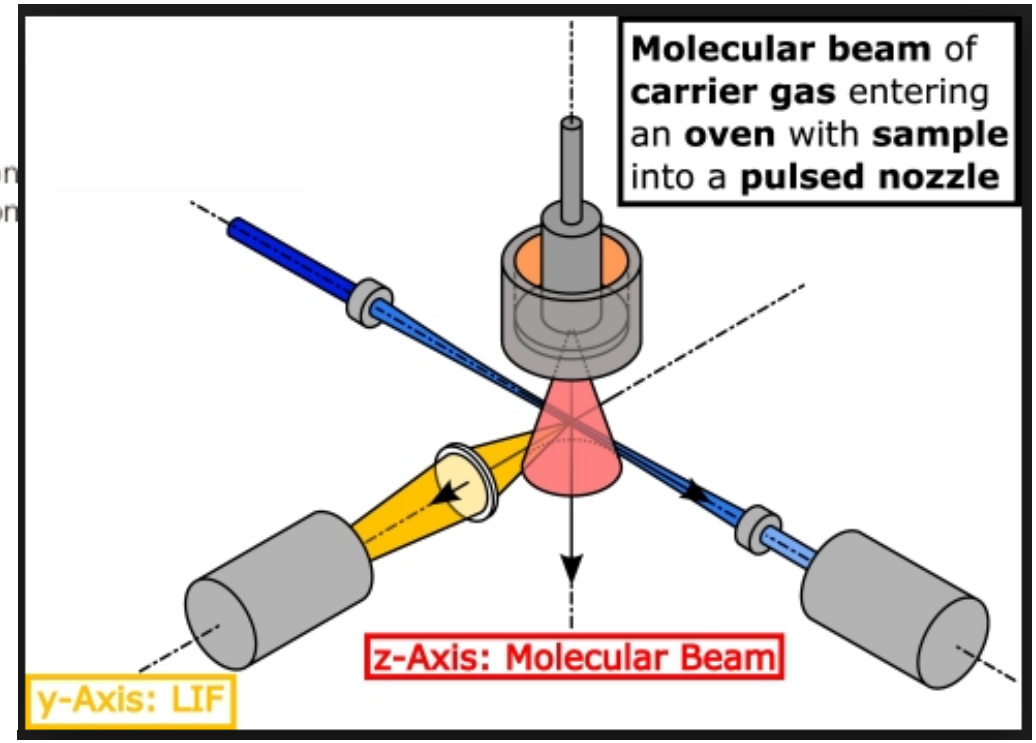

Action spectroscopy in molecular beam

UV/vis (electronic spectroscopy)

Lase

- Tu
- Fi

Conical intersection may quickly remove electronic energy in non-radiative process → $\Phi \approx 0$

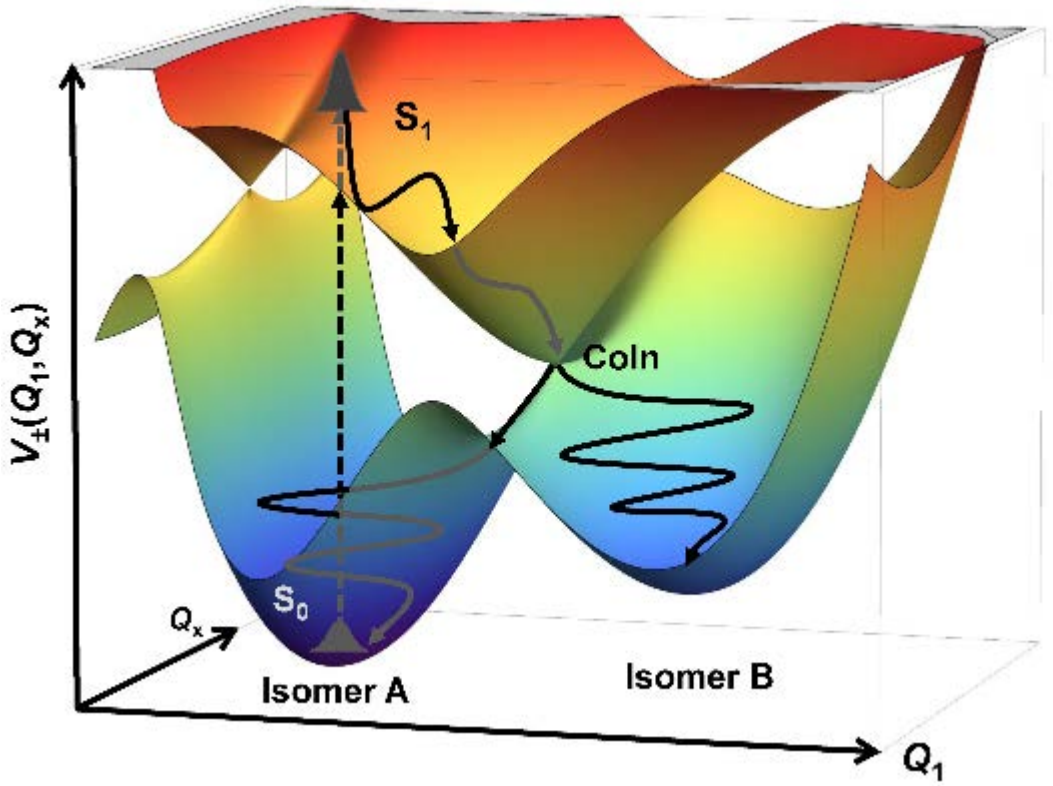

absorption

fluorescence

v'' = 0

r beam of
as entering
with sample
sed nozzle

z-Axis: Molecular Beam

y-Axis: LIF

Photochemical selectivity in guanine–cytosine base-pair structures

Watson-Crick

Ali Abo-Riziq[†], Louis Grace[†], Eyal Nir[†], Martin Kabelac[‡], Pavel Hobza[‡], and Mattanjah S. de Vries[†§]

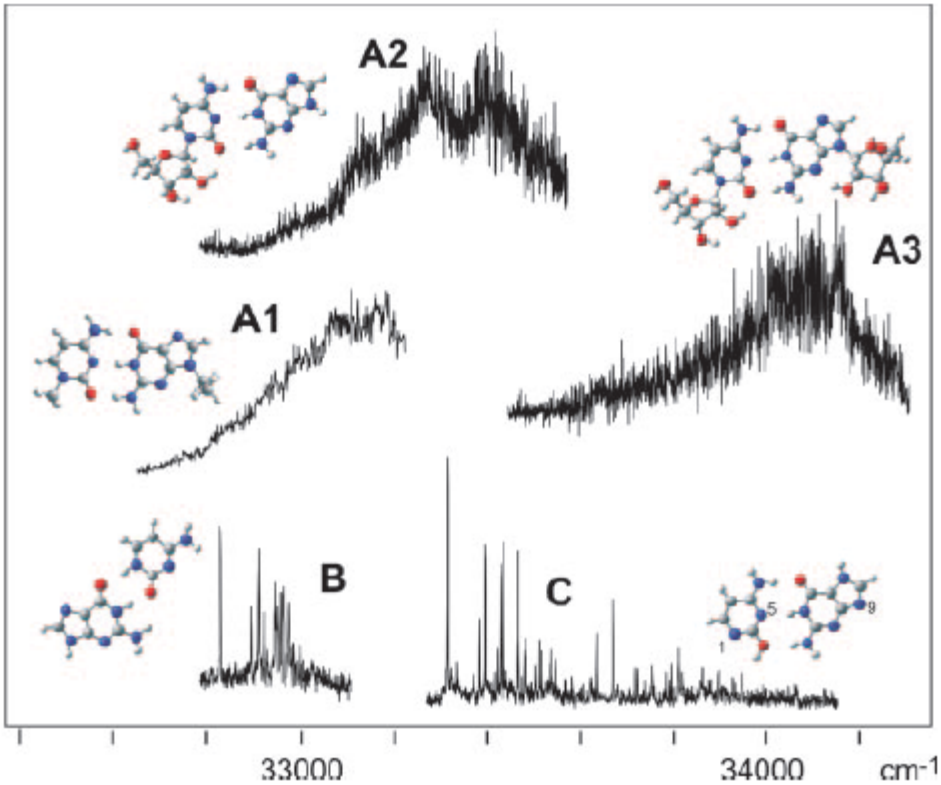

Fig. 2. REMPI spectra recorded at the mass of guanine–cytosine (B and C), 9-ethylguanine-1-methylcytosine (A1), guanine–cytidine (A2), and guanosine–cytidine (A3). All spectra are one-color, two-photon spectra, except B, which is a two-color spectrum with 266 nm for the ionization laser. All spectra were recorded at the parent mass of the respective cluster. The cluster structures in the figure were optimized at the DFT (B3LYP/6–311G**) level.

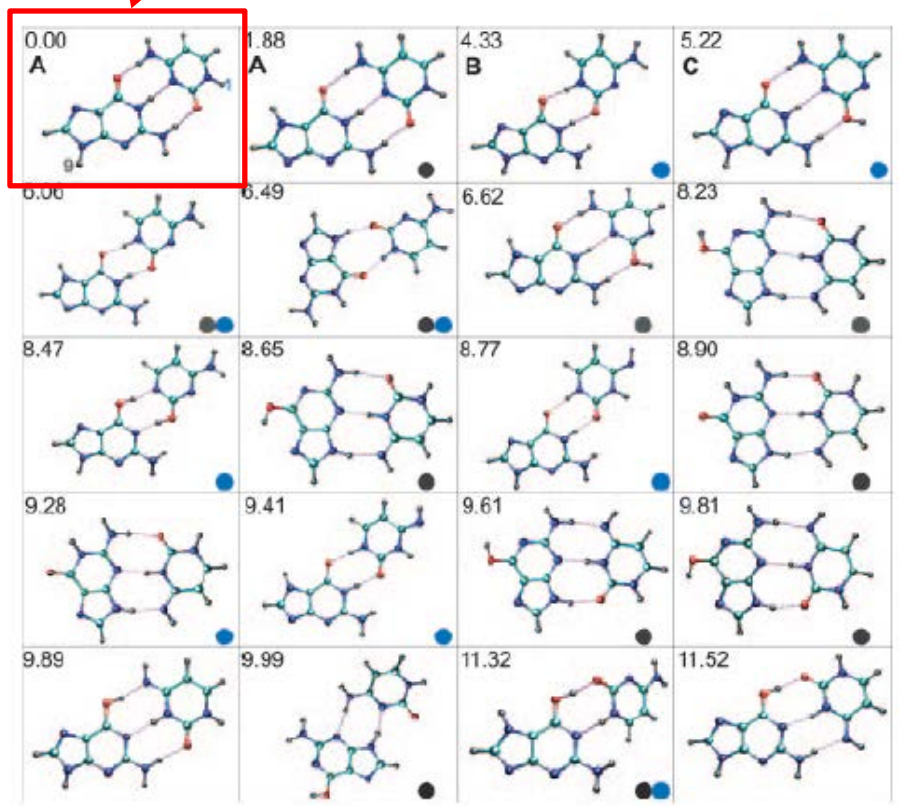

Fig. 1. Twenty lowest-energy hydrogen-bonded GC structures. Stabilization energy for each is indicated in kcal/mol relative to that of the lowest-energy configuration, the WC structure (11). Blue circles indicate structures that are not possible with 1-substituted cytosine, and gray circles indicate structures that are not possible with 9-substituted guanine.

PNAS 2004

Action spectroscopy in molecular beam
UV/vis (electronic spectroscopy)

Resonance enhanced multiphoton ionization(REMPI)
detect **ions** (combine with mass spectrometry!)

- Tune laser λ: excitation spectrum

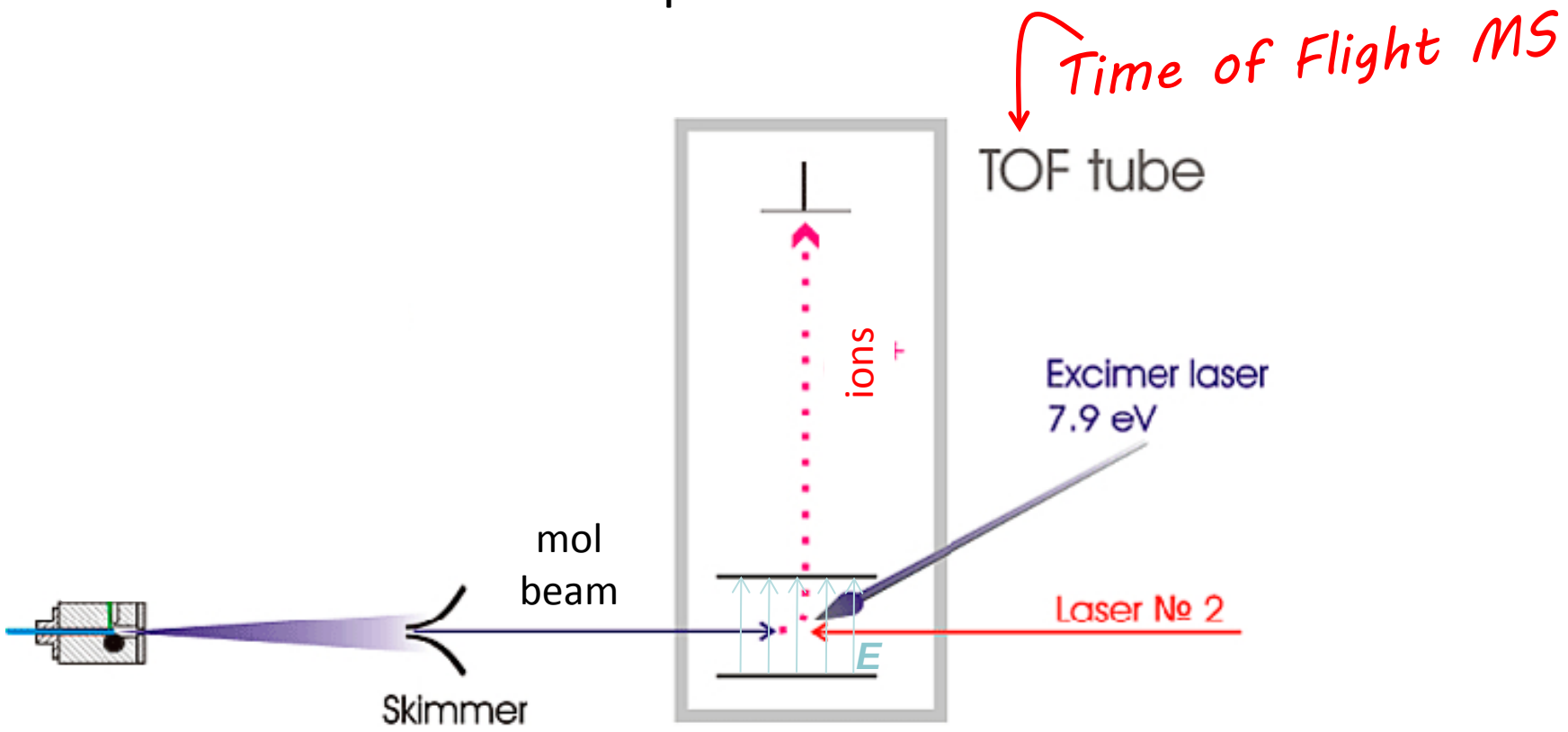

Action spectroscopy in molecular beam
UV/vis (electronic spectroscopy)

Resonance enhanced multiphoton ionization(REMPI)
detect **ions** (combine with mass spectrometry!)

- Tune laser λ: excitation spectrum

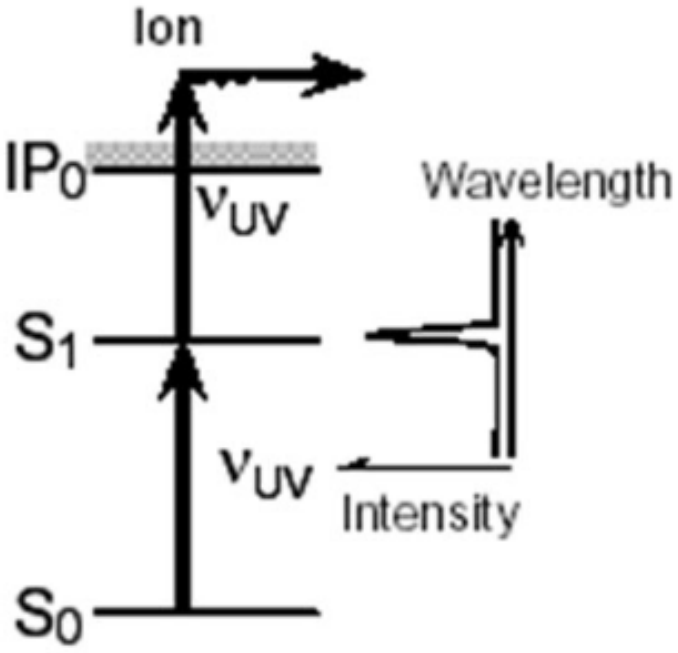

1 + 1 REMPI

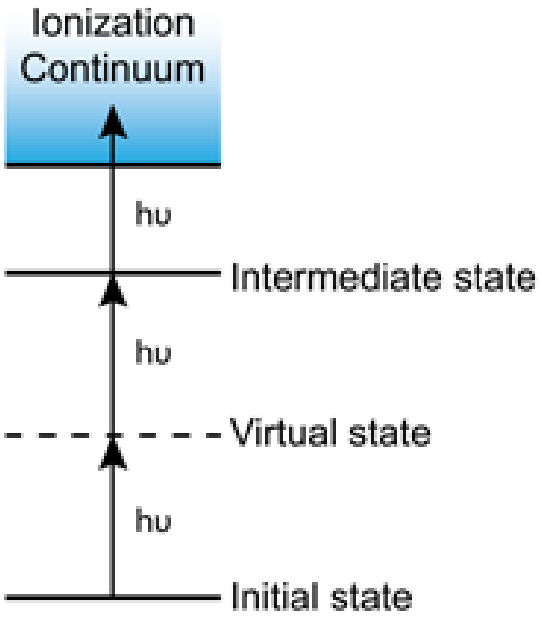

2 + 1 REMPI

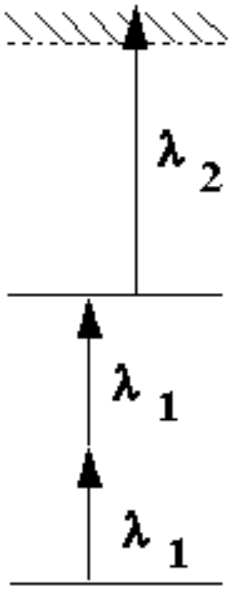

2 + 1' REMPI

Action spectroscopy in molecular beam

IR (vibrational spectroscopy) ?

Mirror reflectivity typically lower and over limited λ range

No fluorescence in IR (Einstein A coefficient ~ ν^3, detectors insensitive in IR, thermal background radiation, …)

IR multiple photon excitation leads to dissociation rather than ionization (IP > D_0)

Action spectroscopy in molecular beam

IR (vibrational spectroscopy) ?

Resonant Ionization Using IR Light: A New Tool To Study the Spectroscopy and Dynamics of Gas-Phase Molecules and Clusters

Gert von Helden,*,† Deniz van Heijnsbergen,† and Gerard Meijer†,‡,§

JPCA 2003

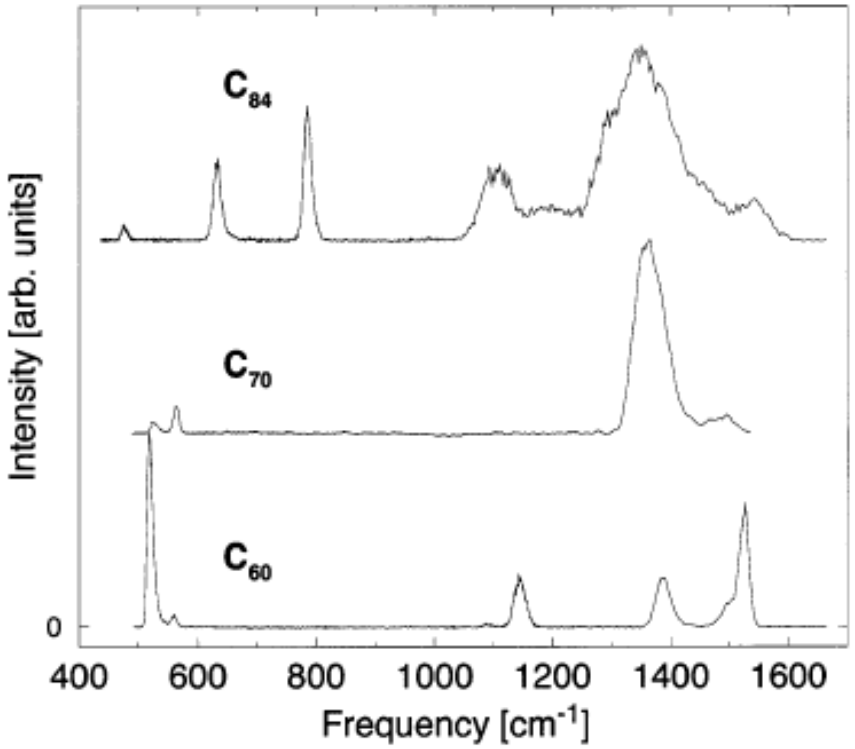

. IR-REMPI spectra for C_{60}, C_{70}, and C_{84}.

Fullerenes have high D_0 and low IP

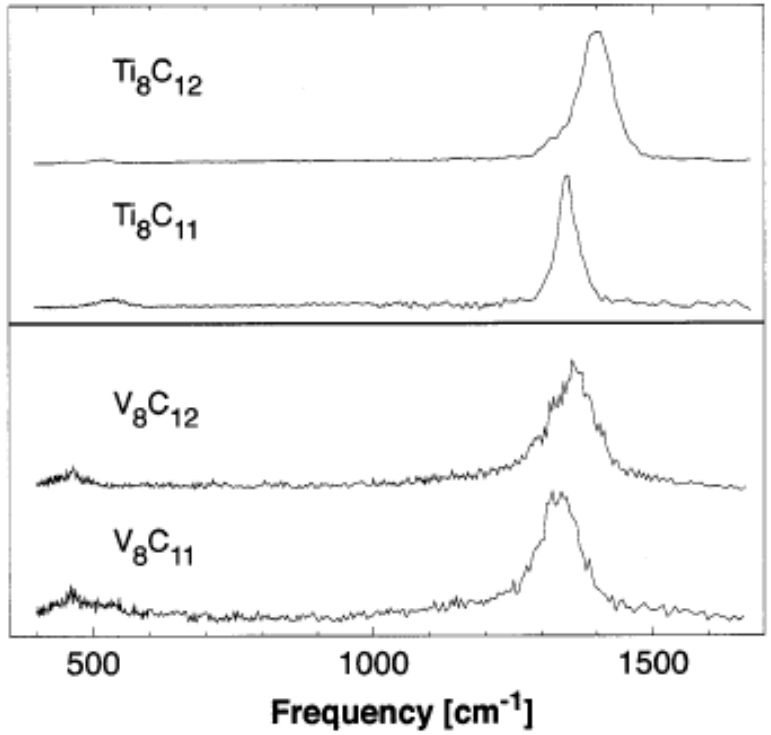

IR-REMPI spectra for Ti_8C_{12}, Ti_8C_{11}, V_8C_{12}, and V_8C_{11}.

Transition metals have low IP

Molecular beam / REMPI / ToF MS

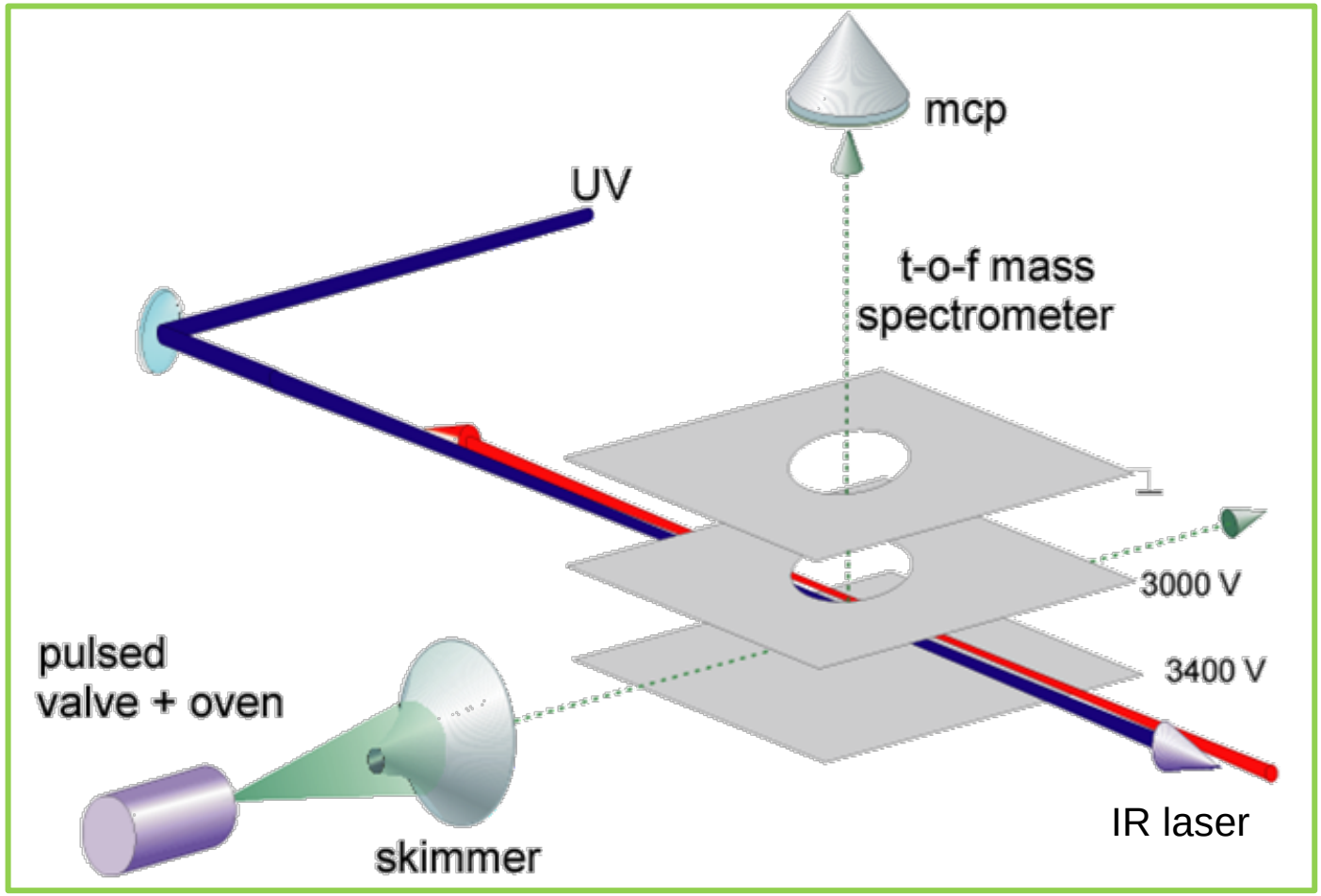

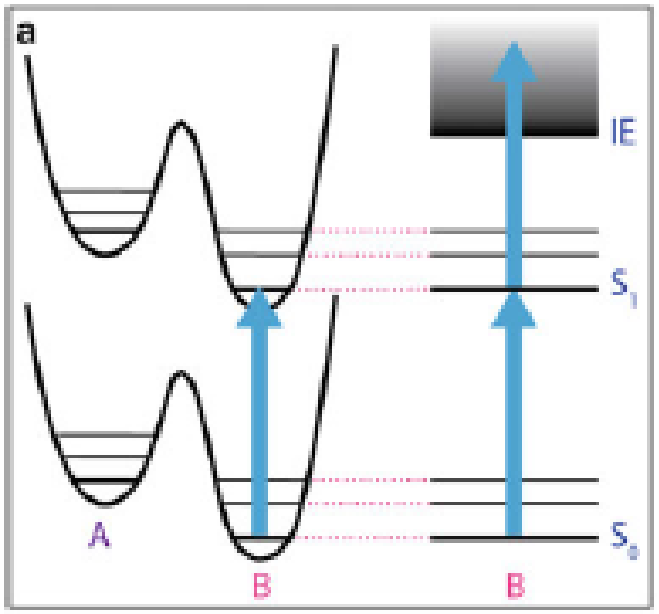

REMPI is conformation specific!

$S_1 \leftarrow S_0$ transition is slightly different for different conformers of the same molecule

Excite one specific conformer with narrow-band laser

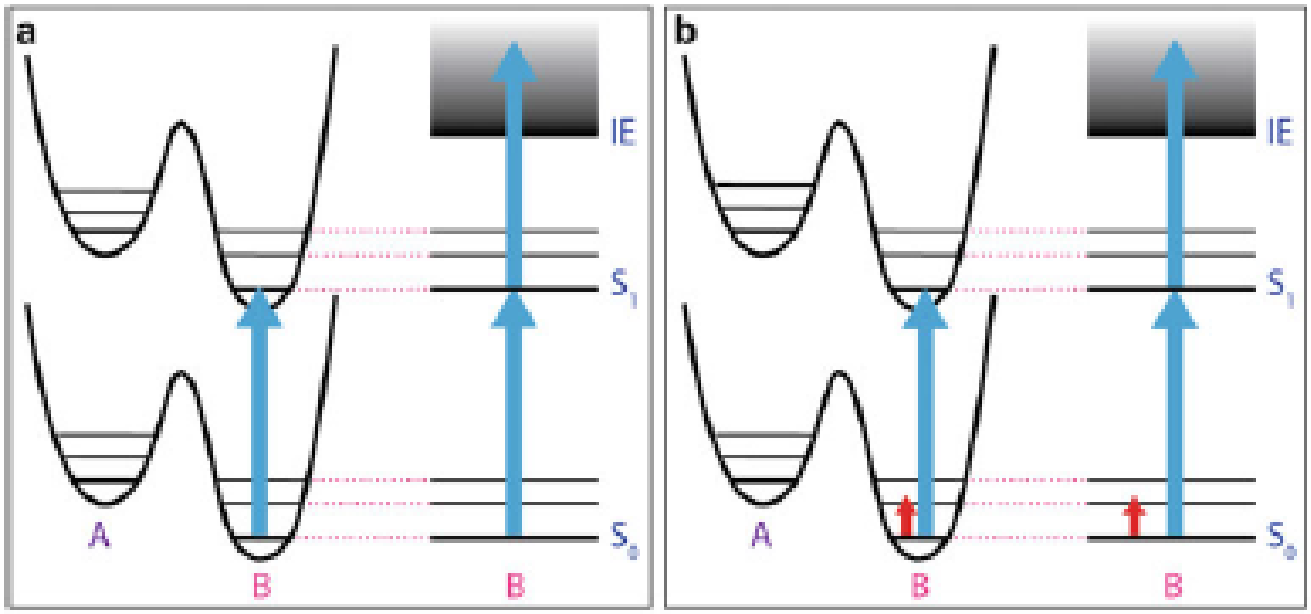

Combine UV and IR

- UV selects one conformer
- IR probes that specific conformer

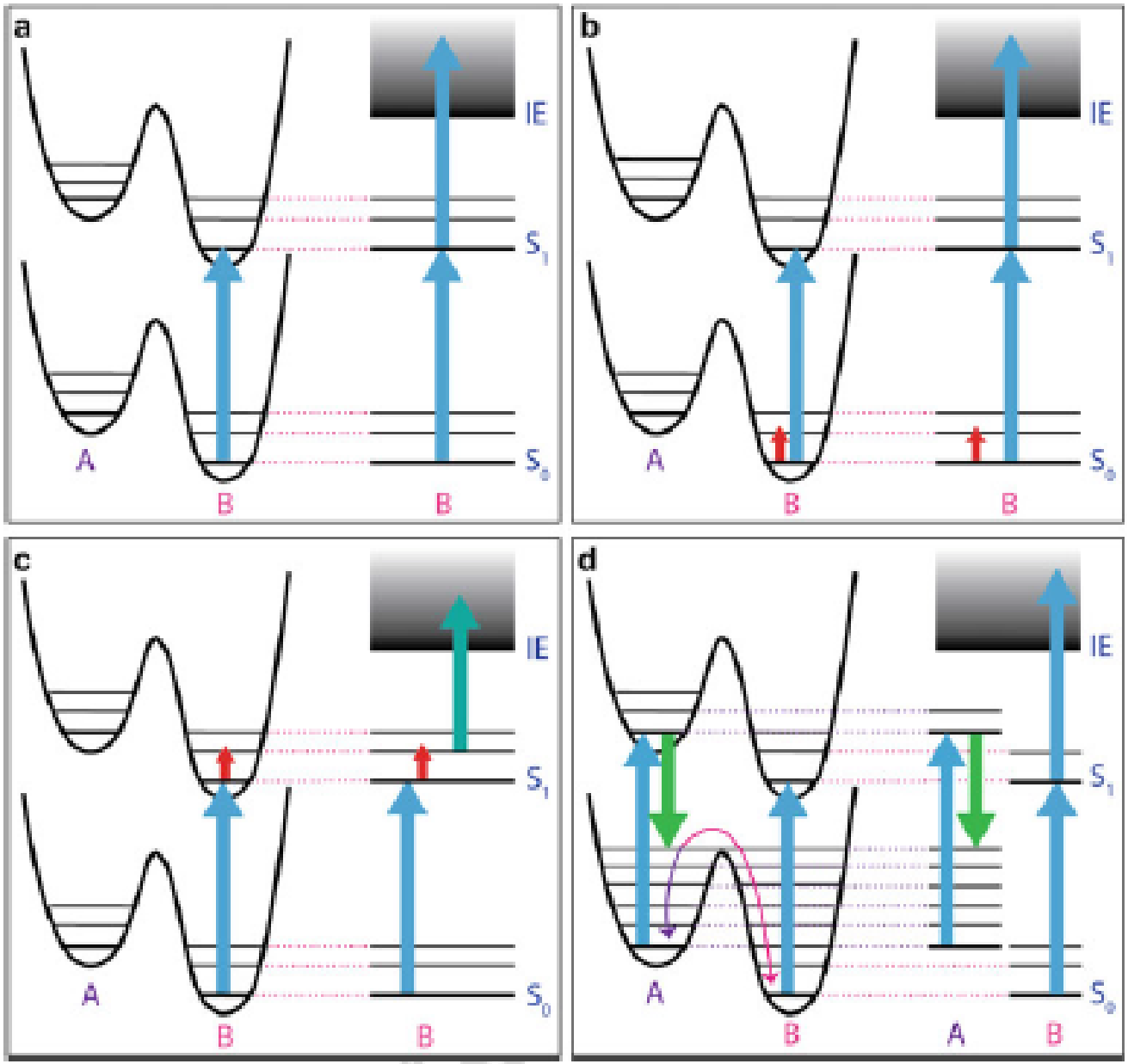
a
IE
S1
S0
A
B
B
b
IE
S1
S0
A
B
B
c
IE
S1
S0
A
B
B
d
IE
S1
S0
A
B
A
B

IR-UV ion dip spectroscopy

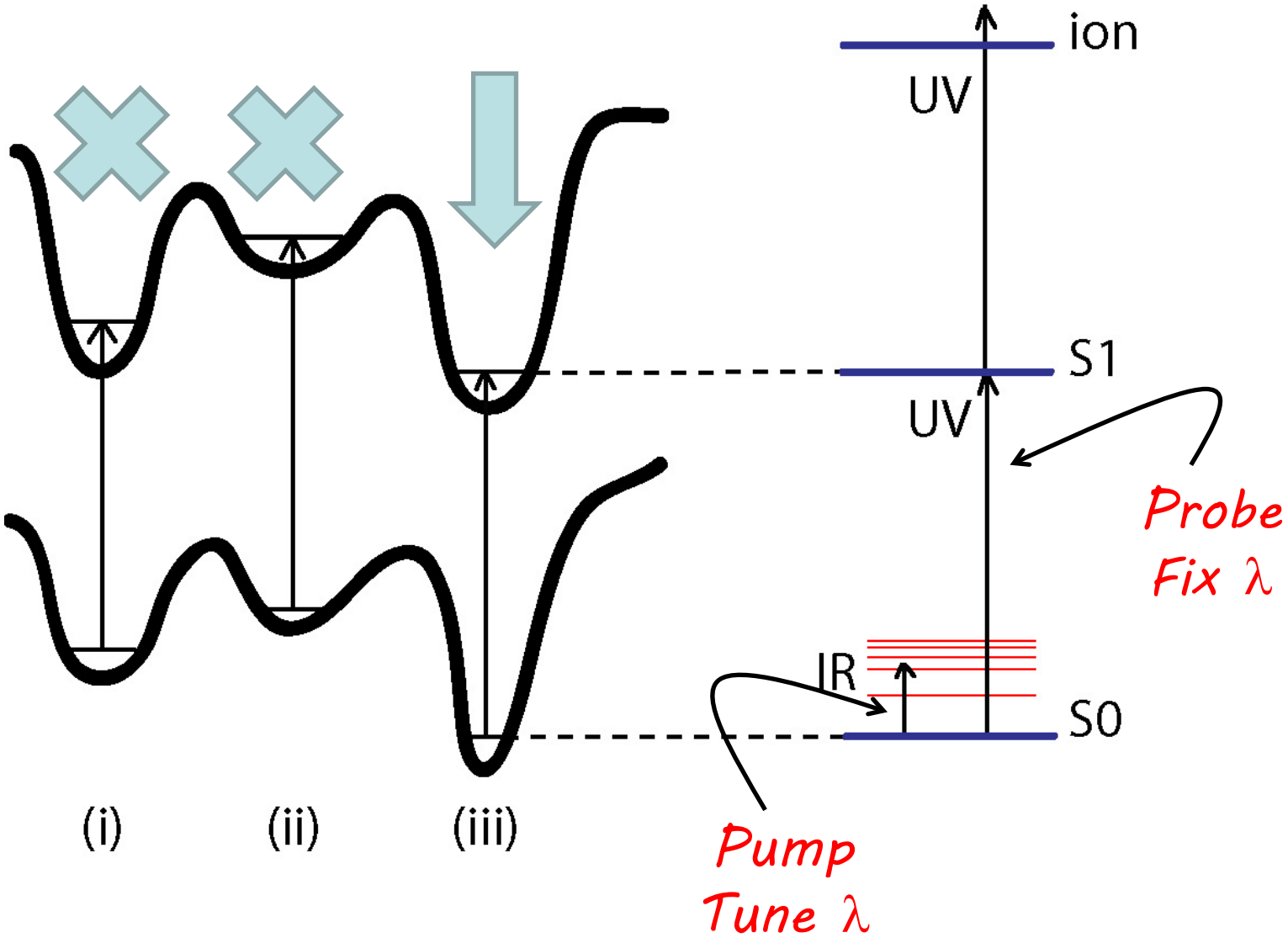

IR ion-dip spectroscopy

Combine with UV ionization (REMPI) spectroscopy

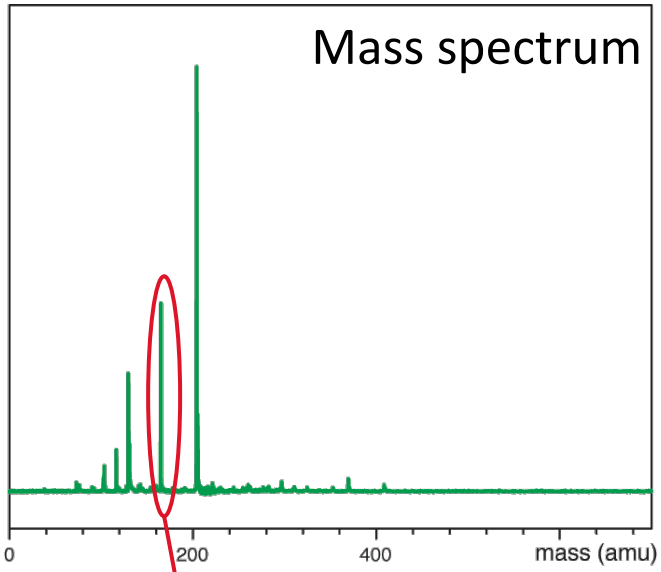

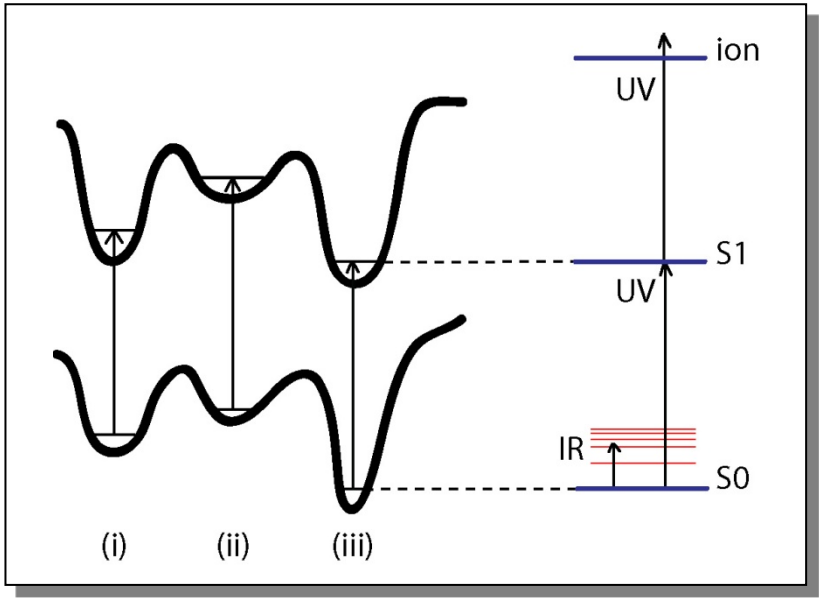

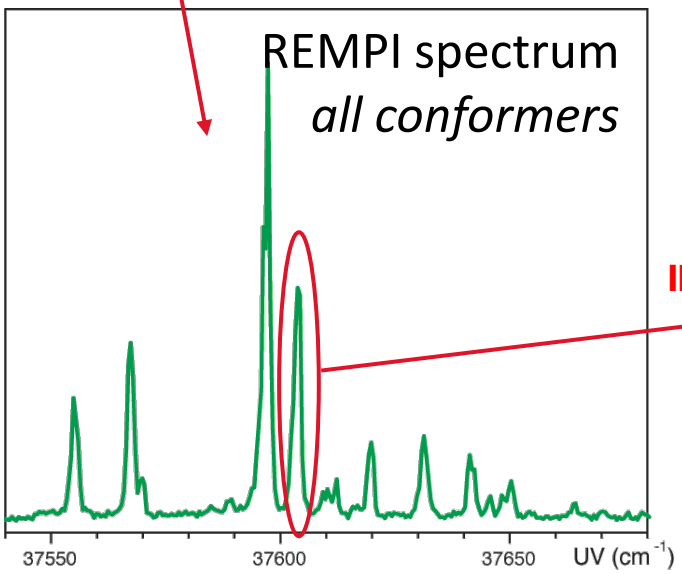

IR scan

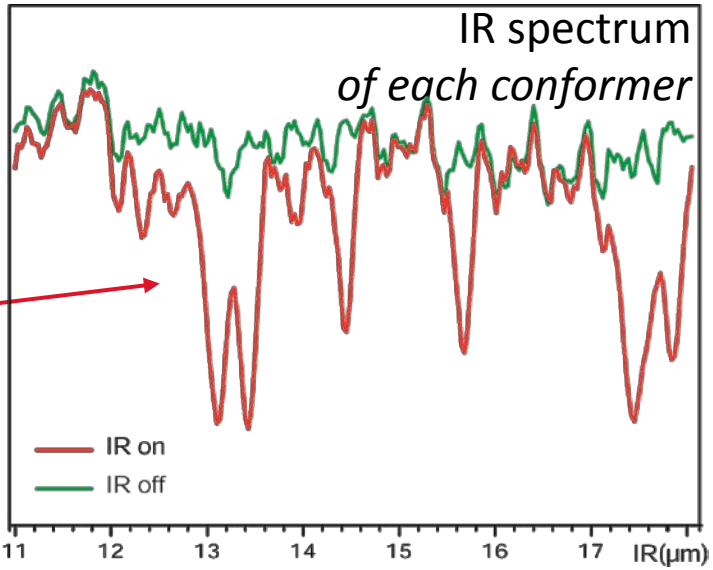

IR-UV hole-burning spectroscopy

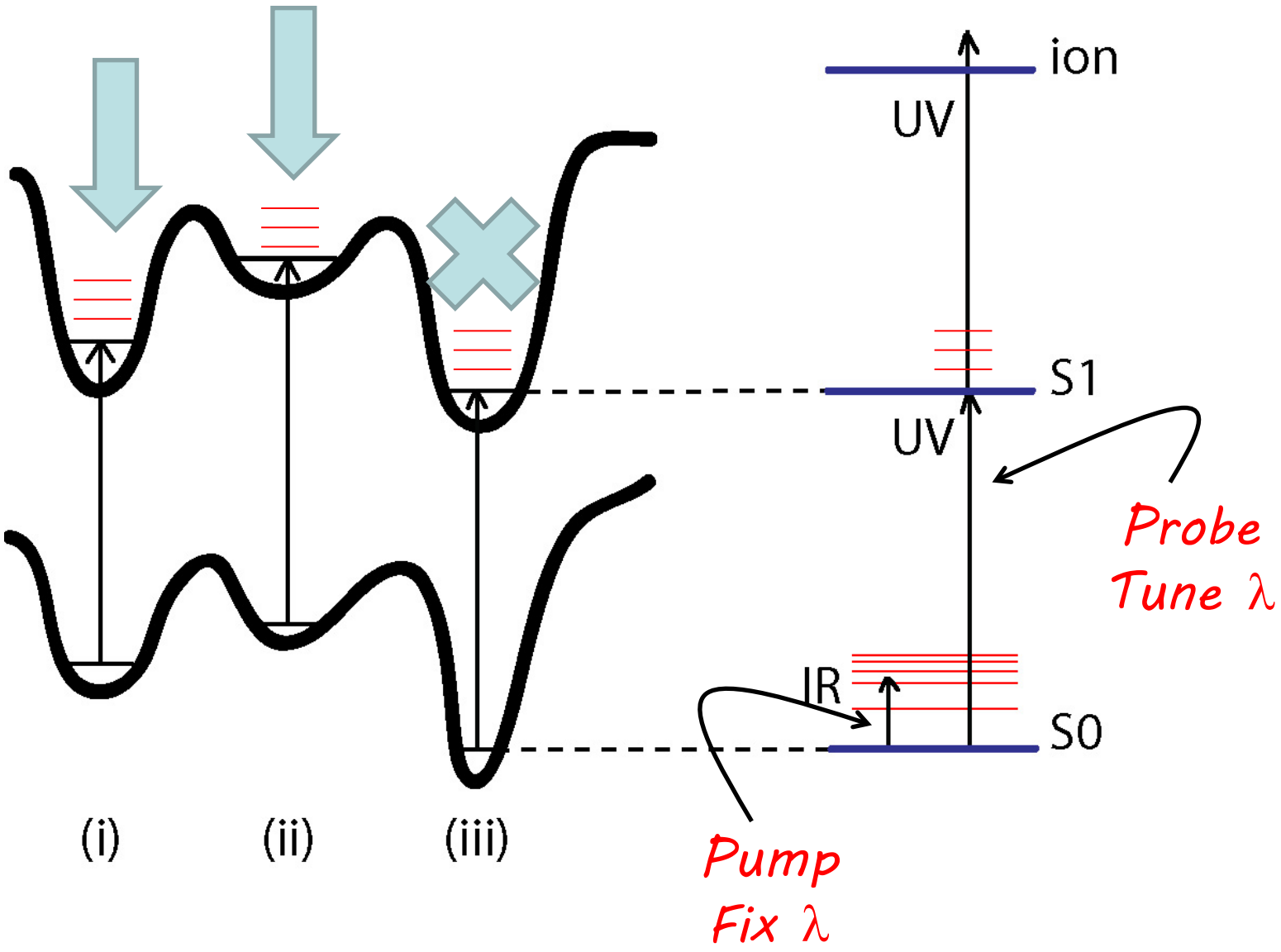

Ion dip spectroscopy

Neutral molecules in beam

Conformer selective due to UV excitation step !

Application to tryptophan

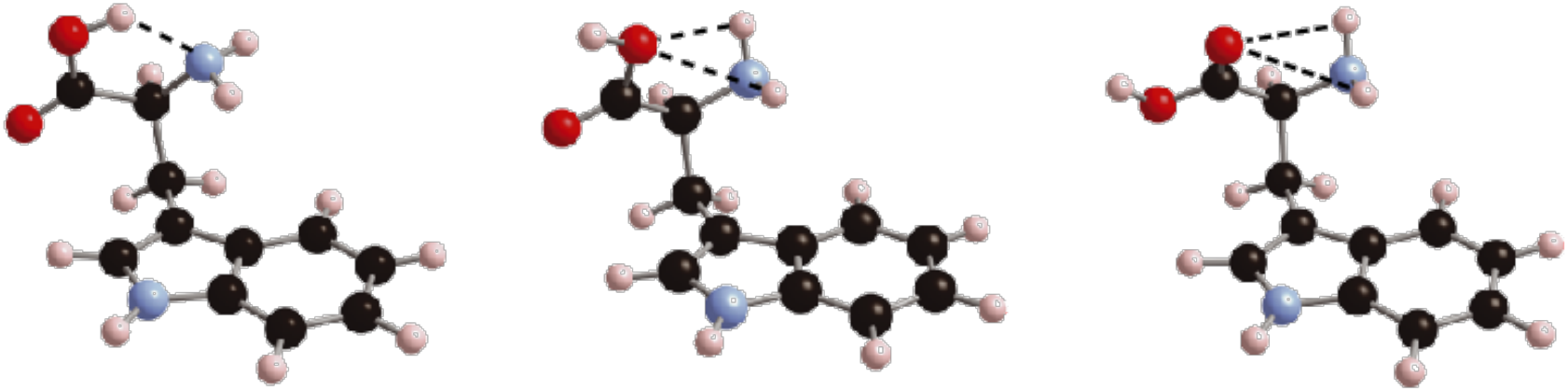

- Different conformers with different H-bonding network
- Stabilization by intramolecular hydrogen bonds
- Can we see differences in the IR spectrum ?

REMPI spectroscopy of tryptophan

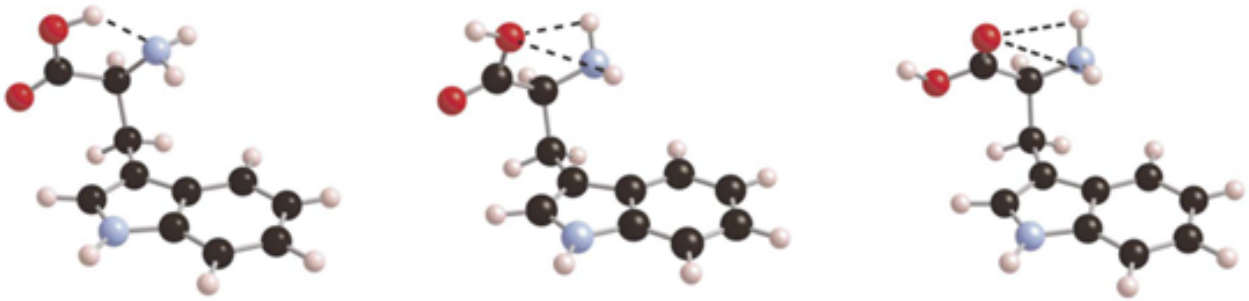

tryptophan

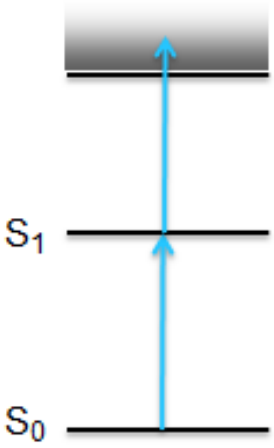

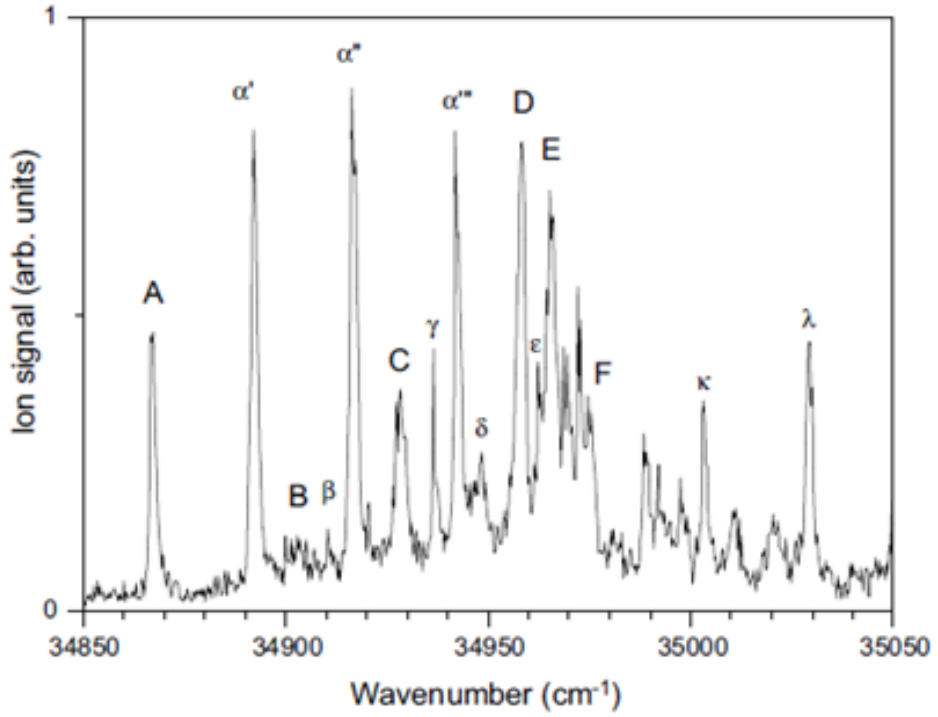

Ion dip spectroscopy of tryptophan

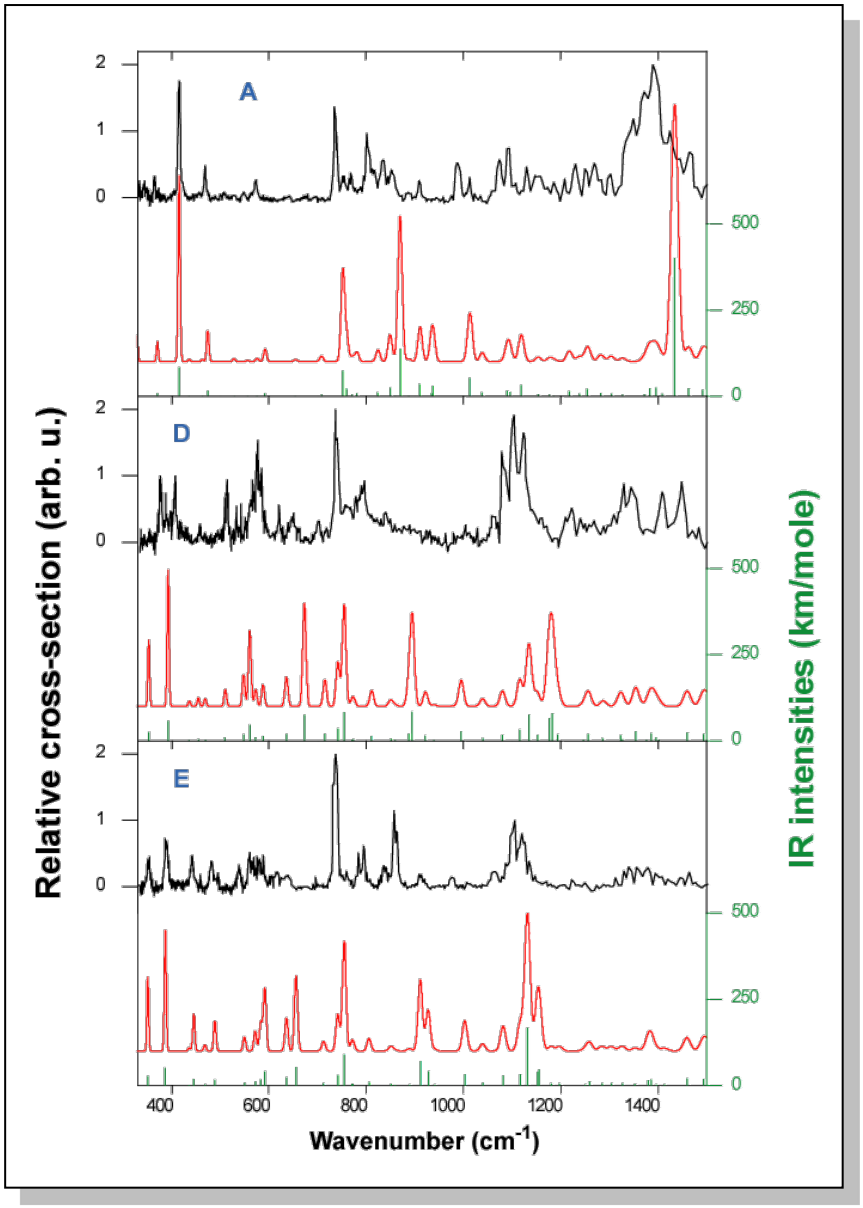

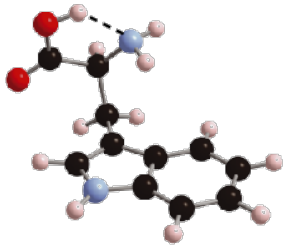

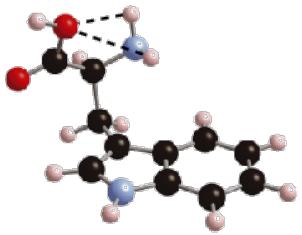

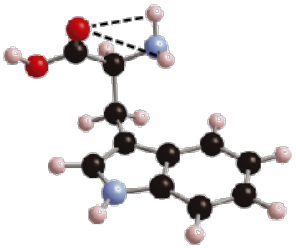

Fixed UV wavelength

Scan IR wavelength

Bakker, MacAleese, Meijer, von Helden, *Phys. Rev. Lett.* **91** 203003 (2003)

IR-VUV double resonance spectroscopy

If no chromophore is present: valine

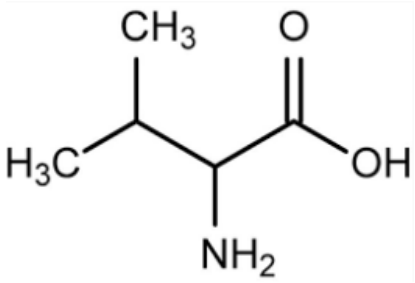

VUV
118 nm

Not conformer selective

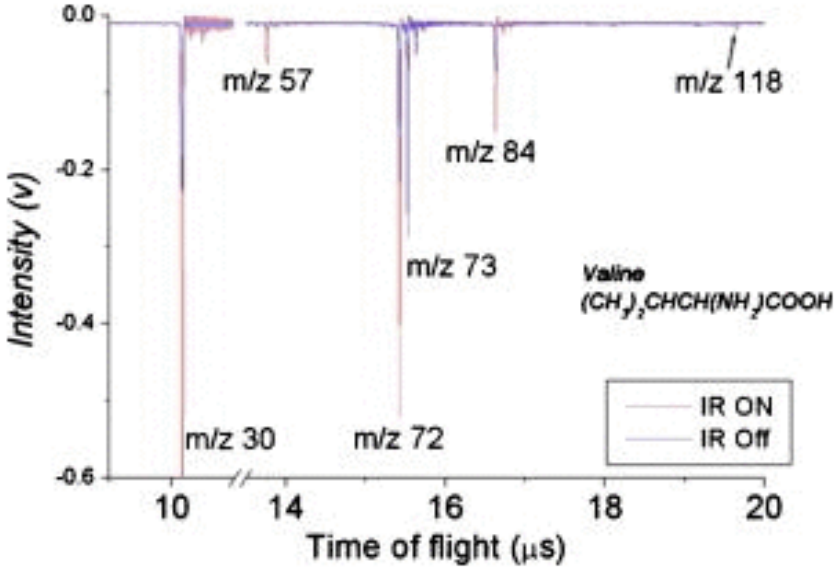

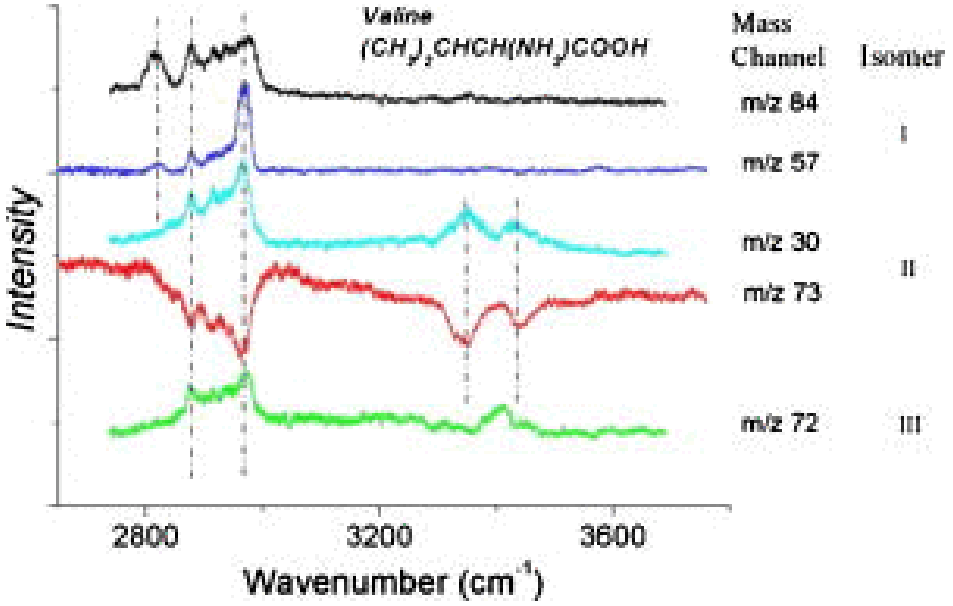

IR-VUV double resonance spectroscopy

If no chromophore is present: NMA

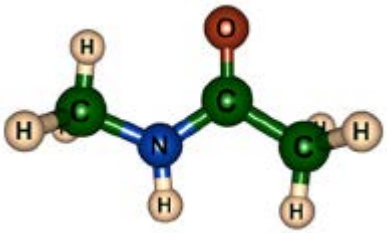

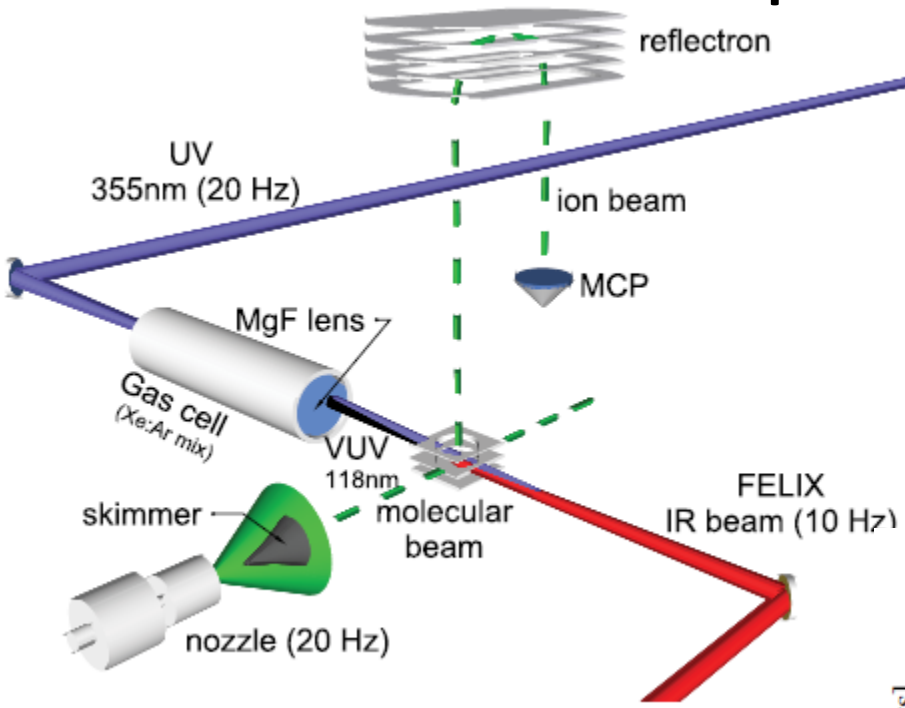

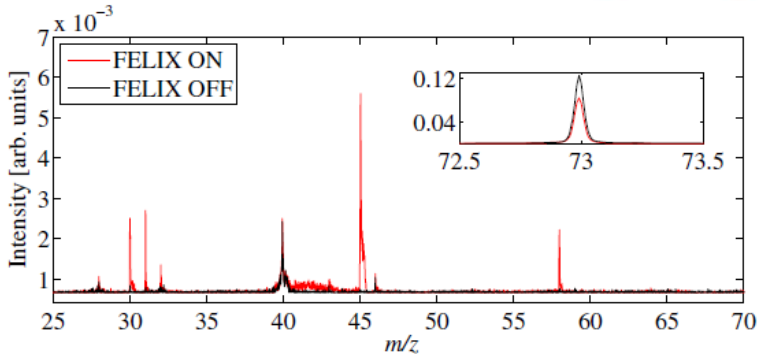

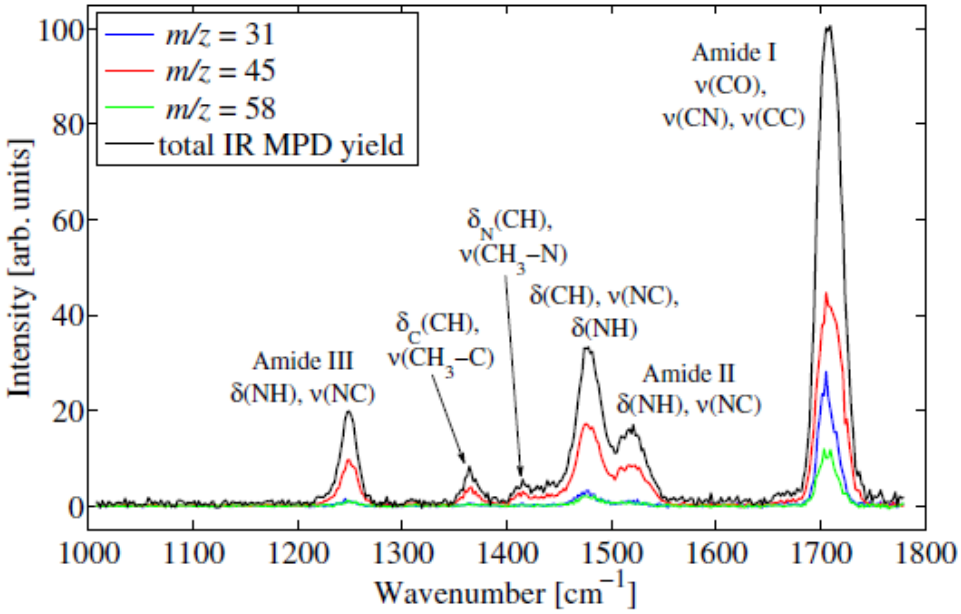

IR photodissociation
VUV ionization of fragments
Background free
No conformer selectivity

Yatsyna et al. PRL 2016

A Journal of the Gesellschaft Deutscher Chemiker
Angewandte
GDCh
International Edition
Chemie
www.angewandte.org
2014–53/14

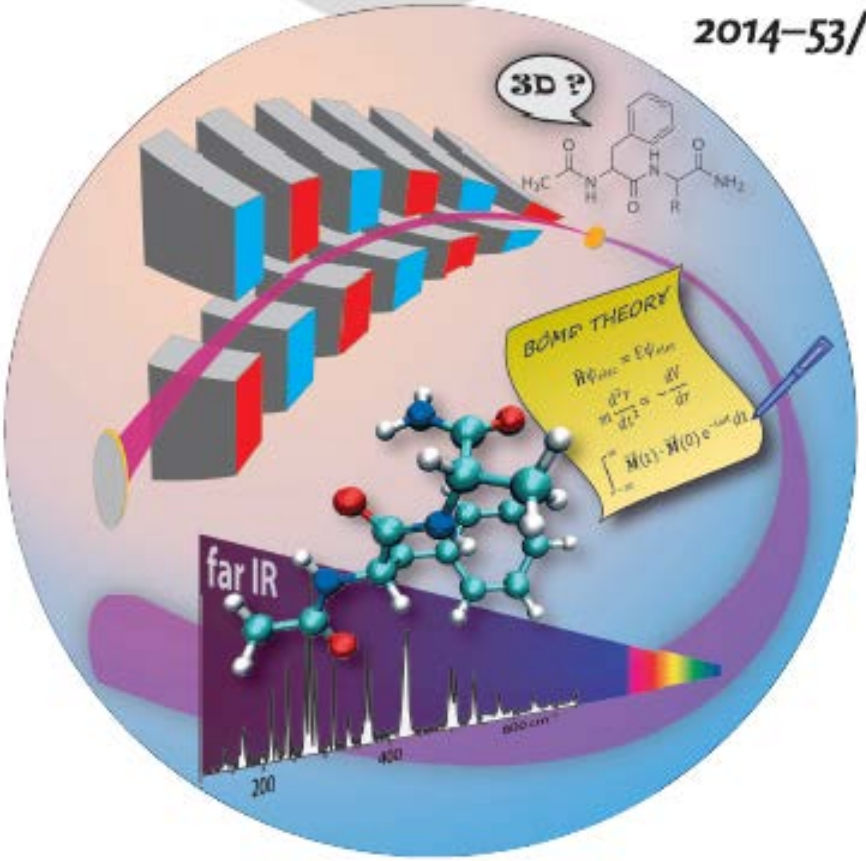

Soft vibrational modes ...

... are typically delocalized over the entire molecule. A far-infrared spectrum is therefore expected to contain detailed information on the global conformational structure of peptides. In their Communication on page 3663 ff., M.-P. Gaigeot, A. M. Rijs, and co-workers show that conformation-selective far-IR spectroscopic experiments combined with Born–Oppenheimer molecular dynamics (BOMD) simulations provide an alternative approach to decipher this information.

WILEY-VCH

Spectroscopy in far-IR

- Delocalized modes
- Shallow potentials
- Large amplitude motions

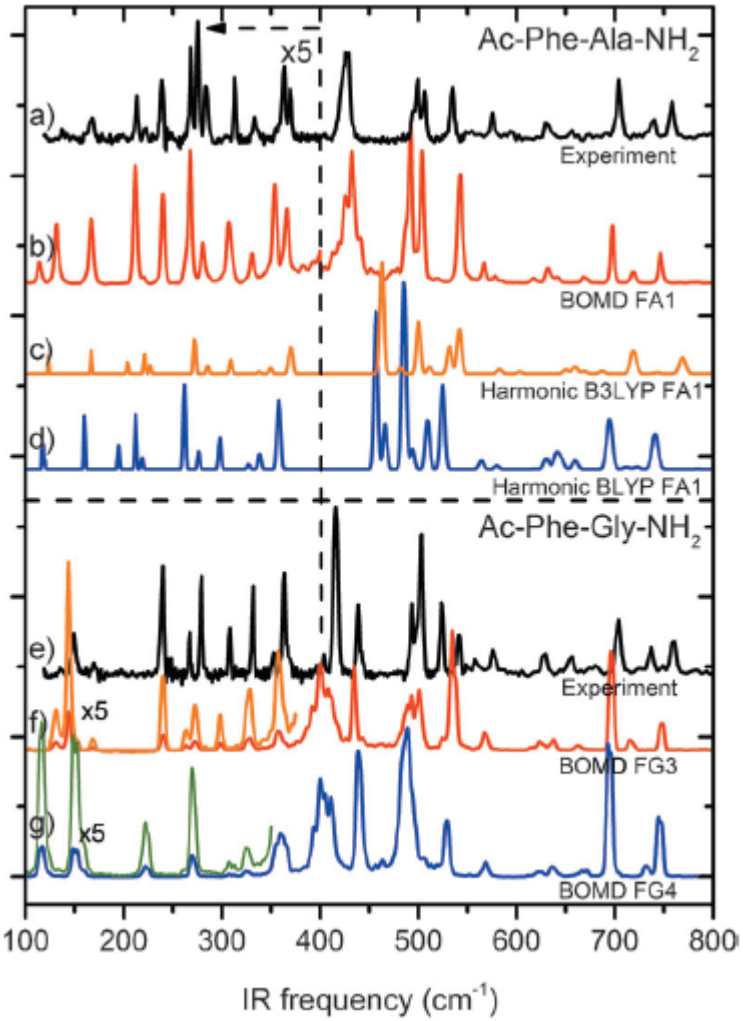

Normal modes – localized vs. delocalized

NH bend 1561 cm-1

CO stretch 1729 cm-1

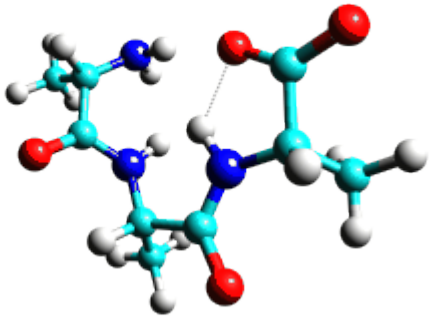

CH stretch 3094 cm-1

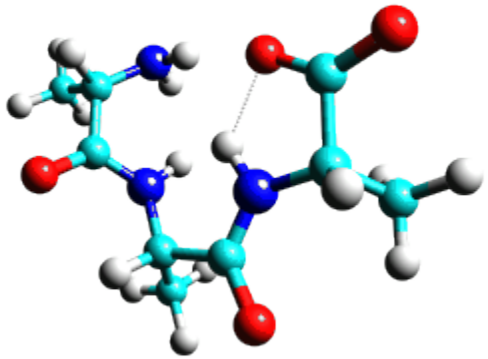

delocalized 661 cm-1

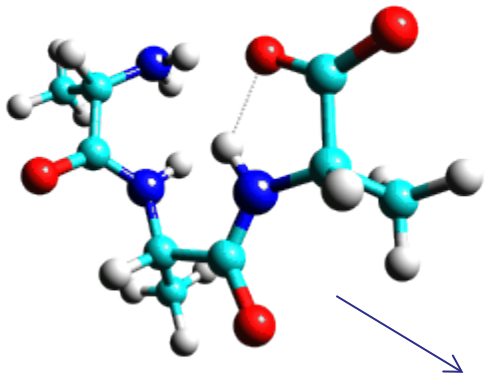

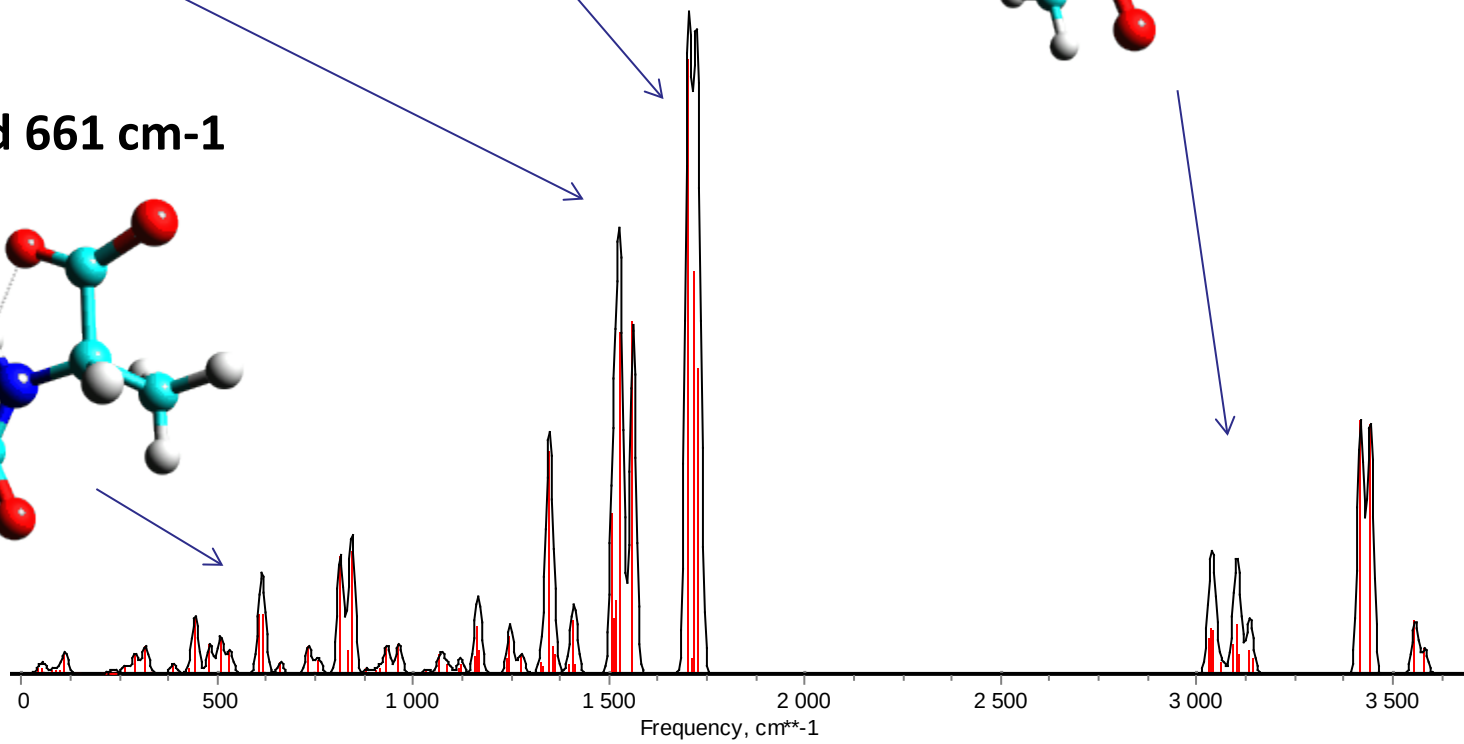

Born-Oppenheimer Molecular Dynamics

Alternative method to compute IR frequencies

$$\hat{H}_e(\mathbf{r};\mathbf{q})\Psi(\mathbf{r};\mathbf{q}) = E_e(\mathbf{q})\Psi(\mathbf{r};\mathbf{q})$$

$$-\frac{\partial E_e}{\partial q_i} = m_i \frac{d^2 q_i}{dt^2}$$

Solve t.i. Schrodinger eq for nuclear geometry ***q*** *(single point calc of electronic wavefunction)*

Determine PES derivatives to calculate new atom positions

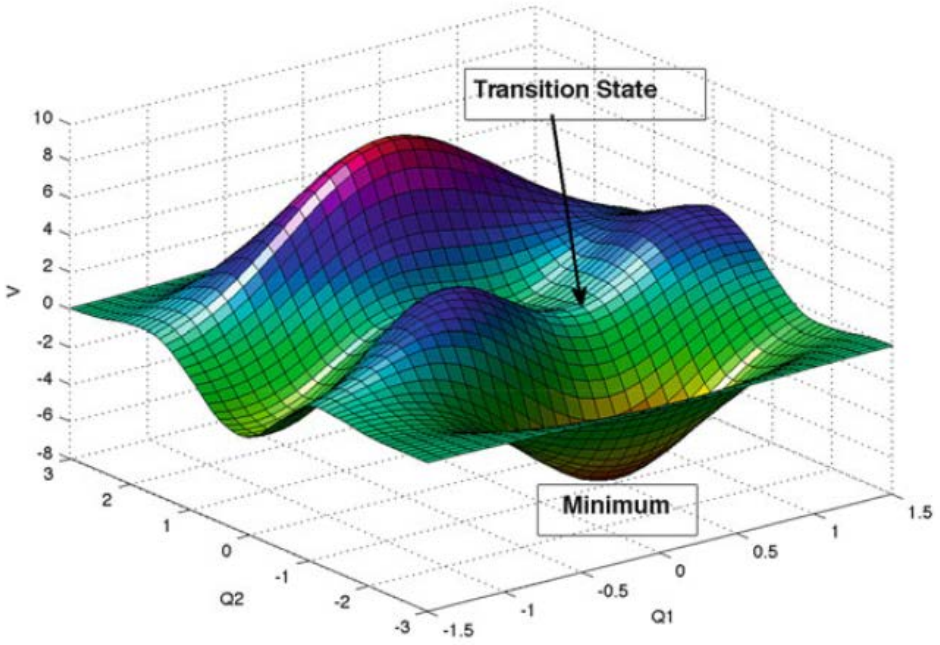

Trajectory on 'on-the-fly' calculated PES

Take FT of fluctuating dipole moment over trajectory

$$I(\omega) = \frac{2\pi\beta\omega^2}{3cV}\int_{-\infty}^{\infty} \mathrm{d}t \langle \delta\mathbf{M}(t)\cdot\delta\mathbf{M}(0)\rangle \exp(i\omega t)$$

Probing dynamics

Finding the barriers between different conformers

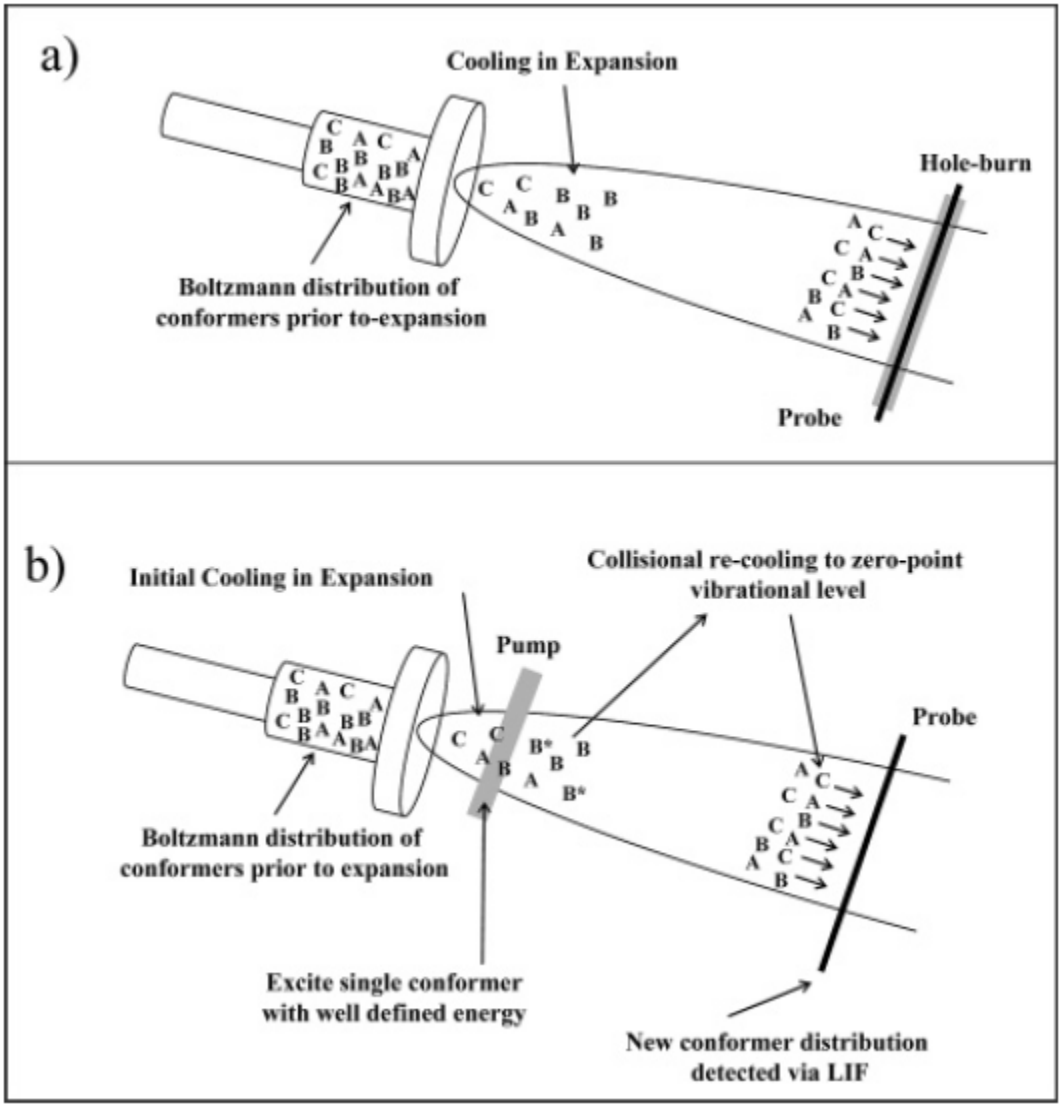

LIF spectrum
no pump

Difference
spectra
pump
on/off

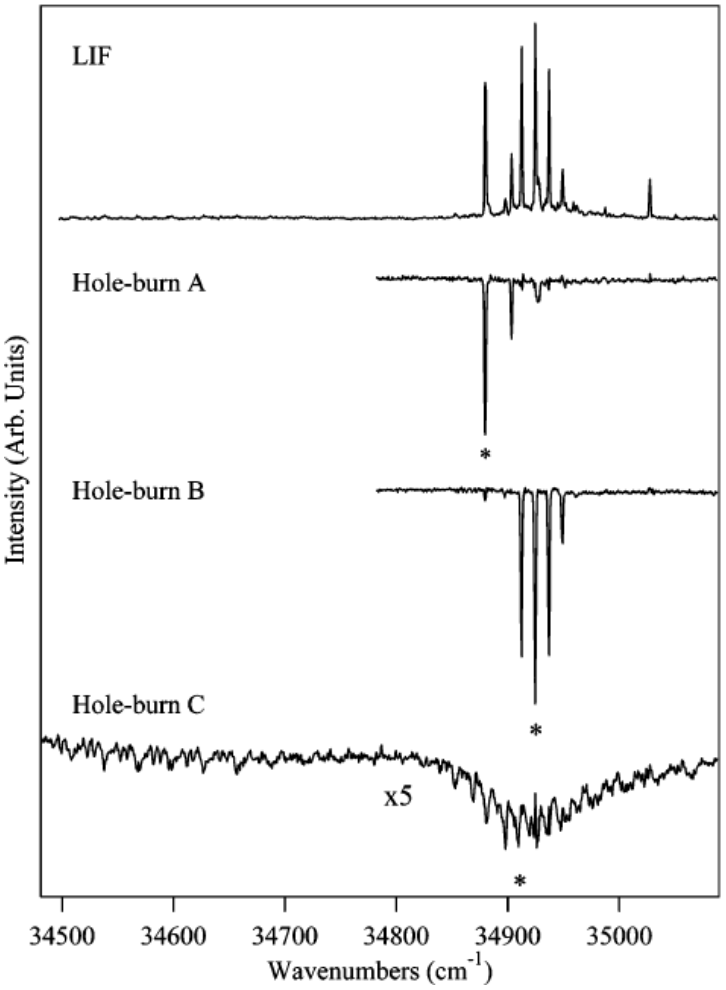

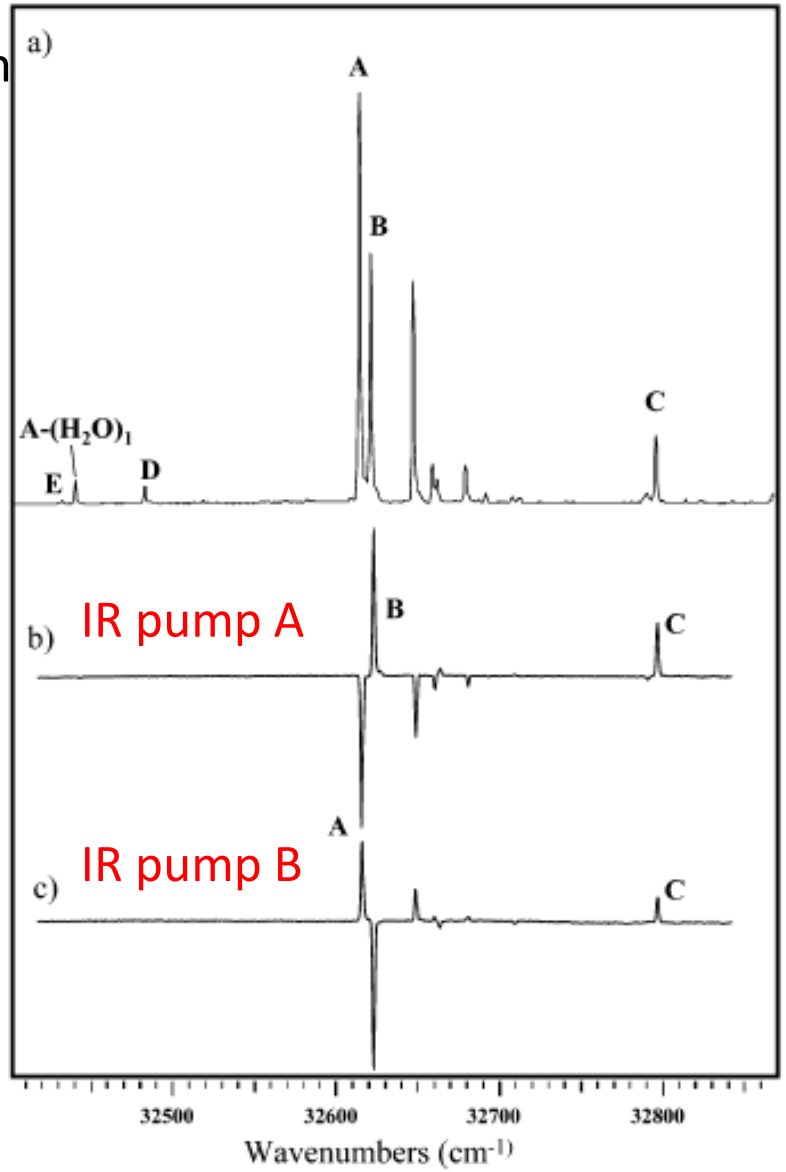

Figure 5. (a) LIF spectrum of melatonin and (b), (c) IR−UV hole-filling spectra following conformation-selective excitation of conformers A and B with the infrared laser, respectively. [Reproduced from ref 74, with permission. Copyright 2004 AAAS.]

Probing dynamics

Finding the barriers between different conformers

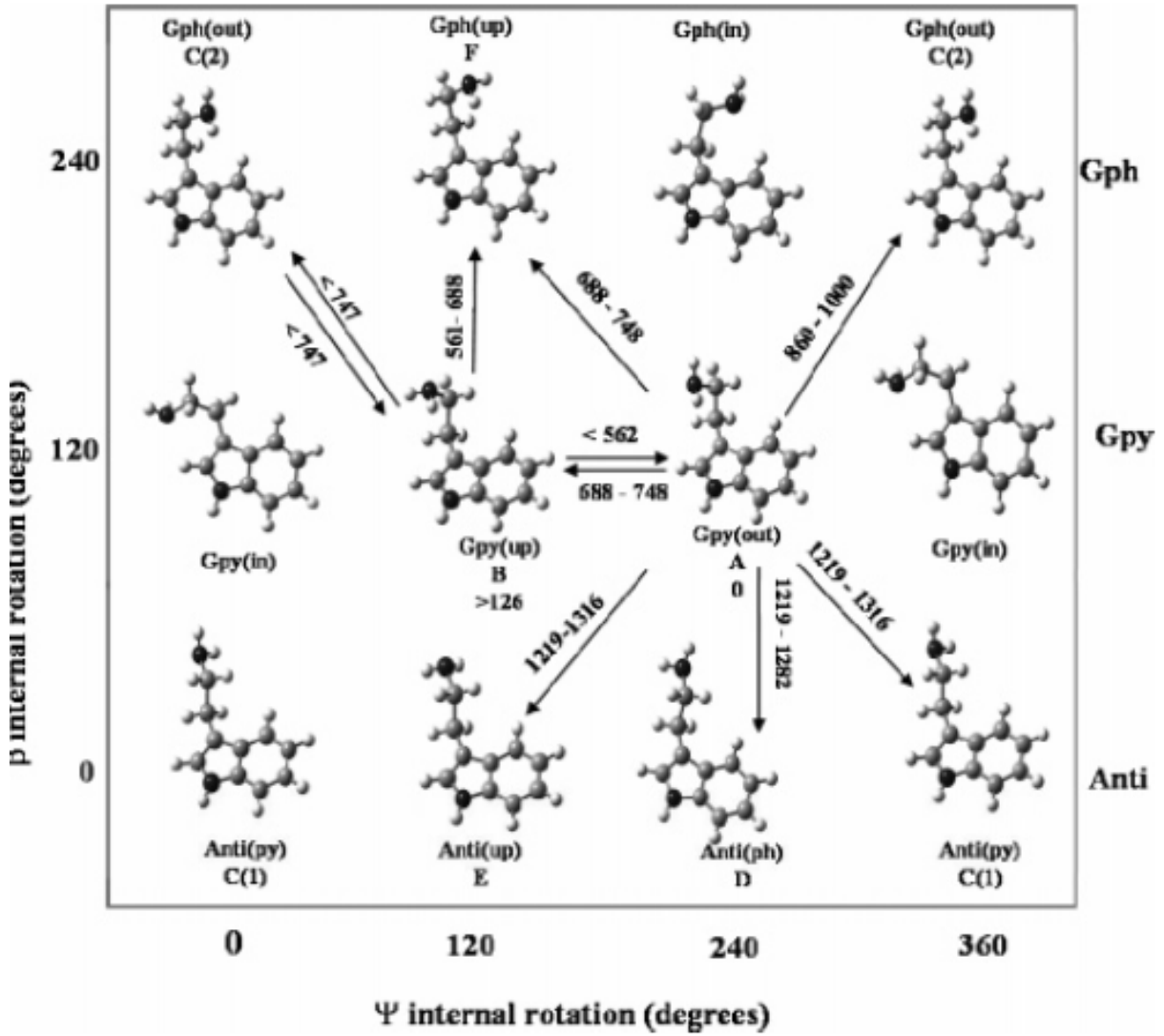

Mass spectrometers

Determine molecular weight based on trajectories of ionized molecule in electric or magnetic field

Using E- and B-fields to measure molecular weights

Forces

Gravitational force can be ignored!

$F = ma = q(E + vB)$

where q = charge

E = electrical field

v = velocity

B = magnetic field

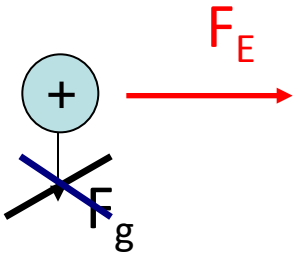

$F_E >> F_g$

$F_L >> F_g$

Gravitational force: $F_g = mg$ = atomic mass x 1.66×10^{-27} [kg] x 9.8 [m/s^2] ≈ **10^{-26}** x amu [N]

Electrical force: $F_E = qE = 1.602 \times 10^{-19}$ [C] x E-field [V/m] ~ **10^{-19}** x field [N]

Lorentz force: $F_L = qvB = 1.602 \times 10^{-19}$ [C] x 400 [m/s] x B-field [T] ~ **10^{-16} N** x B-field [N]

Time-of-flight (TOF) mass spectrometer

Wiley McLaren type

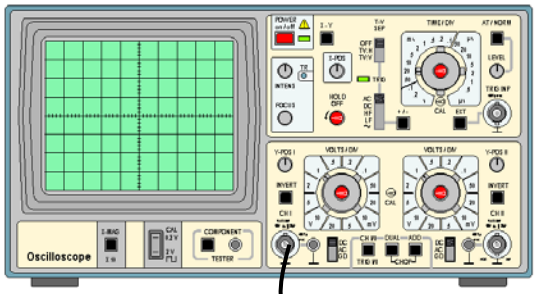

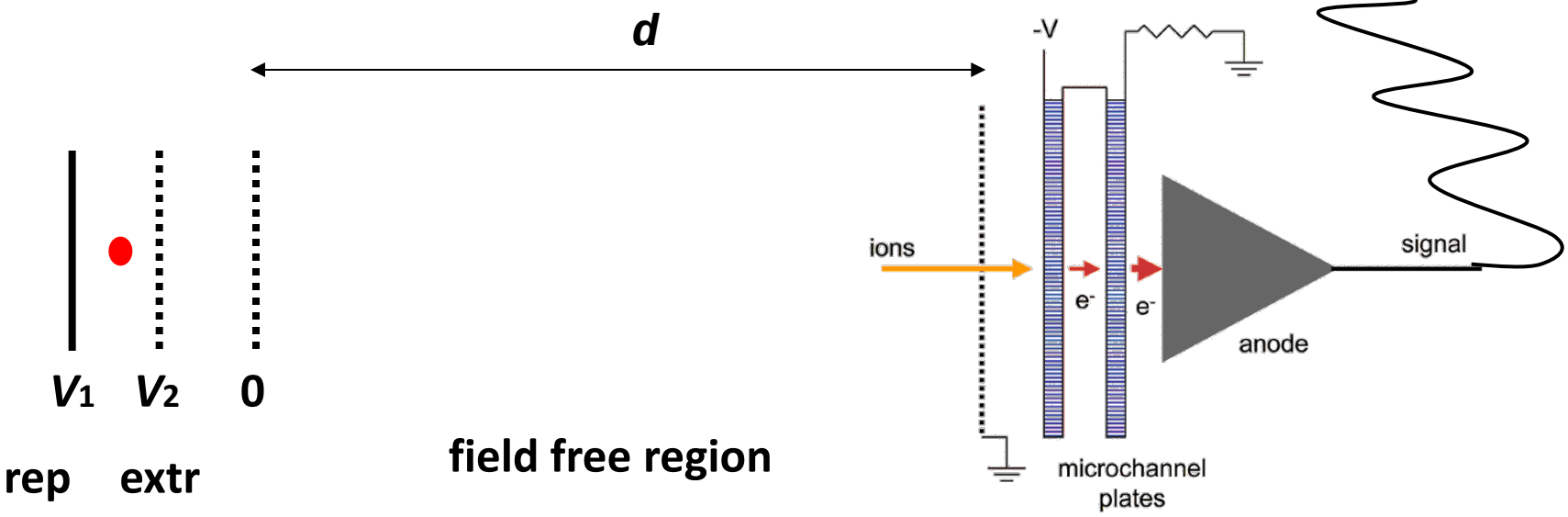

$V_1 > V_2$

MCP detector

$$E_p = qU = E_k = \frac{1}{2}mv^2 \quad , \quad U = (V_1+V_2)/2$$

$$\rightarrow \quad v = \sqrt{\frac{2qU}{m}} \qquad t = \frac{d}{\sqrt{2U}}\sqrt{\frac{m}{q}}$$

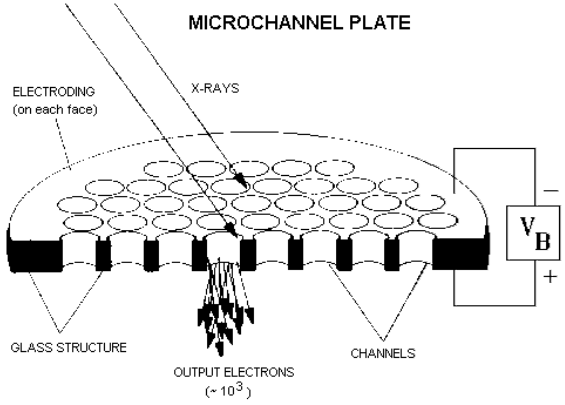

Wiley McLaren type TOF

Space focusing

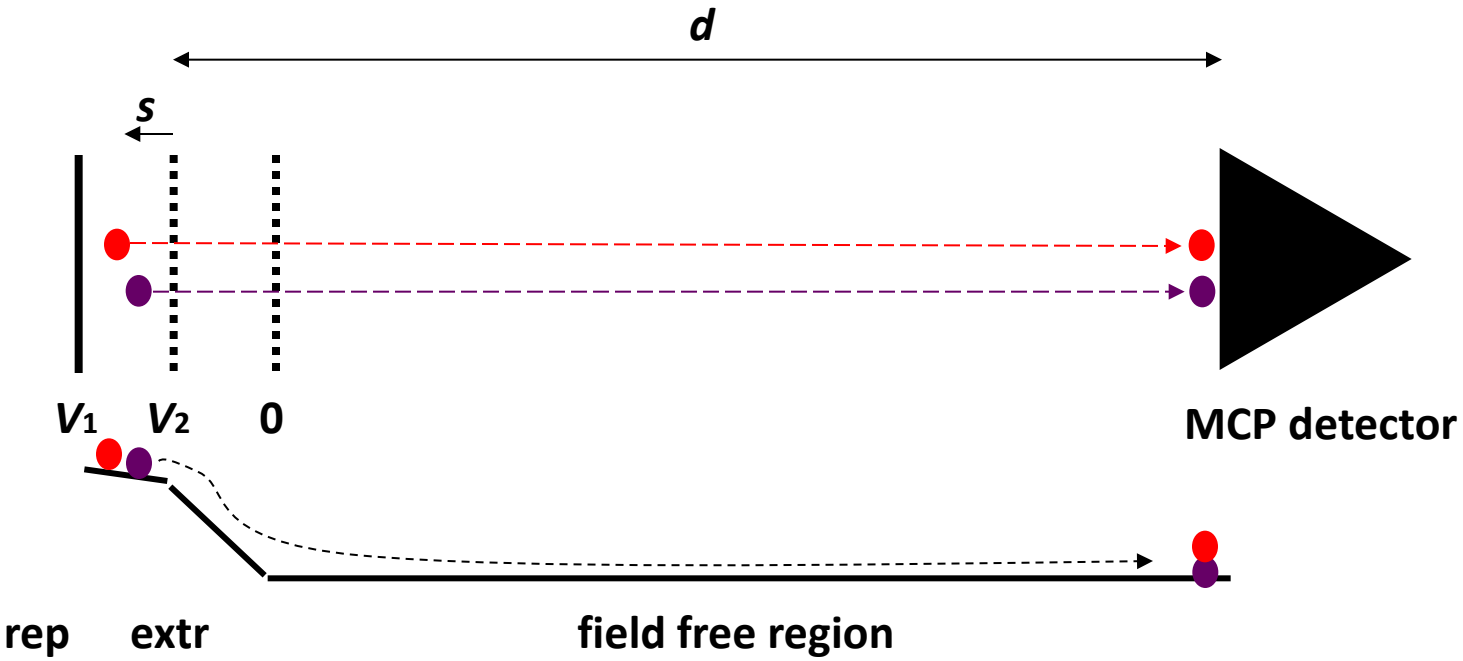

$dt/ds = 0$ ➡ V_1/V_2 : space focusing

Space focusing corrects for spread in kinetic energy

Wiley, McLaren, *Rev. Sci. Instrum.* **26**, 1150 (1955)

Lorentz force

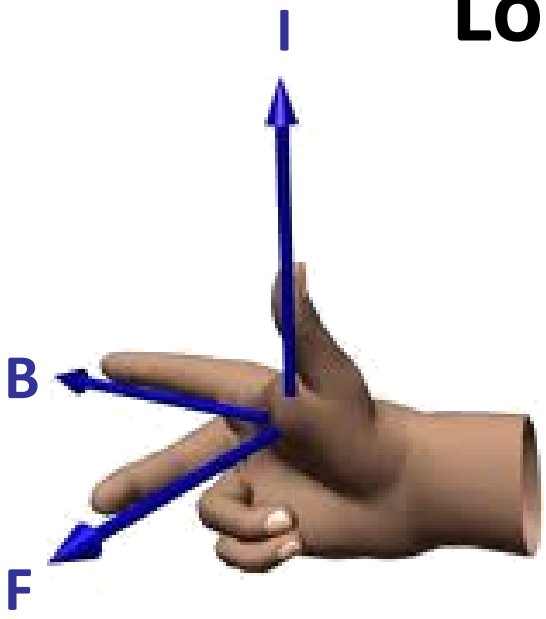

Right-hand rule (for + ions)
Thumb: ion velocity **v**
Index: magnetic field **B**
Middle finger: Lorentz force $\mathbf{F_L}$

$$\vec{F}_L = q\vec{v} \otimes \vec{B}$$

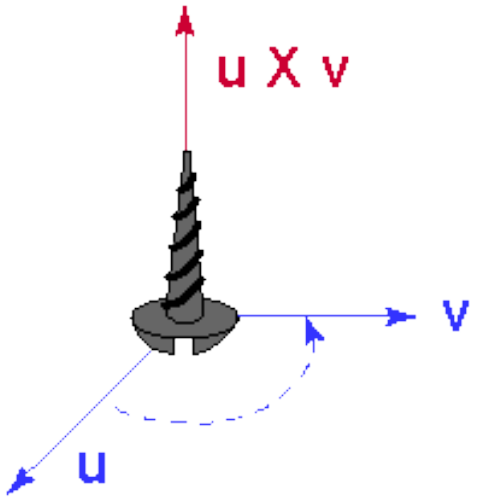

Absolute value only:

$$F_L = qvB(\sin\alpha)$$

α = angle between **v** and **B**
$\alpha = 90^o \rightarrow \sin(90^o) = 1$

Ions moving in B-field

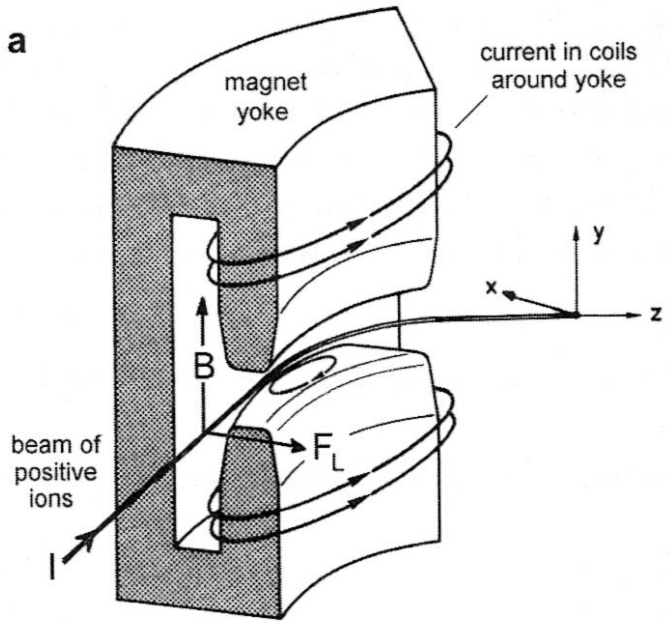

$\mathbf{F_L}$ always perpendicular to **v**
→ ion traverses a circular path

$$F_L = qvB = F_C = \frac{m\,v^2}{r}$$

F_C=centripetal force

$$r = \frac{m\,v}{qB}$$

<u>Momentum</u> – magnetic sector is a momentum analyzer

Remember from TOF: $v = \sqrt{\frac{2qU}{m}}$

$$\frac{m}{q} = \frac{r^2 B^2}{2U}$$

Select KE with electrostatic analyzer (ESA)

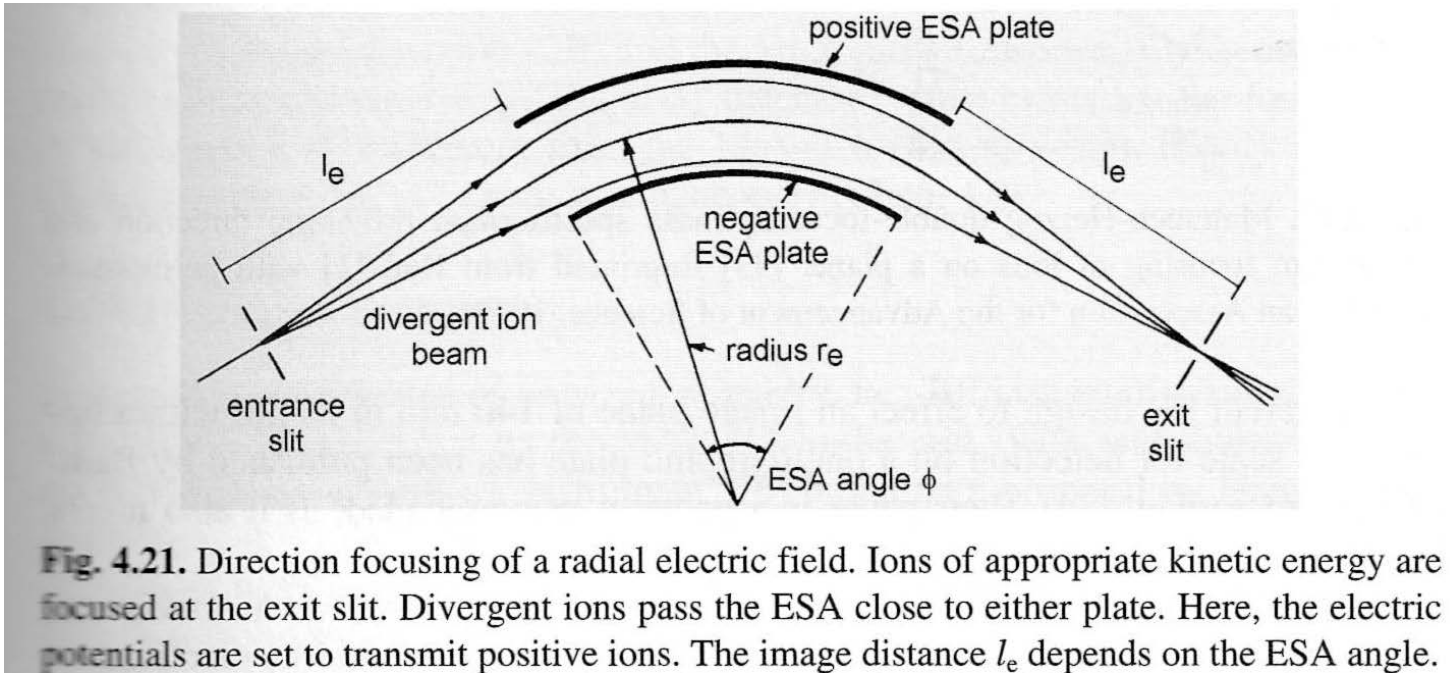

Fig. 4.21. Direction focusing of a radial electric field. Ions of appropriate kinetic energy are focused at the exit slit. Divergent ions pass the ESA close to either plate. Here, the electric potentials are set to transmit positive ions. The image distance l_e depends on the ESA angle.

$$F_e = qE = F_C = \frac{m\,v^2}{r}$$

Kinetic energy selector

$$r = \frac{m\,v^2}{qE}$$

substituting $v = \sqrt{\frac{2qU}{m}}$ gives $r = \frac{2U}{E}$

Double-focusing sector instruments

'Forward' geometry: first electrostatic, then magnetic (EB)

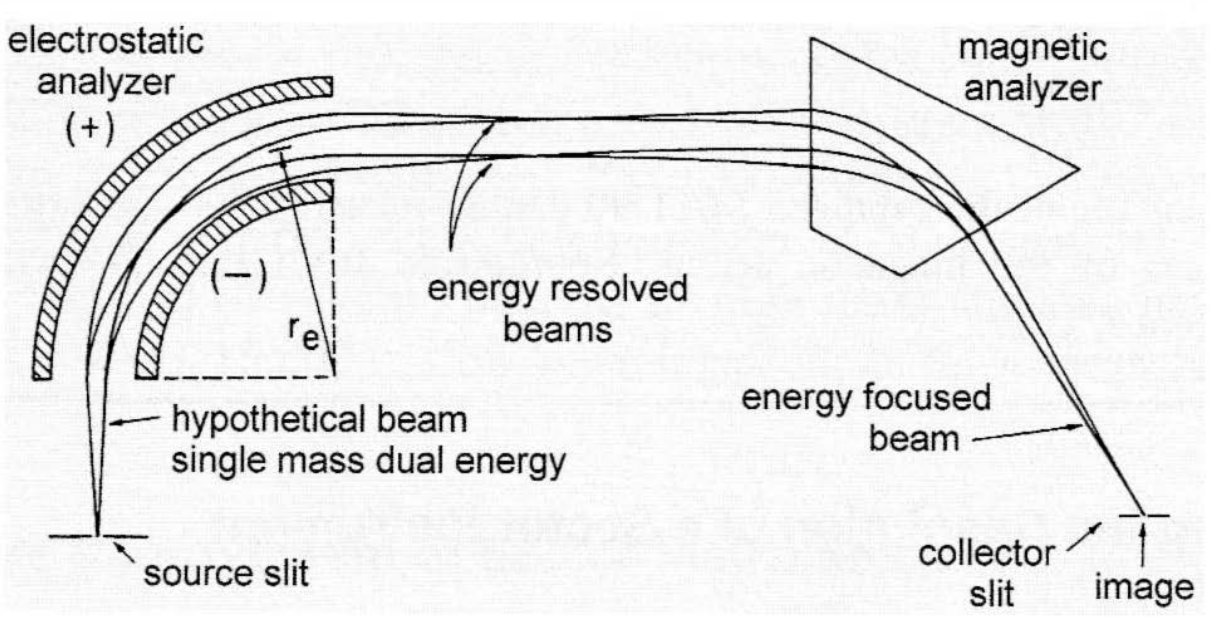

Nier-Johnson geometry

No slit after electrostatic analyzer

R>10,000 possible

Fourier transform ion cyclotron resonance

FTICR MS

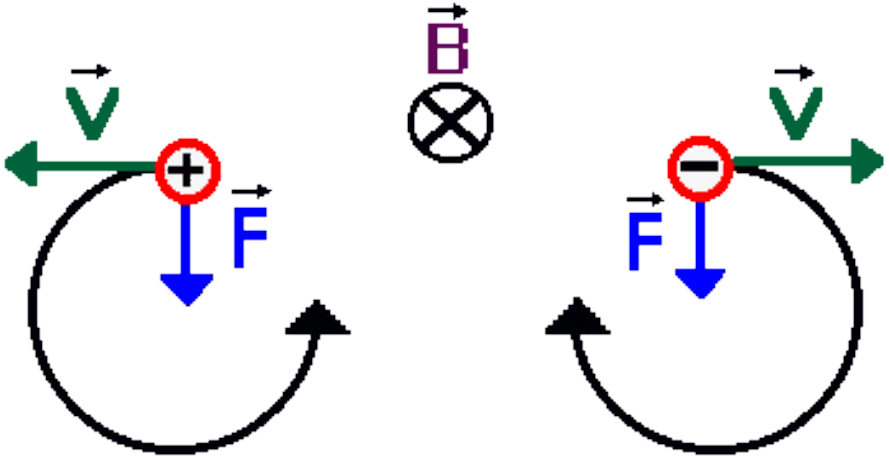

Lorentz force

$$qvB = m \cdot \frac{v^2}{r}$$

$$v = \omega \cdot r$$

$$\omega = \frac{qB}{m}$$

ω=angular frequency of the ion (rad s^{-1})
q=charge (C)
B=magnetic field strength (T)
m=mass (kg)

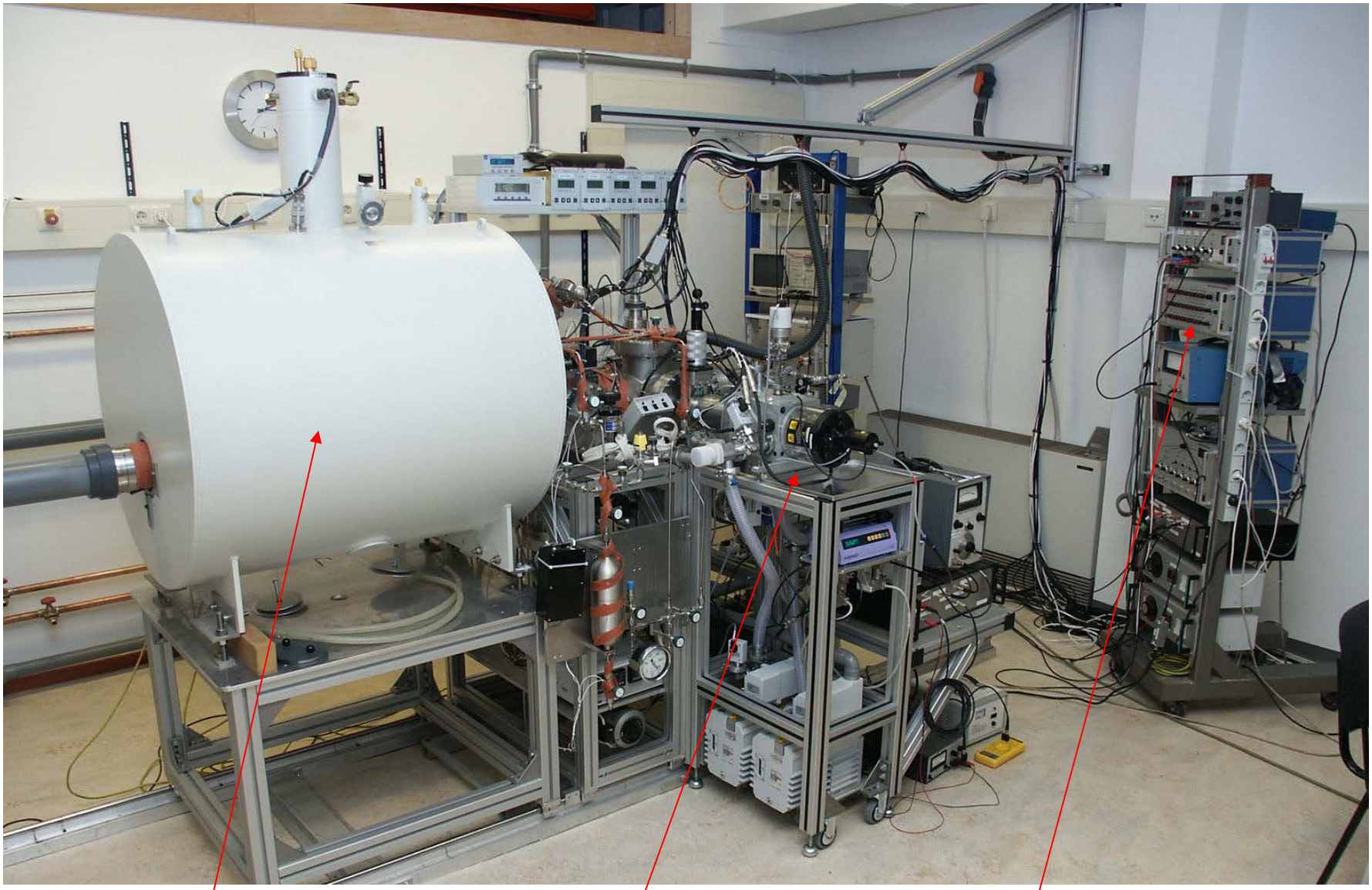
4.7 T actively shielded magnet
ESI source (Z-Spray)
Ion optics controls

Excitation and Detection of the ions

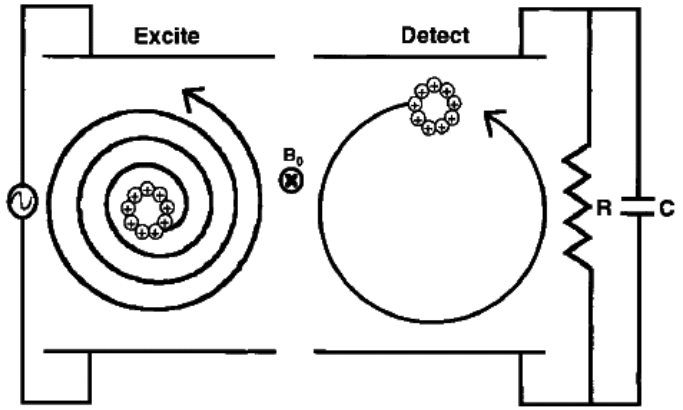

Initial cyclotron radius is very small and ions have a random phase

→ **excite**

coherent motion of ion packet induces image current between two oppositely placed electrodes

→ **detect**

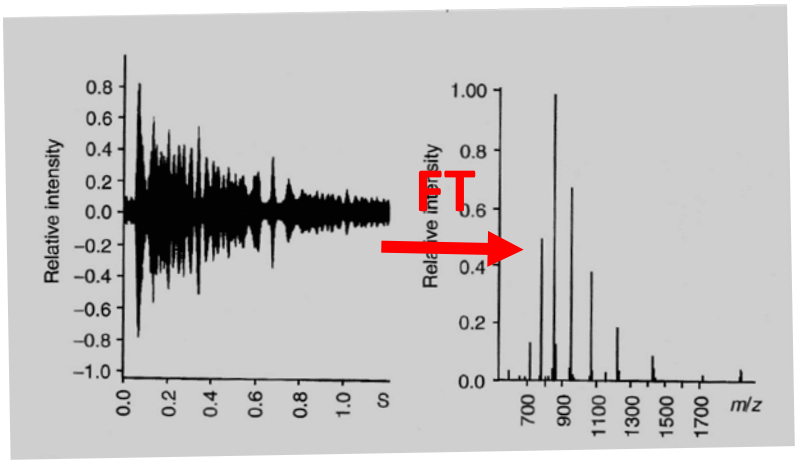

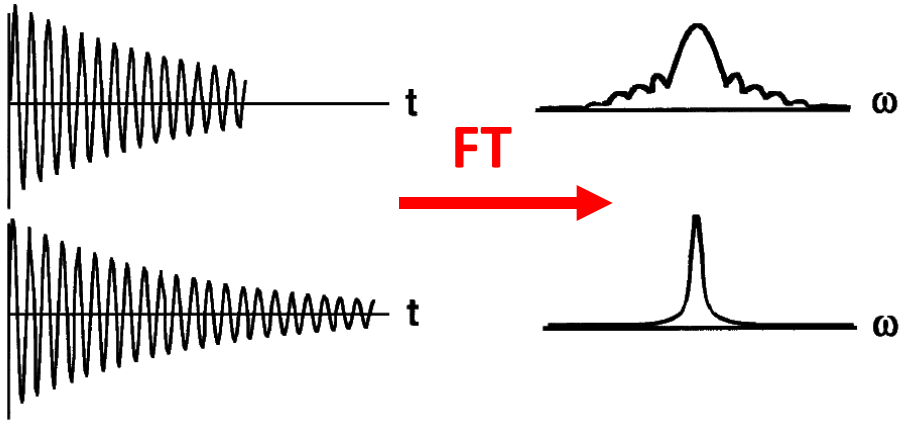

Excitation and Detection of the ions

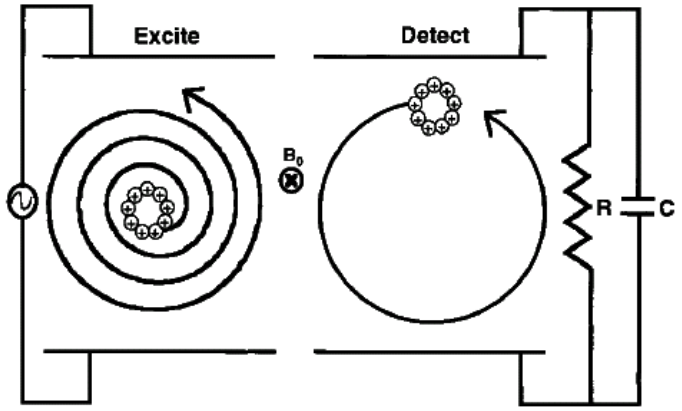

Mass-selective excitation also for ion manipulation:

1. Collisional activation
2. ejection

$$r = \frac{V_{p-p} T_{\text{excite}}}{2dB_0}$$ (S.I. units).

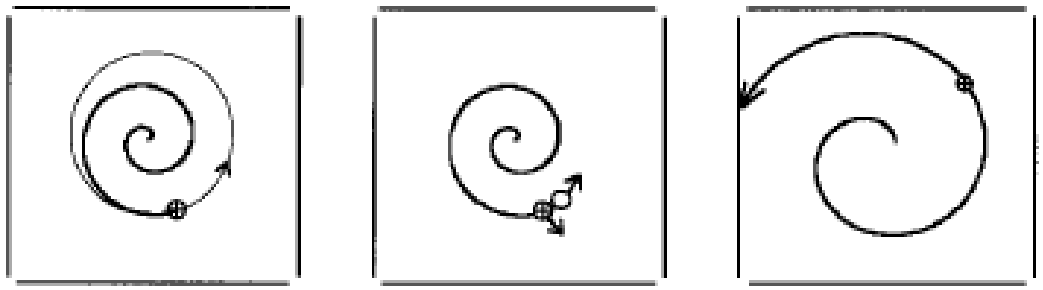

FIGURE 5. Uses for ion cyclotron excitation. Left: Acceleration of ions to form a spatially coherent packet at detectable orbital radius. Middle: Increase in ion kinetic energy to above the threshold for collision-activated dissociation or reaction. Right: Ejection of ions of a given mass-to-charge ratio.

Resolution and accuracy

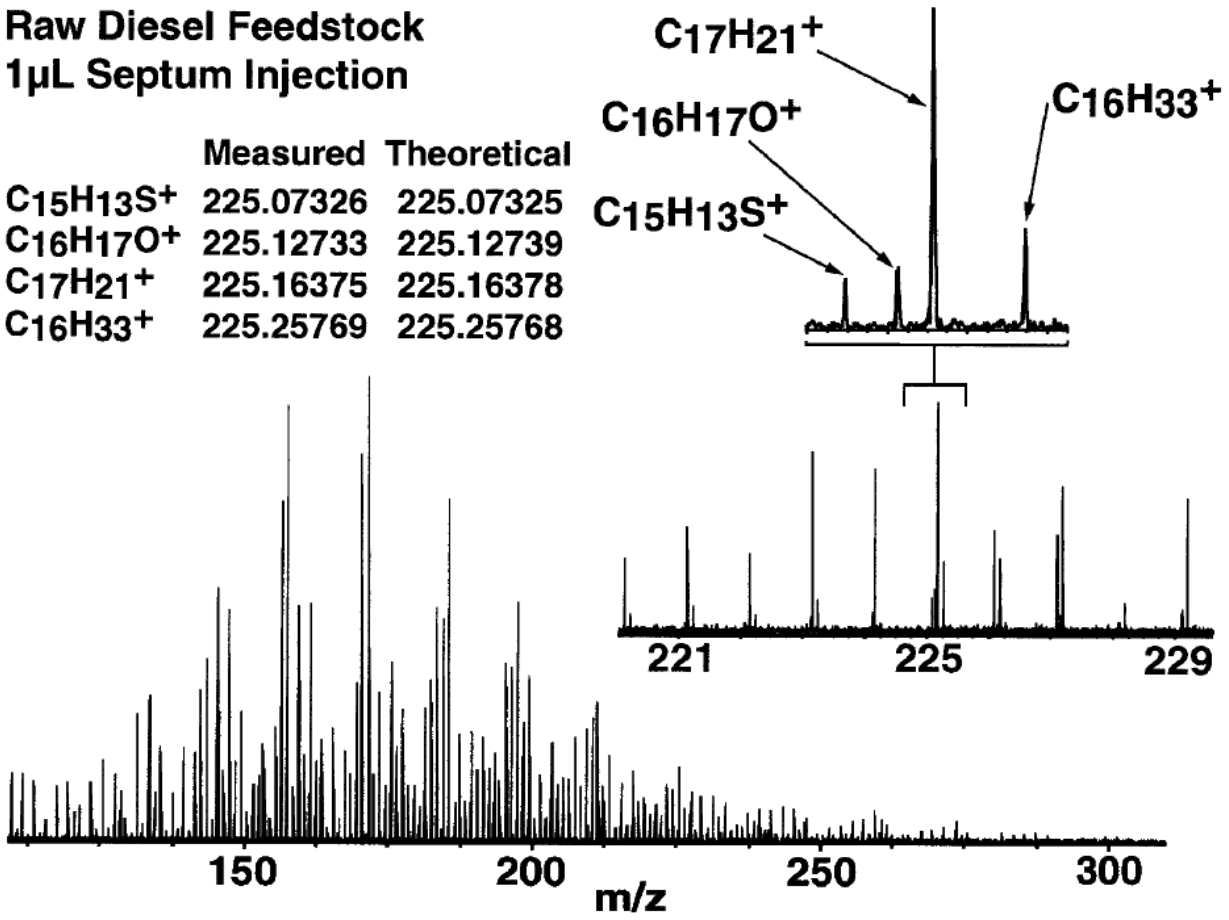

Same nominal mass, but different elemental formulae. e.g. to determine S-content in crude oil

Marshall et al.
NHMFL, Tallahassee, FL

Quadrupole mass analyzer

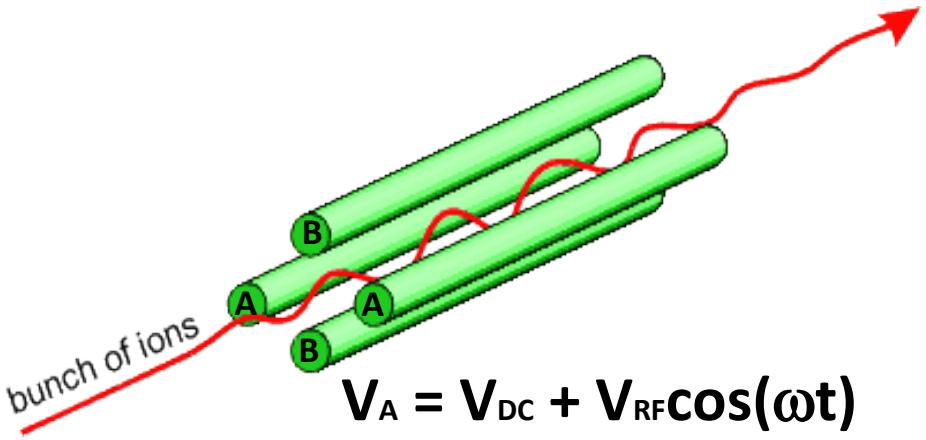

$V_A = V_{DC} + V_{RF}\cos(\omega t)$

$V_B = -V_{DC} - V_{RF}\cos(\omega t)$

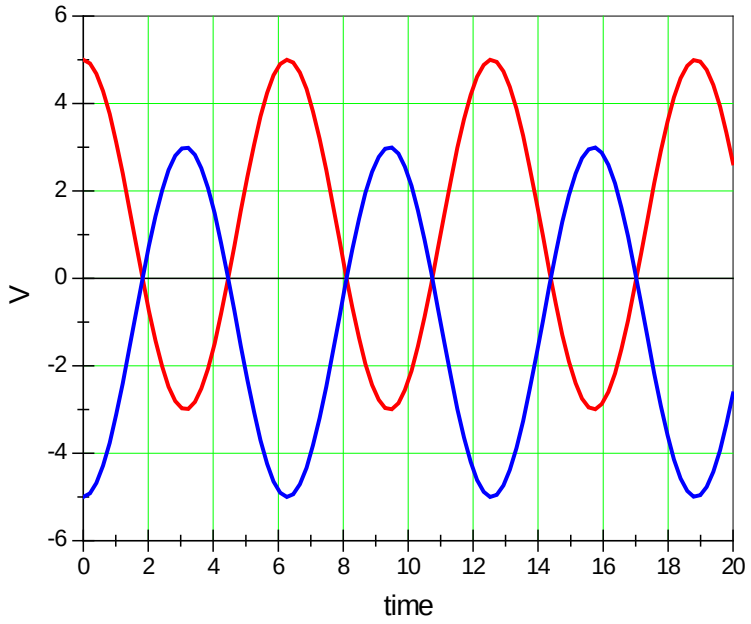

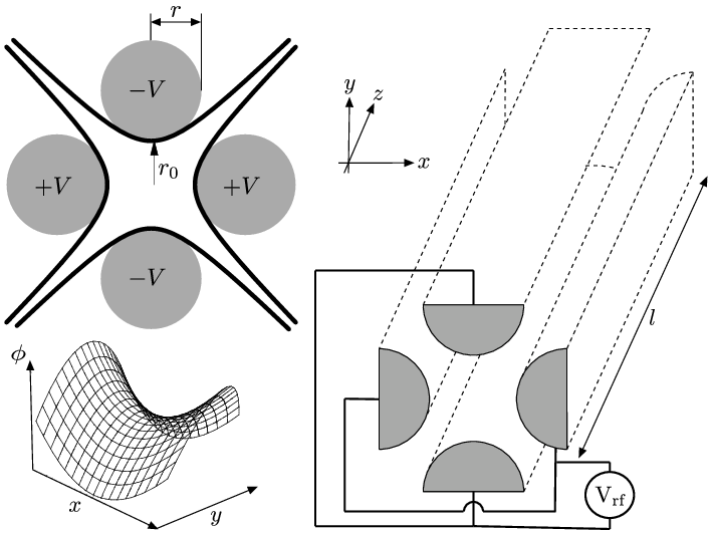

3-D quadrupole ion trap (QIT)
a.k.a. Paul trap

Wolfgang Paul (1913 – 1993)
Nobel Prize Physics 1989

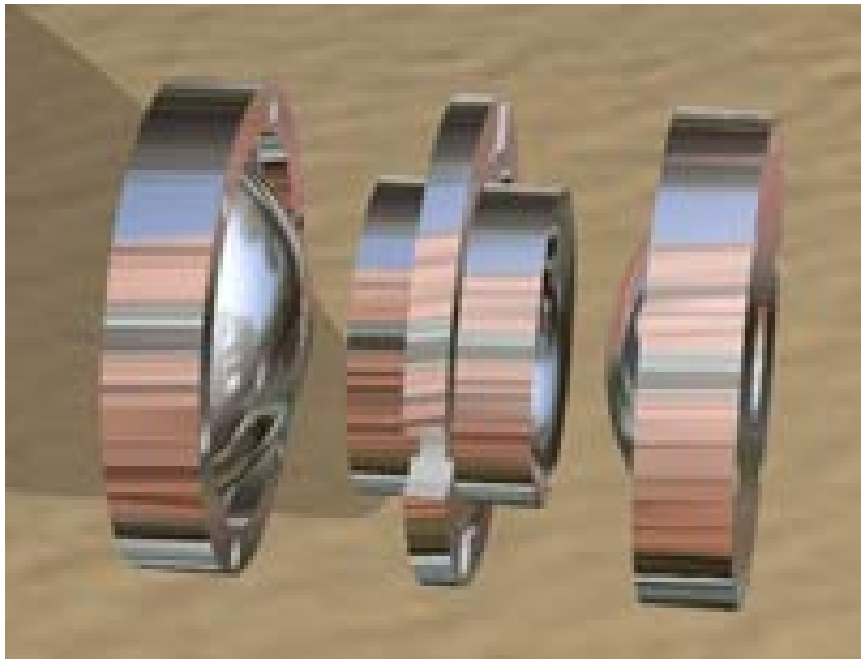

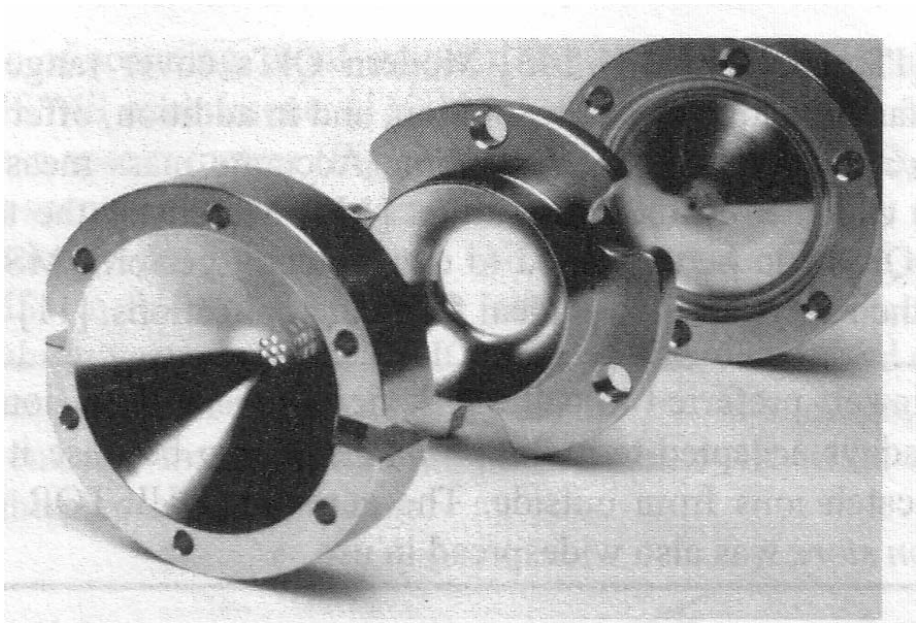

1 ring electrode (middle) and two end-cap electrodes.

Stability diagram in z-dimension

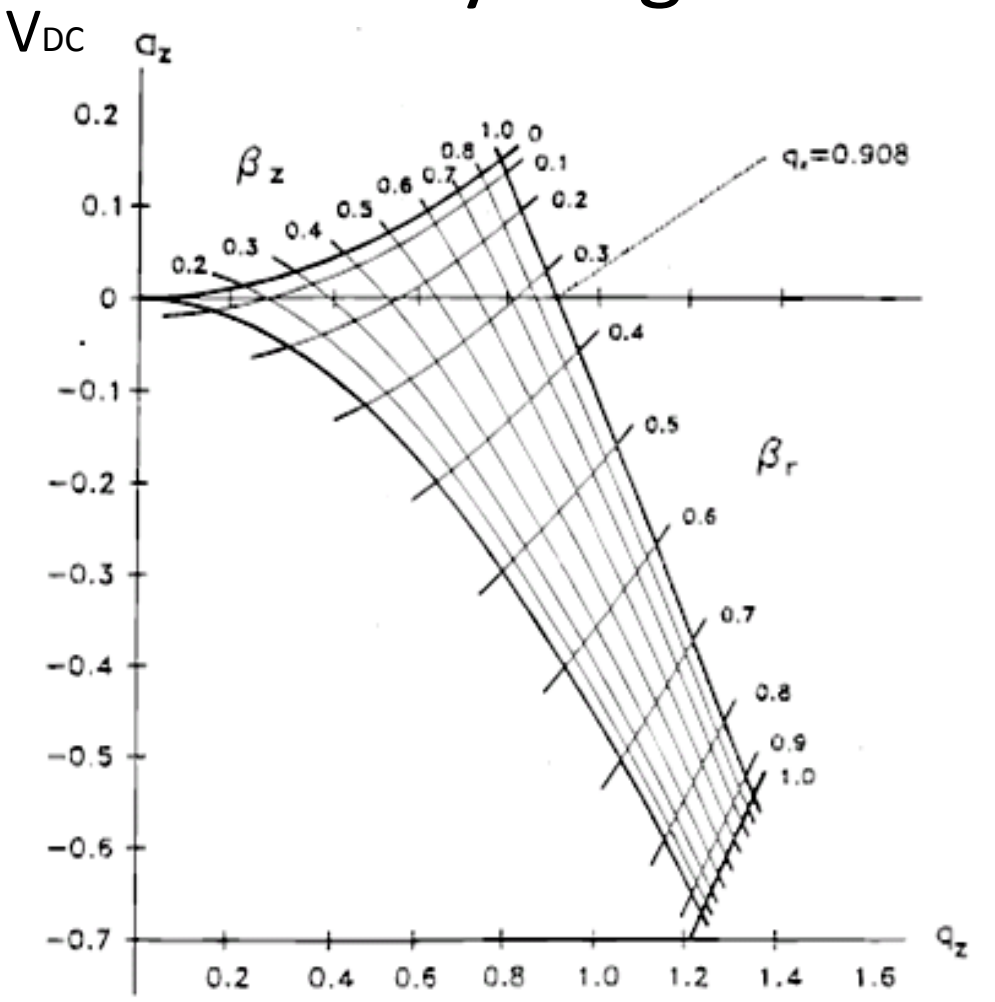

Figure 7. Stability diagram in (a_z, q_z) space for the region of simultaneous stability in both the r- and z-directions near the origin for the three-dimensional quadrupole ion trap; the iso-β_r and iso-β_z lines are shown in the diagram. The q_z-axis intersects the $\beta_z = 1$ boundary at $q_z = 0.908$, which corresponds to q_{max} in the mass-selective instability mode.

Note: DC voltage between ring and end-cap electrodes

If V_{DC}=0, a_z=0
Very similar to quadrupole filter (transmit wide range of *m/z*'s), in QIT trap wide range of *m/z*'s.

For a_z=0, β_z=1 q_z=0.908 (outside of q_z<0.4 limit)

Ejection at the stability limit

If U=0, a_z=0

$$q_z = \frac{8eV}{m(r_0^2 + 2z_0^2)\Omega^2}$$

- q value inversely dependent on m/z → higher m/z ions have lower q values
- if q > 0.908 ion will be ejected along the direction of the end-caps
- by increasing the rf ring electrode voltage, progressively higher m/z can be ejected from the trap

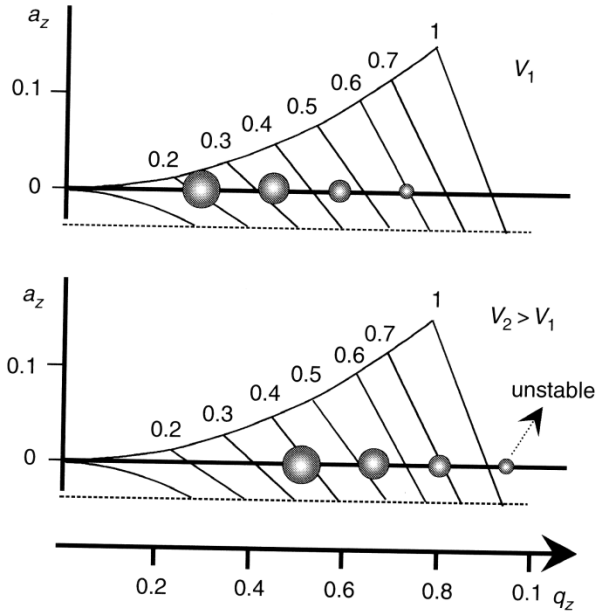

Figure 2.20
At a fixed value of the RF potential V applied to the ring electrode, heavier ions will have lower β_z values and thus lower secular frequencies. If V is increased, β_z values increase for all the ions, as do the secular frequencies. In the example given, the lightest ion now has a β_z value larger than unity and is thus expelled from the trap. The highest mass that can be analyzed depends on the limit V value that can be applied: around 7000–8000 V from zero to peak. For a trap having $r_0 = 1$ cm and operating at a ν frequency of 1.1 MHz, the highest detectable mass-to-charge ratio is about 650 Th